Title: *Tbx1* Heterozygosity in the Oligodendrocyte Lineage Shifts Myelinated Axon Composition in the Mouse Fimbria Without Behavioral Impairments

Authors:

Anne Marie Wells, PhD[1,2+], Takaki Tanifuji, MD, PhD[2+], Takeshi Takano, PhD[2,3+], Arumu Endo, MD.[2], Gina Kang, B.Sc.[2], Marisa Esparza, B.Sc.[2], Qian Shi, PhD[4], Manzoor A. Bhat, PhD[4], Noboru Hiroi, PhD[2, 4,5**]

AM Wells: wellsa1@livemail.uthscsa.edu
T Tanifuji: kjh.goodby@gmail.com
T. Takano: takanot@uthscsa.edu
A. Endo: endo@uthscsa.edu
G. Kang: kangg@uthscsa.edu
M. Esparza: esparzam1@uthscsa.edu
Q. Shi: shiQ@uthscsa.edu
M. Bhat: bhatm@uthscsa.edu
N. Hiroi: hiroi@uthscsa.edu

+ These authors equally contributed to the work.

[1]South Texas Medical Scientist Training Program (STX-MSTP), [2]Department of Pharmacology, [4]Department of Cellular and Integrative Physiology, [5]Department of Cell Systems and Anatomy, University of Texas Health Science Center, San Antonio, TX 78229, USA; [3]Tokyo Denki University, Saitama 350-0394, Japan

ORCID: 0000-0002-6846-5969

****Corresponding Author**
Noboru Hiroi, PhD
hiroi@uthscsa.edu
Department of Pharmacology
Department of Cellular and Integrative Physiology
Department of Cell Systems and Anatomy
University of Texas Health Science Center, San Antonio
Room 211B
7703 Floyd Curl Drive
San Antonio, TX 78229
+1 210 567 4169 (tel)

# of figures: 9
# of supplementary figures: 2
# of supplementary tables: 3

ABSTRACT

Constitutive heterozygosity of *Tbx1*, a T-box transcription factor gene in the 22q11.2 deleted region, produces behavioral deficits and alters myelinated axon composition in the mouse fimbria. However, the cellular origins of these effects—and whether axon changes causally drive behavioral impairments—remain unclear. Prior data link *Tbx1* heterozygosity to reduced oligodendrocyte precursor cell (OPC) markers in the fimbria in mice, raising the hypothesis that *Tbx1* deficiency specifically in the oligodendrocyte lineage contributes to myelin and behavioral phenotypes. To test this hypothesis, we first showed via *in vitro* siRNA knockdown that *Tbx1* regulates both OPCs and mature oligodendrocytes. We then generated conditional *Pdgfrα*Cre;*Tbx1*+/flox mice to initiate *Tbx1* heterozygosity in OPCs. These mice exhibited Cre-mediated recombination in *Pdgfrα*-expressing brain regions and OPC progeny in the fimbria. At 1 month of age, male mutants displayed enhanced spontaneous alternation in the T-maze relative to wild-type littermates—an effect absent at 2 months. No differences appeared in neonatal ultrasonic vocalizations, social interaction, novel object approach, anxiety-like behavior (elevated plus maze), or open-field locomotion and thigmotaxis. Electron microscopic analysis demonstrated a compositional shift in myelinated axons within the fimbria of adult male mutants: increased numbers in the 300–800 nm diameter range and decreased numbers at ~1,200 nm and ~1,400 nm, with unchanged myelin thickness across diameters. These results demonstrate that *Tbx1* heterozygosity in the oligodendrocyte lineage drives a selective shift toward smaller myelinated axons in the fimbria and a transient cognitive enhancement, but does not recapitulate the full myelination abnormalities or the broader cognitive/social deficits observed in constitutive *Tbx1* heterozygotes. Thus, *Tbx1* function in non-oligodendrocyte lineage cells likely exerts non-cell-autonomous effects on myelination that contribute to neurodevelopmental behavioral impairments.

Key Words
Tbx1, *Pdgfrα*, 22q11.2 CNV, social behavior, cognition, fimbria, axon, myelination

INTRODUCTION

Cognitive and social impairments serve as predictors of mental illness(1, 2). Infants later diagnosed with autism spectrum disorder (ASD) exhibit delays and deviations in various aspects of motor, social, and language development(3-11). Similarly, children who later develop full-scale symptoms of schizophrenia show delays in the development of social cognition, working memory, attention, and processing speed(12-16), and these deficits remain integral to the disorder following its onset(17, 18).

These dimensional deficits in mental illness have genetic underpinnings. Copy number variations (CNVs)--which are deletions or duplications of up to several million base pairs at specific chromosomal loci encompassing numerous protein-coding genes-- present high odds ratios and penetrance rates for cognitive and social deficits(19, 20) as well as mental illnesses(21-23).

Individuals carrying 1.5Mb to 3.0Mb hemizygous deletions of human chromosome 22q11.2 exhibit cognitive, social, and emotional impairments from childhood (24-26) and are diagnosed at elevated rates with anxiety disorders, attention-deficit hyperactivity disorder, ASD, intellectual disability, and schizophrenia(27, 28). Duplication of 22q11.2 is associated with epilepsy, ID, ADHD, and ASD at rates higher than those of non-carriers(29-45). However, the mechanisms by which how more than 40 protein-coding genes in 22q11.2 contribute to dimensional deficits and clinical diagnoses remain poorly understood in humans.

Several rare inherited cases of variants in the human *TBX1* gene, a T-box transcription factor gene located within the 22q11.2 CNV, are associated with ASD, schizophrenia, and intellectual disability in the absence of 22q11.2 CNVs(46-51). However, due to their rarity, the statistical reliability of the association between *TBX1* variants and mental illness is limited. Moreover, these patients often carry variants in other single genes throughout the genome(49), complicating the establishment of causality from these associations.

The deletion or overexpression of small murine chromosomal regions or single genes orthologous to human chromosome 22q11.2 offers a complementary approach (1, 52-56). Constitutive overexpression of several hundred kilobase pair segments of the mouse ortholog of 22q11.2 recapitulates distinct social and cognitive deficits linked to 22q11.2 duplication(52, 57), suggesting the presence of driver genes within this segment responsible for distinct behavioral phenotypes. *Tbx1* is one of the genes within a 200 kb segment of 22q11.2, overexpression and hemizygous deletion of which result in deficits in social behavior, repetitive behavior, and prepulse inhibition (50, 52).

The heterozygous deletion of *Tbx1* alone results in impairments in neonatal social communication(58-60), as well as post-pubertal and adult deficits in social interaction(58), social incentive learning(61), acoustic, but not non-acoustic, prepulse inhibition(50, 61), spatial memory acquisition in the Morris water maze and the speed to complete simple discrimination and reversal phases of attentional set-shifting, in the absence of non-specific deficits of motor speed (62). The fimbria of post-pubertal *Tbx1* heterozygous mice displays a lack of large myelinated axons, enhanced myelination of medium-sized axons, a compositional shift of myelinated axons to smaller sizes, and a gene expression profile suggestive of defective oligodendrocyte precursor cells(62). Furthermore, the volume of the secondary motor cortex and amygdala, regions involved in the vocal network(63), is reduced in post-pubertal *Tbx1* heterozygous mice (61). Additionally, virally induced overexpression of *Tbx1* in the hippocampus negatively impacts the developmental maturation of working memory capacity(64).

The cellular and developmental origins of the effects of *Tbx1* deficiency on oligodendrocyte precursor cells remain unknown. During the embryonic period, oligodendrocyte precursor cells emerge from embryonic neural progenitor cells in the medial ganglionic eminence of the ventricular zones around E12.5, followed by a second wave from the lateral ganglionic eminence at E15.5. Oligodendrocyte precursor cells continue to be generated from neural progenitor cells in the subventricular zone during the neonatal period (65-69).

Single-cell transcriptomic analyses have revealed that *Tbx1* is expressed in a more diverse array of cell types than previously indicated by *in situ* hybridization and immunocytochemical studies. In one analysis, involving 1.13 million cells from whole mouse embryos, *Tbx1* was detectable in mesodermal and ectodermal cells from E6.5 to E8.5, in ectodermal cells including those of the neural crest and neural tube at E8.25, in radial glial cells and oligodendrocytes at E10.5, and in neurons and oligodendrocytes at E10.5 and E12.5(70). In the mouse brain, *Tbx1* is detectable in cell clusters with signatures indicative of endothelial cells and Neurog2-positive radial glia at E18 and radial glial cells in the neonatal mouse brain(70). Similarly, another single-cell combinatorial indexing (sci)-RNA-seq analysis of approximately 2 million cells from mouse embryos at E9.5 to E13.3 identified *Tbx1* in endothelial cells, various types of neurons and their progenitors, neural progenitor cells, neural tube, and oligodendrocyte progenitor cells(71). Given that single-cell transcriptomic analyses are capable of detecting rare or transitional cell types with large numbers of cells, these studies suggest that *Tbx1* is present in radial glial cells and neural progenitor cells, as well as their progeny

Our previous work demonstrated that *Tbx1* heterozygosity initiated in neural progenitor cells during the neonatal period recapitulates some behavioral deficits associated with constitutive *Tbx1* heterozygosity(72). As neural progenitor cells during the neonatal period give rise to oligodendrocyte precursor cells, oligodendrocytes, neural progenitor cells, and neurons(65-69), we sought to determine whether the effects of *Tbx1* heterozygosity within the oligodendrocyte lineage induces behavioral and anatomical phenotypes. Our findings indicate that *Tbx1* heterozygosity in the oligodendrocyte lineage induces a compositional shift in myelinated axons in the fimbria, while no affecting myelin integrity, large myelinated axons, or behavior. These results suggest a more critical role for *Tbx1* in neurogenesis lineage.

METHODS

Mice

All protocols for animal handling and use were approved by the Institutional Animal Care and Use Committee (IACUC) of the University of Texas Health Science Center at San Antonio (UTHSCSA) in accordance with National Institutes of Health (NIH) guidelines. Mice were housed in a vivarium with a standard light phase from 7 am to 9 pm).
C57BL/6J mice: We used 1- and 2-month-old male C57BL6/J mice (Jax #000664, Jackson Laboratory, Bar Harbor, ME) as stimulus mice for social interaction.

*Pdgfrα*Cre;*Tbx1*$^{+/flox}$ mice: To conditionally induce *Tbx1* heterozygosity in oligodendrocyte precursor cells, we chose a *Pdgfrα*Cre line that initiates Cre synthesis earlier than a *Cspg4*Cre line to better induce recombination in the oligodendrocyte lineage(73). The *Pdgfrα*- promoter drives Cre-based recombination most robustly in oligodendrocyte precursor cells (74), but also in astrocytes, neurons, fibroblast-like cells, endothelial cells, vascular and leptomeningeal cells, and pericytes in the mouse brain(74-77).

We crossed hemizygous *Pdgfrα*Cre mice with *Tbx1*$^{+/flox}$ mice to generate *PdgfrαCre;Tbx1*$^{+/flox}$ mice. *PdgfrαCre* breeder mice (C57BL/6-Tg(*Pdgfrα*-Cre)1Clc/J; Jax #013148, Jackson

Laboratory, Bar Harbor, ME) have a mixed C57BL/6J;C57BL/6N background. We backcrossed non-congenic *Tbx1*$^{+/flox}$ mice(78) to C57BL/6J for more than 10 generations and confirmed that there was Cre-dependent recombination in a congenic *Tbx1*$^{+/flox}$ mice(72). The genetic background of *Pdgfr*αCre and *Tbx1*$^{+/flox}$ lines were mixed C57BL/6J;C57BL/6N and C57BL/6J, respectively. These two C57BL/6 substrains have many behavioral differences(79). To avoid the confounding effects of their unequal genetic backgrounds(80), we used only an F1 generation derived from crosses of the *Pdgfr*αCre and *Tbx1*$^{+/flox}$ lines.

PdgfrαCre*;ROSA-tdTomato* mice: We crossed hemizygous *Pdgfr*αCre mice (C57BL/6-Tg(*Pdgfr*αCre)1Clc/J; Jax #013148, Jackson Laboratory, Bar Harbor, ME) with homozygous congenic *ROSA-CAG-tdTomato* mice (B6.Cg-*Gt(ROSA)26Sor*$^{tm14(CAG-tdTomato)Hze}$/J, Jax # 007914, Jackson Lab, Bar Harbor, ME) to generate *Pdgfr*αCre*;ROSA-CAG-tdTomato* mice. This ROSA line expresses tdTomato in the hippocampus without the action of Cre (http://connectivity.brain-map.org/transgenic/experiment/81560256)

We determined the genotypes of the mice using our previously published protocol with primers shown in **Table S1**. The sex of the mice was determined by inspection of their external genitalia.

In vitro cell culture of oligodendrocytes

Lateral ventricle tissues, including the subventricular zone (SVZ), were obtained from postnatal day 1-2 (P1-2) C57BL/6J pups. Cells were isolated in culture, with each culture derived from a single mouse. The cells were cultured in a medium (DMEM/F12, HEPES [11320–032, Gibco, Grand Island, NY, USA]) supplemented with N2 (17502048, Gibco, Grand Island, NY, USA), B27 (17504044, Gibco, Grand Island, NY, USA), epidermal growth factor (EGF) at a concentration of 20 ng/ml (AF100-15, Peprotech, Cranbury, NJ, USA). After two to four passages, the cells were dissociated from the spheres using StemPro Accutase Cell Dissociation Reagent (A1110501, Gibco, Grand Island, NY, USA). The cells were then divided into equal portions and plated on each Poly-L-ornithine (P4957, Sigma, St. Louis, MO, USA) and Bovine Fibronectin (1030-FN, R&D Systems, Minneapolis, MN, USA)-coated 6well plate (Corning, 351146, Corning, NY, USA,). The cells were cultured for 144 hours in medium with 5% fetal bovine serum after withdrawing EGF from the medium to induce and maintain differentiation. At the time of EGF withdrawal, we applied *Tbx1* siRNA (10nM, cat#4390771, s74767, Invitrogen; Thermo Fisher Scientific, Waltham, MA, USA) and control siRNA-A (10nM, cat#4390843, Invitrogen; Thermo Fisher Scientific, Waltham, MA, USA) together with siLentFect™ Lipid Reagent for RNAi, 0.5 ml (BIO-RAD, cat# 1703360, Hercules, CA, USA).

Quantitative reverse transcription polymerase chain reaction (qRT-PCR)

In accordance with our published procedure(62), total RNA was extracted using an RNeasy Plus Mini Kit (Cat#74134, Qiagen, Germantown, USA). Complementary DNA (cDNA) was synthesized from total RNA using SuperScript IV VILO Master Mix (Cat#11766050, Invitrogen, Carlsbad, USA). qRT-PCR reactions were performed in triplicate on a QuantStudio 6 Flex Real-Time PCR System (Cat#4485694, Applied Biosystems, Waltham, USA) using the TaqMan Fast Advanced Master Mix (Cat#4444963, Applied Biosystems, Waltham, USA). We used TaqMan® Gene Expression Assays (cat# 4331182, Thermo Fisher, Waltham, MA, USA). The Taqman probes are listed in the Supplementary Material (**Table S2**). Data were analyzed using the ΔΔCt method and normalized to the reference gene *Pgk1*; we had an identical pattern of results with another reference gene *18S*.

Whole brain tissue clearing and index matching

We used the SHIELD and SmartBatch+ (LifeCanvas Sciences, Cambridge, MA) standard pipelines for preserving and electrophoretic clearing(81) to visualize tdTomato in the brains of *Pdgfra*Cre;ROSA-CAG-tdTomato mice. We performed transcardial perfusion of 1-month old mice with ice-cold 0.9% NaCl in dH_2O, followed by 4% paraformaldehyde (PFA) in phosphate-buffered saline (PBS). Brains were preserved using SHIELD as follows: perfused brains were 1) removed from the cranium and fixed in 4% PFA in PBS overnight at 4°C with gentle shaking; 2) incubated in SHIELD OFF solution (dH_2O + SHIELD Buffer [cat#SH-Bf] + SHIELD Epoxy Buffer [cat#SH-Ex]) solution at 4°C with gentle shaking for 3 days; 3) incubated in pre-warmed SHIELD ON Buffer (cat#SH-ON) at 37°C for 1 day with gentle shaking; 4) incubated in the delipidation buffer (cat#DB) for 3 days at 45°C with gentle shaking. Final clearing by electrophoresis was performed with the SmartBatch+ device, with the delipidation buffer inside the clearing cup containing the samples and conduction buffer (cat#CB) for 30 h. Cleared brains were index-matched using a solution of 50% EasyIndex (RI = 1.52, cat#EI-500-1.52) + 50% dH_2O with shaking at 37°C for 1 day, then 100% EasyIndex for one additional day until brains were transparent(81).

Light sheet microscopy

We used a Zeiss Lightsheet 7 Microscope housed in the UTHSCSA Optical Imaging Core to perform volumetric light sheet imaging of cleared *Pdgfrα*Cre;ROSA-CAG-tdTomato brains using a pair of 5×/0.1 focusing illumination objectives and a Fluar 2.5×/0.12 detection objective at identical settings. Image tiles were stitched together using Zeiss Zen Blue software (ver 3.4). 3D volume analysis was performed with Imaris (Oxford Instruments, ver 10.02). Peak intensity of the tdTomato signal was segmented, and volumetric measurements (mm^3) and peak intensities of the total volume (arbitrary units) were calculated for each volume in each mouse.

Immunofluorescence

*Pdgfrα*Cre;ROSA-*tdTomato* mice were sacrificed at 1 month of age. Mice were deeply anesthetized using 4–5% isoflurane and perfused transcardially with 0.9% saline followed by 4% PFA. Brains were extracted and post-fixed in 4% PFA overnight at 4°C, followed by cryoprotection in glycerol overnight at 4°C. Coronal 60-μm thick sections were cut with a freezing microtome. For immunofluorescence labeling, sections were washed in 0.1 M PBS, blocked with 5% normal donkey serum in PBS, and incubated overnight at room temperature, as we described previously(62, 72). We used a well-validated primary rabbit antibody against myelin basic protein (1:200, MBP, ab40390, Abcam) and Donkey anti-rabbit IgG-Alexa Fluor 488 (1:200, A21206, Invitrogen), together with a nuclear marker (DAPI,1:25,000, D3571, Invitrogen). MBP is a marker of mature oligodendrocytes(82, 83). We captured images of sections that were mounted and cover-slipped with Vectashield® anti-fade mounting medium (H-1000) using a Keyence microscope (BZ-X800) microscope with BZX Hardware Module and Zeiss LSM 710 confocal microscope at the UT Health Optical Imaging Core.

Double staining of tdTomato with markers of oligodendrocytes

We captured a series of coronal brain sections from *Pdgfrα*Cre*;ROSA-tdTomato* mice using a Keyence BZ-X800 microscope with BZX Hardware Module and a Zeiss LSM 710 confocal microscope at the UT Health Optical Imaging Core. We used the DAPI signal to identify the anatomical boundaries of landmark structures in each image, cross-matched with equivalent levels in the Allen Brain Atlas (Allen Reference Atlas – Mouse Brain [brain atlas]. Available from *atlas.brain-map.org*). We then used a color scale to represent the level of tdTomato intensity within the delineated anatomical boundaries.

Behavioral Analysis

Male neonatal mice were tested for vocalization resulting from maternal separation at P8 and P12, followed by additional behavioral tests at 1 and 2 months of age, corresponding to peripubertal and post-pubertal, adolescent periods(84), respectively; early signs of puberty begin around 1 month of age(85). Because body weight can alter behavior in mice(86) and *Pdgfrα* regulates progenitor differentiation into adipocytes(87, 88), we measured body weight at the beginning of behavioral tests. Our behavioral battery included reciprocal social interaction, novel object approach, spontaneous alternation in a T-maze, elevated plus maze, and locomotor activity and thigmotaxis in an inescapable open field(52, 57-59, 64, 89-91).

The order of the behavioral assays was based on the stress level; behaviors that occur in a home cage-like setting was given first (i.e., social interaction and novel object approach). T-maze and elevated plus maze tests permit choices and are thus considered less stressful than an inescapable open field. At least a one-day interval was provided between behavioral tests to reduce the likelihood of carryover effects(61, 62, 92), except for the T-maze, in which three different delays were given on three consecutive days.

Mice were assigned randomly to experimental groups and tested during the light phase. Experimenters were blinded to genotypes. Social interaction, novel object approach, and behaviors in the elevated plus maze were recorded using a Basler GigE camera, with video images stored in Ethovision v18 software (Noldus Information Technology, Leesburg, VA). Video images of social interaction and novel object approach were manually scored according to our established criteria. Various parameters of the elevated plus maze were automatically analyzed by Ethovision. The time point of each arm entry was recorded for spontaneous alternation, and the data were subsequently tallied manually. Locomotor activity and thigmotaxis in an inescapable open field were analyzed using Med Associates Activity Monitor 7 Software (Fairfax, VT).

<u>Ultrasonic vocalization</u> Pups were tested for vocalization induced by maternal separation at postnatal days 8 and 12. A cage containing the mother and a litter was transferred to the test room 30 min before testing. Ultrasonic vocalization was recorded for 5 min by UltraSoundGate (Avisoft, Germany) connected to a computer equipped with Avisoft-RECORDER software (Avisoft, Germany) in a test chamber (18 cm long × 18 cm wide × 30 cm high). The sampling rate and lower cutoff frequency were set at 250 kHz (format, 16-bit) and 10 kHz, respectively. A frequency window from 15–150 kHz was used for analysis. Call detection was provided by an automatic threshold-based algorithm and a hold-time mechanism (hold time = 10 ms). Sonograms were inspected, and mechanical noises were eliminated from the analysis. We used the VocalMat software, which has the lowest false positive and false negative rates(93), to determine call types. This software typically detects only the most salient components of the harmonic call type and classifies this call type differently. As the harmonic call type is often affected in genetic mouse models of neuropsychiatric disorders(58, 59, 86, 94), we manually inspected all call types and re-classified such cases as harmonic calls.

<u>Reciprocal Social Interaction Test</u> A test mouse and an age-matched unfamiliar C57BL/6J mouse as a stimulus subject were simultaneously placed in a cage (28.5 cm long × 17.5 cm wide × 12.5 cm high). Mouse behavior was recorded during two 5-min sessions with a 30-min interval between sessions. Video images were scored manually for affiliative and aggressive social interaction by a rater blinded to genotype. The following reciprocal social behaviors were scored by the duration of interaction (minimum of 1 s): aggressive (tail rattle, bite/kicks, sideway offense, boxing/wrestling), affiliative, non-aggressive (mount, pursuit, olfactory investigation,

309 allogrooming, escape/leap), or passive (side-by-side, submissive). We analyzed the sum of time
310 engaged in affiliative, active, and passive social interactions, but passive behavior was rarely
311 seen in our experimental set-up (72, 86, 91, 94).

312 Novel Object Approach A test mouse was placed in a cage (28.5 cm long × 17.5 cm wide × 12.5
313 cm high) with an empty, non-secured 50-mL Falcon tube (3 cm diameter × 8.5 cm long) lying on
314 its side. Videos of mouse interactions with the tube were used to manually score approach
315 behavior by two independent analysts blinded to genotype with an inter-rater reliability of >99%.
316 Approach behavior was scored for olfactory or non-olfactory investigations with a minimum
317 duration of 1 s. Time spent near the tube was also analyzed.

318 Spontaneous Alternation in a T-Maze A test mouse was placed in the start site of the long arm
319 of a black plexiglass T-maze (21.5 cm long × 10.5 cm wide × 20.5 cm high) and allowed to enter
320 the maze and explore either the left or right short arms (31 cm long × 10.25 cm wide × 20.5 cm
321 high) of the cage. We imposed 0 s, 15 s, or 30 s interval delays to maze reentry for 10 trials, and
322 the three interval trials were given on three consecutive days. We manually scored the
323 percentages of alternation and latency to reach the alternated and non-alternated arms.
324
325 Elevated Plus Maze Test Mice were placed in the center stage (5 × 5 cm) of the maze apparatus
326 with four arms (30 × 5 cm) and permitted to explore two closed arms and two open arms
327 extending from the center platform of the maze for 5 min. The maze was positioned 53 cm
328 above the floor. The time spent in visits and the frequency of visits to the two open and two
329 closed arms were analyzed.

330 Open Field Mice were placed in an open-field cage (27.3 cm × 27.3 cm × 20.2 cm; Med
331 Associates, Fairfax, VT) and permitted to explore the cage for 30 min. We measured the
332 distance and velocity of motor activity and duration of time spent in the center (19.05 cm ×
333 19.05 cm central square) versus the margin of an open field, using the activity monitor software
334 (Med Associates, Fairfax, VT).

335 **Electron Microscopy (EM)**
336 We prepared tissue for EM to characterize myelination in the fimbria of *Pdgfrα*Cre;*Tbx1*$^{+/flox}$ mice
337 as we described previously(62). After behavioral assays were completed at 1 and 2 months of
338 age, 4–5-month-old male *Pdgfrα*Cre;*Tbx1*$^{+/flox}$ (N=3) and five control mice, including
339 *Pdgfrα*Cre;*Tbx1*$^{+/+}$ (N=2), wild-type (WT);*Tbx1*$^{+/flox}$ (N=2), and WT;*Tbx1*$^{+/+}$ (N=1), were
340 anesthetized with 4.5% isoflurane in a chamber, and anesthesia was maintained by a nose cone
341 with 2.0% isoflurane. The animals were transcardially perfused with 120 mL of 0.9% saline
342 followed by fixation with 120 mL of 0.1 M buffer (pH 7.4; cat#11653 Electron Microscopy Science,
343 Hatfield, PA) with 2.5% sodium glutaraldehyde (cat#16310, Electron Microscopy Sciences,
344 Hatfield, PA) and 2.5% paraformaldehyde (cat#19202, Electron Microscopy Sciences, Hatfield,
345 PA). Brains were extracted and post-fixed in the same solution at 4°C for 7 weeks. The fimbria
346 from the two hemispheres were obtained separately using a vibratome and placed in 0.1 M
347 sodium cacodylate buffer overnight. Tissues were rinsed with 0.1 M sodium cacodylate buffer to
348 remove aldehydes and placed in 2% osmium tetroxide solution (OsO_4; cat#19150, Electron
349 Microscopy Sciences, Hatfield, PA) in 0.1 M sodium cacodylate buffer for 1 h. Tissues were
350 dehydrated in a series of ethanol solutions and embedded in molds containing Polybed resin
351 (Poly/Red® 812 Embedding media, cat#08791-500 Polysciences, Inc., Warrington, PA). We cut
352 100-nm sections and collected them on square 150-mesh copper grids (cat#7551C,
353 Polysciences, Inc., Warrington, PA) and stained them with uranyl acetate (7 g in 100 mL deionized
354 water)/Reynold's lead citrate (1.33 g lead nitrate,1.76 g sodium citrate in 30 mL triple-distilled
355 water, 8 mL 1 N NaOH). Uranyl acetate stains membranous structures and structures containing

nucleic acid; lead citrate binds to RNA-containing structures and the hydroxyl groups of carbohydrates.

Each fimbria section was viewed in the EM grid squares. Images were screened at 1,000× magnification. For each section, we used all grid images that contained fimbria tissue with round axons without wrinkles, folds, or tears in the sections. One image was captured at the center of each grid field at 20,000× magnification. Images were analyzed by MyelTracer(95). Only axons whose myelin was fully within the image were analyzed quantitatively.

We obtained multiple images for each animal from a section of the right and left hemispheres. The positions of sections sliced from the fimbria varied between the two hemispheres and did not necessarily match the two sides; in one case, only one hemisphere was available because of the accidental loss of a tissue slice. The number of images varied across tissue slices, resulting in unequal image numbers. Many axons from each grid square and many grid squares from each hemisphere were analyzed for each animal. As the number of images and positions of each image varied between the two hemispheres and did not match between the two sides, the hemisphere could not be used as a replicate. Thus, we pooled data for each animal as a technical replicate; data points within and across images were technical replicates. As there was considerable variability in the data, we could not average the values for each animal. The averages of the total axon diameter per genotype were also not appropriate for this data set, as axon numbers differed between genotypes at specific axon diameters (≥300 nm to <400 nm; ≥1,200 nm to <1300 nm) (genotype × axon diameter range, $F(27,5880) = 6.336$, $P < 1.0 \times 10^{-4}$). Thus, linear mixed models were used, as reported previously(62). Data were assessed for the number of myelinated axons, the thickness of myelination, and the g-ratio along a 100 nm unit axon diameter. Data from different images and hemispheres were embedded in random models.

Statistical Analysis

We used SPSS (v29.0.2.0 (20), IBM Corporation) to perform all statistical analyses. Among-group and between-group comparisons of the data were performed using analysis of variance (ANOVA) and Student's two-tailed t-test ($\alpha = 0.05$). We determined normality and homogeneity of variance using the Shapiro-Wilk test and Levene's homogeneity of variance test, respectively If either assumption was violated, we analyzed the data using a linear mixed model, Kruskal Wallis tests, or Mann–Whitney U tests. The Greenhouse–Geisser correction was applied if sphericity was violated and the estimated epsilon was less than 0.75. If multiple tests were applied to a data set, the significance level was adjusted using the Benjamini–Hochberg correction, with a false discovery rate of 5%. We used GraphPad Prism software (v9; GraphPad Software, San Diego, CA) to generate all graphs. All statistical analyses are presented in Table S3.

Data Availability

All data that support the findings and conclusions are provided within the article. All raw data and additional information are available upon request.

List of abbreviations

CNVs, Copy number variations
ASD, Autism Spectrum disorder
scRNA-seq, single cell RNA-seq
Pdgfra, Platelet-derived growth factor receptor alpha
MAG, Myelin associated glycoprotein

MOG, Myelin oligodendrocyte glycoprotein,
MBP, myelin basic protein

Declarations

Ethics approval and consent to participate

All protocols for animal handling and use were approved by the Institutional Animal Care and Use Committee (IACUC) of the University of Texas Health Science Center at San Antonio (UTHSCSA) in accordance with National Institutes of Health (NIH) guidelines.

Consent for publication

Not applicable

Availability of data and materials

All data and materials are available upon request.

Competing interests

The authors declare no competing interests.

Funding

T. Takano, GK, ME, TH, and NH were supported by the National Institute of Health (R01MH099660; R01DC015776). T. Tanifuji was supported by SENSHIN Medical Research Foundation and Uehara Memorial Foundation. QS and MAB were supported by the National Institute of Health (R01GM063074). AMW was funded by F30MH134482, UT Health San Antonio CTSA T32 (T32R004545), UT Health San Antonio Neuroscience T32 (T32NS082145), STX-MSTP (NIH T32GM113896/T32GM145432), and SfN NSP Fellowship (R25NS089462). The Zeiss Lightsheet 7 microscope was funded by the NIH S10 grant 1S10OD030383. The content is solely the responsibility of the authors and does not necessarily represent the official views of the National Institutes of Health.

Authors' contributions

Anne Marie Wells: Conducted lightsheet brain analysis, perfused mice and applied MyelTracer to images for electron microscopy, genotyping, social interaction assessments, and manuscript writing.

Takaki Tanifuji: Performed qRT-PCR analysis, immunofluorescent staining, confocal imaging and analyses, electron microscopy image capturing, and figure preparation.

Takeshi Takano: Conducted statistical analyses and prepared all figures except for immunofluorescent images.

Arumu Endo: Performed qRT-PCR analysis and figure preparation.

Gina Kang: Conducted all behavioral testing.

Marisa Esparza: Managed breeder maintenance, ensured quality control of data input, performed statistical analyses, conducted mouse perfusion, and carried out genotyping.

Qian Shi: Responsible for electron microscopy preparation and manuscript writing.

Manzoor A. Bhat: Engaged in electron microscopy preparation and manuscript writing.

Noboru Hiroi: Designed all experiments, supervised all personnel, prepared electron microscopy samples, captured electron microscopy images, performed immunofluorescent staining, and prepared figures for immunofluorescent staining and wrote the manuscript.

Acknowledgments

The LifeCanvas device was purchased with generous donations by 10 scientists at UT Health San Antonio. We thank Dr. Bernice Morrow for providing *Tbx1*$^{+/flox}$ breeders, Ms. Monica D. Alarcon for technical assistance with EM analysis, and Dr. Lacey B. Sell for her help with MyelTracer software.

455 **RESULTS**

456 Effects of *Tbx1* Knockdown on Markers of Oligodendrocyte Lineage *In Vitro*

457 We first determined the earliest step along the oligodendrocyte lineage at which *Tbx1* deficiency
458 has an effect. To this end, we developed an *in vitro* screening assay that capitalizes on the
459 capacity of neonatal neural progenitor cells, derived from the subventricular zone of C57BL/6J
460 pups sacrificed on postnatal day 2, to generate neuronal precursor cells and oligodendrocyte
461 precursor cells(69). We evaluated the expression of *Cspg4*, a marker of oligodendrocyte
462 precursor cells, as well as *Mag, Mbp, Mog*, and *Plp1*, which are markers indicative of maturing
463 and mature myelinating oligodendrocytes (65), at 144 hours after EGF withdrawal (i.e.,
464 differentiation) and *Tbx1* siRNA application.

465 *Tbx1* siRNA significantly reduced mRNA levels of *Tbx1, Cspg4*, and all markers of mature
466 oligodendrocytes, with *Pgk1* as (**Figure 1**) and *18S* (**Table S3-Figure 1**) as reference genes.
467 These *in vitro* findings are consistent with our *in vivo* data indicating that *Cspg4* (also known as
468 *Ng2*) was reduced in the fimbria of *Tbx1* heterozygous mice(62).

469 As our culture includes both neuronal (58, 72) and oligodendrocyte (see **Figure 1**) lineages, as
470 well as remaining neural progenitor cells, how *Tbx1* knockdown induces changes in the
471 expression of myelin marker genes remains unclear. *Tbx1* knockdown in oligodendrocyte
472 precursor cells may reduce myelin markers in a cell-autonomous manner; alternatively,
473 reductions in *Tbx1* in neonatal neural progenitor cells or their neuronal progeny may indirectly
474 regulate these markers of oligodendrocytes.

475

476 Localization of Recombination in *Pdgfrα-Cre*;ROSA-tdTomato Mice

477 Given our data suggesting that *Tbx1* deficiency begins to affect the stage of oligodendrocyte
478 precursor cells (see **Figure 1**), we initiated *Tbx1* heterozygosity in oligodendrocyte precursor
479 cells using a conditional heterozygous mouse model, where Cre-based initiation of *Tbx1*
480 heterozygosity is guided by the promoter of *Pdgfrα*, a gene expressed in oligodendrocyte
481 precursor cells of both embryonic and post-embryonic origins. We first assessed the extent of
482 *PdgfrαCre*-mediated recombination throughout the brain, employing a tissue clearing technique
483 (SmartBatch+) and conducting lightsheet microscopy to visualize the 3D volume of tdTomato
484 signals in the brains of PdgfrαCre;ROSA-tdTomato mice (**Figure 2A**). The highest levels of
485 tdTomato expression were observed in a pair of arch-shaped structures located along the lateral
486 and third ventricles. Additionally, clusters of tdTomato signals were detected on the ventral
487 surface of the posterior brain, while lower levels of signals were seen throughout other regions.

488 To identify brain regions with tdTomato signals in PdgfrαCre;ROSA-tdTomato mice, we analyzed
489 a series of coronal sections from 1-month-old PdgfrαCre;ROSA-tdTomato mice. High levels of
490 tdTomato signals were present in the striatum, superficial layers of the neocortex (**Figure 2BC**),
491 choroid plexus within the lateral ventricle (**Figure 2ED**) and the fimbria (**Figure 2F**). This
492 expression pattern, driven by the *Pdgfrα* promoter, is consistent with previously reported
493 distributions of *Pdgfrα* mRNA and protein, as well as recombination activity associated with the
494 *Pdgfrα* promoter in the mouse brain (96-98). Moreover, the most intense staining of the choroid
495 plexus is consistent with the intensely tdTomato+ structures resembling the shapes of the lateral
496 and third ventricles (see **Figure 2A**).

497 Embryonic Pdgfra-positive cells give rise to distinct pre-oligodendrocyte precursor cells by the
498 perinatal period, but they exhibit similar profiles by postnatal and adult periods(65, 99).
499 PdgfraCre is expected to induce recombination in oligodendrocyte precursor cells(74). Once
500 tdTomato is expressed through recombination in the PdgfraCre;ROSA-tdTomato mouse line, it
501 remains expressed in their progeny, such as mature oligodendrocytes and myelinated fibers. As
502 myelination of the fimbria is selectively affected in constitutive *Tbx1* heterozygous mice(62), we
503 examined whether tdTomato was colocalized with MBP, a marker of mature oligodendrocytes
504 and myelinated fibers, in the fimbria(100). MBP-positive fibers were present throughout the
505 fimbria (**Figure 3AB**). TdTomato signals were more prominent laterally than medially (**Figure**
506 **3C**) and was colocalized with MBP-positive fibers (**Figure 3D**) in the fimbria. These data
507 establish that tdTomato triggered by PdgfraCre in PdgfraCre;ROSA-tdTomato mice is present in
508 myelinated fibers in the fimbria.

509 Intense tdTomato signals were present in the choroid plexus located laterally to the lateral
510 surface of the fimbria (**Figure 2D**). The cell types in the mouse choroid plexus that express
511 *Pdgfra* include fibroblasts, mural cells, and endothelial cells in the embryo, and fibroblasts,
512 macrophages from the post-embryonic period in the mouse brain; while gene profiles indicative
513 of oligodendrocyte precursor-like cells are detectable during the embryonic period, their genuine
514 location within the choroid plexus remains unclear (70, 101-103). The robust tdTomato signal
515 observed in the choroid plexus at 1 month of age likely originates from some or all of these cell
516 types.

517 <u>Effects of *Tbx1* Heterozygosity in Oligodendrocyte Precursor Cells on Behaviors</u>

518 The rate of growth could affect behavior; PdgfrαCre;*Tbx1*$^{+/flox}$, termed o*Tbx1*$^{+/-}$ mice, may exhibit
519 developmental delays, and their phenotypes could reflect a delayed development compared to
520 their wild-type littermates. However, neonatal o*Tbx1*$^{+/+}$ and o*Tbx1*$^{+/-}$ mice demonstrated
521 indistinguishable increases in body weights (**Figure S1**).

522 To determine how *Tbx1* heterozygosity in oligodendrocyte precursor cells and their progeny
523 affects behavior, mice were tested for social communication during the neonatal period and a
524 battery of social, cognitive, anxiety-related, and motor behaviors at one and two months of age,
525 as myelination peaks around the fourth to fifth postnatal week in rodents(104, 105) and mice
526 reach adolescence around 2 months of age(84). Constitutive *Tbx1* heterozygous mice exhibit
527 impairments in 1) neonatal social communication as early as P7, 2) social behaviors, 3) working
528 memory/cognitive flexibility in a T-maze and attentional set shifting, and 4) affect-related
529 behaviors in an inescapable open field, though not in an elevated plus maze(58-62) around
530 adolescence.

531 We first measured differences among the three control mice: PdgfraCre;*Tbx1*$^{+/+,}$ WT;*Tbx1*$^{+/flox}$,
532 and WT;*Tbx1*$^{+/+}$. There was no significant difference among the controls for any behavioral
533 measure, expect for three time points of total margin time in the open field (see **Table S3-**
534 **Figure 8B**); therefore, we collapsed all the control genotypes into a single control group as
535 *oTbx1*$^{+/+}$ for comparison with *oTbx1*$^{+/-}$ (70).

536 Constitutive *Tbx1*$^{+/-}$ mice exhibit various neonatal, peri-adolescent, and postnatal behavioral
537 phenotypes(58, 59). Therefore, we tested mice for neonatal ultrasonic vocalization on P8 and
538 P12–P13 and performed additional tests with peripubertal (1 month) and adolescent (2 months)
539 mice with 1–2 day intervals between tasks to mitigate potential carryover effects of prior
540 testing(92).

541 We found no differences among o*Tbx1*$^{+/-}$ pups in the number, percentage, and duration of
542 various neonatal vocal call types on P8 and P12 (**Figure 4A–C**). At 1 and 2 months of age, mice
543 were sequentially tested for social interaction, novel object approach, spontaneous alternation in
544 a T-maze, anxiety-related behavior in an elevated plus maze, and locomotor activity and
545 thigmotaxis in an inescapable open field. o*Tbx1*$^{+/-}$ mice and o*Tbx1*$^{+/+}$ mice were
546 indistinguishable in social interaction (**Figure 5A**) and novel object approach (**Figure 5B**). In a
547 T-maze, o*Tbx1*$^{+/-}$ mice, at 1 month of age exhibited better spontaneous alternation rates at the
548 longest delay (**Figure 6A**); otherwise, o*Tbx1*$^{+/+}$ and o*Tbx1*$^{+/-}$ mice were indistinguishable in rates
549 of spontaneous alternation at 2 months of age and in latencies to correct choices at 1 and 2
550 months of age (**Figure 6B–D**).

551 The two genotypes were indistinguishable in the percentage of time spent in open arms (F**igure**
552 **7A**) and visits to open arms (**Figure 7B**) of the elevated plus maze.

553 We evaluated motor activity and anxiety-related behavior in the stressful open-field task(58, 62)
554 where there is no opportunity to escape to closed space. In this task, o*Tbx1*$^{+/-}$ and o*Tbx1*$^{+/+}$
555 mice were indistinguishable in distance traveled at both 1 month and 2 months of age (**Figure**
556 **8A,B**) and time spent in the margin zone (**Figure 8C,D**).

557 While conditional *Tbx1* heterozygosity in the oligodendrocyte cell lineage resulted in improved
558 spontaneous alternation with the longest inter-trial delay at one month of age, this phenotype
559 contrasts with the impaired spontaneous alternation observed in constitutive *Tbx1* heterozygous
560 mice (58, 62). Moreover, this conditional *Tbx1* heterozygosity did not replicate the altered
561 neonatal vocalizations, peri-adolescent or postnatal social interaction deficits, or heightened
562 responses to novel, non-social objects or thigmotaxis seen in constitutive *Tbx1* heterozygous
563 mice(58).

564

565 <u>Effects of *Tbx1* Heterozygosity in Oligodendrocyte Precursor Cells on Myelinated Axons in the</u>
566 <u>Fimbria</u>

567 After behavioral testing, we examined myelinated axons in the fimbria using electron
568 microscopy. Constitutive *Tbx1* heterozygosity selectively alters the ultrastructure in the fimbria,
569 resulting in a higher proportion of myelinated axons measuring 200–600 nm diameter and a
570 lower proportion of axons ≥700 nm and <1,200 nm diameters. Furthermore, the 700–1,500 nm
571 axons exhibited a thicker myelin sheath, with no larger myelinated axons observed in
572 constitutive *Tbx1* heterozygous mice (62). We evaluated whether the ultrastructural alterations
573 of the fimbria of constitutive *Tbx1*$^{+/-}$ mice were recapitulated in o*Tbx1*$^{+/-}$ mice.

574 Densely packed axons were observed in the fimbria (**Figure 9A**). To determine relative myelin
575 thickness, we compared the ratio of the inner axon diameter to the outer fiber diameter (i.e., the
576 g-ratio) (**Figure 9B**). As was the case with constitutive *Tbx1* mice, the g-ratio plateaued at
577 approximately 0.8, the ratio for optimal signal conductance in the brain (88). However, no
578 differences were observed in g-ratios between o*Tbx1*$^{+/-}$ mice and o*Tbx1*$^{+/+}$ mice across the
579 entire range of axon diameters.

580 We separately determined the number and proportion of axons of different diameters. The
581 fimbria of o*Tbx1*$^{+/-}$ mice contained more axons of ≥ 300 nm and <800 nm diameters but fewer
582 axons of >1,200 nm and <1,500 nm diameters compared to o*Tbx1*$^{+/+}$ mice (**Figure 9C**).
583 Consequently, the curve for the relative proportions of axons (y-axis) versus axon diameter (x-
584 axis) shifted to the left in o*Tbx1*$^{+/-}$ mice, compared to o*Tbx1*$^{+/+}$ mice (**Figure 9D**). Consistent with

585 g-ratios, myelin thickness was indistinguishable between o*Tbx1*$^{+/-}$ mice and *oTbx1*$^{+/+}$ mice
586 across all axon diameters (**Figure S2**). Thus, conditional *Tbx1* heterozygosity initiated in
587 oligodendrocyte precursor cells selectively shifted the relative proportion of small to medium
588 myelinated axons in the fimbria but did not affect myelin thickness.

589 In summary, conditional *Tbx1* heterozygosity in the oligodendrocyte lineage shifted the
590 proportion of myelinated axons to smaller sizes without affecting the thickness of myelin in the
591 fimbria.

592

DISCUSSION

The objective of this study was to delineate the cellular origin(s) of the diverse behavioral and myelin phenotypes observed in constitutive *Tbx1* heterozygous mice(58-62). As some of these behavioral phenotypes are recapitulated by initiating *Tbx1* heterozygosity in neonatal progenitor cells (72) and neonatal neural progenitor cells in the subventricular zone are responsible for generating neurons and oligodendrocytes during the neonatal period (68, 69, 106), we reasoned that *Tbx1* deficiency in neonatal neural progenitor cells, neuronal lineage from neural progenitor cells, or oligodendrocyte lineage from oligodendrocyte precursor cells contributes to the observed myelin and associated behavioral phenotypes. This study aimed to investigate the impact of *Tbx1* heterozygosity in the oligodendrocyte lineage on the behavioral and ultrastructural phenotypes.

To achieve this objective, we crossed *Pdgfrα*Cre mice with congenic *Tbx1*$^{+/flox}$ mice to generate *Pdgfrα*Cre;*Tbx1*$^{+/flox}$ (o*Tbx1*$^{+/-)}$ mice. We evaluated a range of social, cognitive, anxiety-related, and motor behaviors, along with the ultrastructural composition of myelin and axons in the fimbria. The o*Tbx1*$^{+/-}$ mice selectively replicated the altered axon sizes in the fimbria observed in constitutive *Tbx1* heterozygous mice. In contrast, while o*Tbx1*$^{+/-}$ exhibited improved spontaneous alternation following a 30-second delay at one month of age—indicative of enhanced working memory and cognitive flexibility-- this was contrary to the impaired spontaneous alternation observed in constitutive *Tbx1* heterozygous mice. This observation supports that suggestion that the final phenotype arises from the cumulative effects of various contributory and opposing factors (54, 80).

Other phenotypes associated with constitutive *Tbx1* heterozygosity were absent in o*Tbx1*$^{+/-}$ mice, including neonatal social communication, responses to social or non-social stimuli, and anxiety-like behaviors in an elevated plus maze and thigmotaxis. These findings indicate that *Tbx1* in the oligodendrocyte lineage does not significantly influence the phenotypes. Combined with the observation that *Tbx1* heterozygosity initiated in neonatal (P1–P5) neural progenitor cells at P1-P5, but not P21–P25, recapitulates the social and cognitive deficits observed in constitutive *Tbx1* heterozygous mice (72), the current negative data suggest that *Tbx1* in neonatal neural progenitor cells or their neuronal lineage may play a principal role in determining the final phenotype (72).

The fimbria of o*Tbx1*$^{+/-}$ mice had more axons of ≥300 nm and <800 nm diameter and fewer axons of ≥1,200 nm and <1,500 nm diameter than o*Tbx1*$^{+/+}$ mice. This was similar to the increase in axons of ≥200 nm and <400 nm and the decrease in axons of ≥700 nm and <1,700 nm axons in constitutive *Tbx1* heterozygous mice. The medium-size axons of constitutive *Tbx1* heterozygous mice have increased myelin thickness and lack large (≥1,700 nm) myelinated axons in the fimbria(62), but these characteristics were absent in o*Tbx1*$^{+/-}$ mice. This selective change in the axon phenotype could result from widespread activities of the *Pdgfrα* promoter in many cell types and regions. Although *Pdgfrα*Cre induces recombination in oligodendrocyte precursor cells, it also triggers recombination in neurons, astrocytes, pericytes, ependyma, perivascular mesenchymal cells, and other cells(74-77, 97, 107, 108). *Tbx1* heterozygosity in neurons might underlie the shift in the axonal composition of neurons. The correlation between altered spontaneous alternation and the increased proportion of small-to-medium myelinated axons in the fimbria does not necessarily indicate causality by oligodendrocyte precursor cells. *Pdgfrα*Cre-induced recombination could have affected phenotypes through other cell types and their progenies in other brain regions. In the mouse brain, *Tbx1* is not detectable in astrocytes or microglia; however, it is significantly present in endothelial cells and neural progenitor cells.

Additionally, *Tbx1* can be detected in immature neurons as well as both excitatory and inhibitory neurons at various developmental stages, ranging from embryonic development to adulthood(70, 71, 109, 110). Further research is necessary to elucidate the effects of Tbx1 in different cell types on phenotypic outcomes.

Several interpretative limitations warrant attention. The general absence of phenotypes may be attributed to the high mortality rate of o*Tbx1*$^{+/-}$ litters, potentially biasing our sample toward mice that were less affected by or recovered more quickly from the mutation's effects. Among male pups in our breeder colony, only 31% and 24% survived to P7 and 2 months of age, respectively. However, two lines of evidence do not support this possibility. First, more mice were alive during the neonatal period than at 1 and 2 months of age, yet neonatal vocalizations on P8 and P12 were normal. Second, our nestinCreERT;*Tbx1*$^{+/flox}$ litters also exhibited a high mortality rate but demonstrated more profound behavioral deficits (72).

We cannot exclude the possibility that the conditional *Tbx1* heterozygosity was incomplete. The *Pdgfrα* promoter induces nearly complete recombination in oligodendrocyte precursor cells, with labels persisting in their mature progeny oligodendrocytes (107, 111); however, this promoter may exhibit variability in some cells, leading to incomplete recombination (112). Furthermore, the lack of behavioral deficits may arise from compensatory processes in oligodendrocyte lineage cells; ablation of specific oligodendrocyte precursor cells did not result in gross behavioral abnormalities (66).

Large-scale human brain imaging studies show alterations in the white matter in CNV carriers(113, 114), as well as idiopathic cases of ASD and schizophrenia (115, 116). Moreover, carriers of hemizygous deletion of 22q11.2 have an altered white matter in the fornix/fimbria(117) and volume alterations of many brain regions(118-120). Together with our previous observations that *Tbx1* heterozygosity during embryonic neurogenesis (61) and in neonatal stem cells (72) likely contribute to volume alterations of specific brain regions and social and cognitive deficits (61), respectively, the present negative results delineate the extent to which *Tbx1* contributes to the behavioral and structural phenotypes of 22q11.2 hemizygosity through different cell types.

668 **Figure legends**

669 **Figure 1**. The relative quantification (RQ) (mean ± SEM) of expression levels at each stage of
670 oligodendrogenesis, as determined by quantitative reverse transcription polymerase chain
671 reaction (qRT-PCR) using *Pgk1* as a reference gene. Three cell clones were derived from three
672 different C57BL/6J pups at postnatal days 2 or 3, with data obtained from three culture wells for
673 each clone, except for one *Tbx1* siRNA-treated clone where *Tbx1* mRNA was undetectable and
674 thus excluded from the analysis. A linear mixed model showed that Tbx1 siRNA reduced
675 expression of all genes tested equally (Treatment, $F(1,89)=14.665$, $p=0.0002386$; Gene,
676 $F(5,89)=0.8440$, $p=0.5222$; Treatment x Gene, $F(5,89)=0.8440$, $p=0.5222$). Mann-Whitney tests
677 confirmed that *Tbx1* siRNA reduced expression of each gene. Statistically significant differences
678 between control siRNA and *Tbx1* siRNA groups are indicated by *, **, and *** for $p<0.05$,
679 $p<0.01$, and $p<0.005$, respectively; they remained significant following Benjamini-Hochberg
680 correction at a 5% false discovery rate (FDR).

681 **Figure 2. A**. A representative lightsheet image of the brain from a 1-month-old male
682 PdgfrαCre;ROSA-tdTomato mouse. Following SmartBatch+ tissue delipification, tdTomato
683 signals were visualized using a Zeiss LSM 7 Lightsheet microscope with a 2.5x objective (N =
684 3). **B-D**. tdTomato expression in 1-month-old PdgfrαCre;ROSA-tdTomato mice is depicted
685 together with blue DAPI signals at the levels of the anterior striatum (**B**), middle striatum (**C**),
686 posterior striatum/fimbria (**D**), anterior lateral ventricle (**E**), middle lateral ventricle (**F**), and
687 fimbria (**H**). Abbreviations: ChPx, choroid plexus; LV, lateral ventricle; Str, striatum; Sept,
688 septum; CC, corpus callosum; CTX, cortex; HGCL, hippocampal granule cell layer; fmb, fimbria;
689 SVZ, subventricular zone. N = 3.

690 **Figure 3**. A Representative Case of Confocal Images of the Fimbria of a 1-Month-Old Male
691 PdgfrαCre;ROSA-tdTomato Mouse. Sections were stained for DAPI (**A**, blue) and MBP (**B**,
692 green). **C**. Red tdTomato signals originated from the PdgfrαCre;ROSA-tdTomato genotype. **D**. A
693 composite image of the three colors is presented; white arrows indicate an area where fibers
694 are positive for both MBP and tdTomato. N = 4. ChPx, choroid plexus; fmb, fimbria.

695 **Figure 4**. The number (**A**), proportion (**B**), and duration (**C**) (mean ± standard error of the mean
696 [SEM]) of 12 call types emitted on postnatal days (P) P8 and P12. The two genotypes exhibited
697 differences in certain interaction effects: **A**. Number: Genotype, $F(1,912)=0.1966$, $p = 0.6576$;
698 Genotype x Postnatal day, $F(1, 912)=4.835$, $p = 0.0281$; Genotype x Call type, $F(11,$
699 $9123)=0.7077$, $p = 0.7319$; Genotype x Postnatal day x Call types, $F(11, 912)=0.3686$, $p =$
700 0.9679. **B**. Proportion: Genotype, $F(1,912)=0.0107$, $p = 0.9176$; Genotype x Postnatal day, $F(1,$
701 $912)=0.0107$, $p = 0.9176$; Genotype x Call type, $F(11, 912)=1.3657$, $p = 0.1837$; Genotype x
702 Postnatal day x Call types, $F(11, 912)=0.7966$, $p = 0.6437$. **C**. Duration: Genotype,
703 $F(1,560)=0.0435$, $p = 0.8349$; Genotype x Postnatal day, $F(1, 560)=0.10519$, $p = 0.7458$;
704 Genotype x Call type, $F(11, 560)=3.361$, $p = 0.00016$; Genotype x Postnatal day x Call types,
705 $F(11, 560)=1.0389$, $p = 0.4101$. However, Mann-Whitney U tests did not reveal any significant
706 genotype effects at any postnatal day for any call type after applying Benjamini-Hochberg
707 corrections at 5% false discovery rate (FDR). **Inset** in **A**: The total number of ultrasonic
708 vocalizations (mean ± SEM) emitted at P8 and P12. The two genotypes did not differ on the two
709 postnatal days (Genotype, $F(1,76)=0.1559$, $p = 0.694$; Genotype x Postnatal day, $F(1,$
710 $76)=1.103$, $p = 0.2969$). **Inset** in **C**: Duration: Genotype, $F(1,32)=0.0002$, $p = 0.9878$; Genotype
711 x Postnatal day, $F(1, 32)=0.3617$, $p = 0.5518$). Ha, harmonic; Sd, step-down; Sh, short; Df,
712 down frequency modulation; Uf, up frequency modulation; Ts, two steps; Fl, flat; Ch, chevron;

Co, complex; Su, step-up; Ms, multiple steps; Rc, reverse chevron. *oTbx1*$^{+/+}$ mice, N = 27; *oTbx1*$^{+/-}$ mice, N = 11 at P8; *oTbx1*$^{+/+}$ mice, N = 30; *oTbx1*$^{+/-}$ mice, N = 12 at P12.

Figure 5. Interaction with Social and Non-Social Stimuli. **A**) Social Interaction. The *oTbx1*$^{+/-}$ (PdgfrαCre;Tbx1$^{+/flox}$) mice and *oTbx1*+/+ mice did not differ in the amount of time (mean ± SEM) spent in affiliative social interaction (1 month: genotype, F(1, 72) = 0.1118, p = 0.739; genotype × session, F(1, 72) = 0.262, p = 0.6102; 2 months: genotype, F(1, 58) = 0.00547, p = 0.9413; genotype x session, F(1, 58) = 1.2175, p = 0.2744). The three genotypes of *oTbx1*+/+ (1 month, N = 8, PdgfrαCre;*Tbx1*$^{+/+}$, N = 10, Wild-type;*Tbx1*$^{+/+}$, N = 9, Wild-type;*Tbx1*$^{+/flox}$; 2 months, N = 8, PdgfrαCre;*Tbx1*$^{+/+}$, N = 6, Wild-type;*Tbx1*$^{+/+}$, N = 7, Wild-type;*Tbx1*$^{+/flox}$) did not show significant differences (1 month: genotype, F(2, 48) = 1.686, p = 0.1960; genotype × session, F(2, 48) = 0.843, p = 0.4366; 2 months: genotype, F(2, 36) = 0.0392, p = 0.9616; genotype x session, F(2, 36) = 0.2382, p = 0.7893), and were thus combined as *oTbx1*+/+. *oTbx1*$^{+/+}$ mice , N = 27; *oTbx1*$^{+/-}$ mice, N = 11 at 1 month; *oTbx1*$^{+/+}$ mice, N = 21; *oTbx1*$^{+/-}$ mice, N = 10 at 2 months. **B**) Approach to a novel, non-social object. The two genotypes did not differ in the amount of time spent in affiliative social interaction (1 month: genotype, F(1, 70) = 2.2507E-05, p = 0.9962; genotype × session, F(1, 70) = 1.0305, p = 0.31354; 2 months: genotype, F(1, 58) = 0.11634, p = 0.7342; genotype × session, F(1, 58) = 0.0821, p = 0.77545). The three genotypes of *oTbx1*$^{+/+}$ (1 month: N = 8, PdgfrαCre;*Tbx1*$^{+/+}$, N = 9, Wild-type;*Tbx1*$^{+/+}$, N = 9, Wild-type;*Tbx1*$^{+/flox}$; 2 months: N = 8, PdgfrαCre;*Tbx1*$^{+/+}$, N = 6, Wild-type;*Tbx1*$^{+/+}$, N = 7, Wild-type;*Tbx1*$^{+/flox}$) did not differ (1 month: genotype, F(2, 46) = 0.1772, p = 0.8382; genotype × session, F(2, 46) = 0.9318, p = 0.4012; 2 months: genotype, F(2, 36) = 0.0580, p = 0.9437; genotype × session, F(2, 36) = 0.6581, p = 0.5239) and were therefore combined as *oTbx1*$^{+/+}$. *oTbx1*$^{+/+}$ mice, N = 26; *oTbx1*$^{+/-}$ mice, N = 11 at 1 month; *oTbx1*$^{+/+}$ mice, N = 21; *oTbx1*$^{+/-}$ mice, N = 10 at 2 months.

Figure 6. Spontaneous alternation in a T-maze. Compared to male *oTbx1*$^{+/+}$ (N = 20) mice, male *oTbx1*$^{+/-}$ (N = 10) mice performed better in the percentage of correct spontaneous alternations (mean ± SEM) at the longest delay (30 s) in a T-maze at 1 month of age, but not at 2 months. Specifically, at 1 month: % alternation, genotype, F(1, 96) = 4.66, p = 0.0333; genotype × delays, F(2,96) = 3.1509, p = 0.0473; at 2 months: genotype, F(1, 81) = 2.047, p = 0.1564; genotype × delays, F(2, 81) = 0.2439, p = 0.7841. The three genotypes of *oTbx1*$^{+/+}$ (1 month: N = 8, PdgfrαCre;*Tbx1*$^{+/+}$, N = 7, Wild-type;*Tbx1*$^{+/+}$, N = 9, Wild-type;*Tbx1*$^{+/flox}$; 2 months: N = 8, PdgfrαCre;*Tbx1*$^{+/+}$, N = 6, Wild-type;*Tbx1*$^{+/+}$, N = 6, Wild-type;*Tbx1*$^{+/flox}$) did not differ (1 month: genotype, F(2, 63) = 0.1046, p = 0.9008; genotype × delays, F(4, 63) = 0.2648, p = 0.8995; 2 months: genotype, F(2, 51) = 0.1197, p = 0.8874; genotype × delays, F(4, 51) = 0.6401, p = 0.6363) and consequently were combined as *oTbx1*$^{+/+}$. *oTbx1*$^{+/-}$ mice exhibited higher levels of alternations at the 30-second delay compared to *oTbx1*+/+ mice, as determined by the Mann-Whitney test (p = 0.0081). **B**) The two groups did not exhibit significant differences in the latency to correct choices in the T-maze at 1 month (genotype, F(1, 96) = 2.181, p = 0.1430; genotype × delays, F(2, 96) = 2.058, p = 0.1332) or at 2 months (genotype, F(1, 81) = 1.1135, p = 0.2944; genotype × delays, F(2, 81) = 2.5825, p = 0.0817). The three genotypes of *oTbx1*$^{+/+}$ (1 month, N=8), PdgfrαCre;*Tbx1*$^{+/+}$ (N=7), Wild-type;*Tbx1*$^{+/+}$ (N=9), and Wild-type;*Tbx1*$^{+/flox}$ (2 months, N=8), PdgfrαCre;*Tbx1*$^{+/+}$ (N=6), Wild-type;*Tbx1*$^{+/+}$ (N=6), and Wild-type;*Tbx1*$^{+/flox}$, demonstrated a significant interaction effect at 1 month of age (genotype, F(2, 63) = 1.5787, p = 0.2143; genotype × session, F(4, 63) = 4.5625, p = 0.00267), but no significant interaction at 2 months of age (genotype, F(2, 51) = 0.1631, p = 0.8500; genotype × session, F(4, 51) = 1.0611, p = 0.3853). However, Mann-Whitney U tests revealed that none of

760 the three genotypes significantly differed from one another at 1 month of age after applying the
761 Benjamini-Hochberg correction (p>0.05 for all pairs). The three genotypes were combined as
762 o*Tbx1*$^{+/+}$. The sample sizes were as follows: *oTbx1*$^{+/+}$ mice, N = 24; *oTbx1*$^{+/-}$ mice, N = 10 at 1
763 month; *oTbx1*$^{+/+}$ mice, N = 20; *oTbx1*$^{+/-}$ mice, N = 9 at 2 months.

764 **Figure 7**. Anxiety-related behavior in an elevated T-maze.The *oTbx1*$^{+/-}$ and *oTbx1*$^{+/+}$ mice did
765 not differ significantly in the relative amount of time spent (mean +SEM) in the open arms of an
766 elevated plus maze (**A**,1 month,U = 100, p = 0.3440; 2 months, U = 98, p = 0.9483) or the
767 frequency of visits to the open arms of the elevated plus maze (**B**, 1 month,t(32) = 1.7412, p =
768 0.0912; 2 months, t(28) = 0.5925, p = 0.5583). The three genotypes of *oTbx1*+/+ (1 month, N=7,
769 PdgfrαCre;*Tbx1*$^{+/+}$, N=7, Wild-type;*Tbx1*$^{+/+}$, N=6, Wild-type;*Tbx1*+/flox; 2 months, N=8,
770 PdgfrαCre;*Tbx1*$^{+/+}$, N=6, Wild-type;*Tbx1*$^{+/+}$, N=6, Wild-type;*Tbx1*$^{+/flox}$) did not differ in the
771 percentage of time spent in open arms (1 month,genotype, F(2, 20) = 0.0745, p = 0.9285; 2
772 months,genotype, F(2, 17) = 2.126, p = 0.1499) or the percentage of visits to open arms (1
773 month,genotype, F(2, 20) = 0.1837, p = 0.8336; 2 months,genotype, F(2, 17) = 1.4821, p =
774 0.2551), and thus were combined as *oTbx1*$^{+/+}$. The sample sizes were: *oTbx1*$^{+/+}$ mice, N = 23;
775 *oTbx1*$^{+/-}$ mice, N = 11 at 1 month; *oTbx1*$^{+/+}$ mice, N = 20; *oTbx1*$^{+/-}$ mice, N = 10 at 2 months.

776 **Figure 8**. Motor Activity and Thigmotaxis. *oTbx1*$^{+/+}$ and *oTbx1*$^{+/-}$ mice exhibited indistinguishable
777 distances traveled at both 1 month and 2 months of age (**A**, 1 month, genotype, F(1, 198) =
778 0.6314, p = 0.4278; genotype × time, F(5, 198) = 0.9551, p = 0.4466; **B**, 2 months, genotype,
779 F(1, 28) = 0.0242, p = 0.87739; genotype × time, F(3.66, 102.485) = 0.5389, p = 0.69188). The
780 Greenhouse–Geisser correction was applied due to a violation of sphericity, with the estimated
781 epsilon being less than 0.75.The three genotypes of *oTbx1*$^{+/+}$ (1 month, N=8, PdgfrαCre;*Tbx1*$^{+/+}$,
782 N=7, Wild-type;*Tbx1*$^{+/+}$, N=9, Wild-type;*Tbx1*$^{+/flox}$; 2 months, N=8, PdgfrαCre;*Tbx1*$^{+/+}$, N=6, Wild-
783 type;*Tbx1*$^{+/+}$, N=6, Wild-type;*Tbx1*$^{+/flox}$) demonstrated differences at both ages (genotype, F(2,
784 21) = 5.475, p = 0.01220; genotype × time, F(7.10, 74.58) = 1.118, p = 0.3611; at 2
785 months,genotype, F(2, 17) = 9.533, p = 0.00167; genotype × time, F(10, 85) = 0.3955, p =
786 0.9453). Comparisons of all pairs using Student's t-tests indicated that no pair reached
787 significance after the Benjamini-Hochberg correction (p>0.05 for all pairs), resulting in their
788 combination as *oTbx1*$^{+/+}$.

789 *oTbx1*$^{+/+}$ and *oTbx1*$^{+/-}$ mice spent equal amounts of time in the margin zone (i.e., thigmotaxis) of
790 the inescapable open field at both 1 and 2 months of age (**C,** 1 month, genotype, F(1, 198) =
791 0.2009, p = 0.6545; genotype × time, F(5,198) = 2.1516, p = 0.0609; **D**, 2 months, genotype,
792 F(1, 168) = 0.08912, p = 0.7657; genotype × time, F(5, 168) = 0.9880, p = 0.4267). The three
793 genotypes of *oTbx1*$^{+/+}$ did not differ at 1 month of age (genotype, F(2, 21) = 0.3687, p = 0.6961;
794 genotype × time, F(5.485, 57.58) = 0.9884, p = 0.4375), but differences were observed at 2
795 months of age (genotype, F(2, 17) = 4.880, p = 0.0211; genotype × time, F(5.049, 42.917) =
796 0.7179, p = 0.6147). Comparisons of all pairs using Student's t-tests revealed that 2-month-old
797 Wild-type;*Tbx1*$^{+/flox}$ and Wild-type;*Tbx1*$^{+/+}$ differed at the first four time points, even after the
798 Benjamini-Hochberg correction (p<0.05). However, these groups had relatively small sample
799 sizes (N=6 for both), and PdgfrαCre;*Tbx1*$^{+/+}$and Wild-type;*Tbx1*$^{+/flox}$ or PdgfrαCre;*Tbx1*$^{+/+}$ and
800 Wild-type;*Tbx1*$^{+/flox}$ did not differ at any time point (p >0.05), thus they were combined as
801 *oTbx1*$^{+/+}$. Sample sizes included *oTbx1*$^{+/+}$ mice, N = 24; *oTbx1*$^{+/-}$ mice, N = 11 at 1 month;
802 *oTbx1*$^{+/+}$ mice, N = 20; *oTbx1*$^{+/-}$ mice, N = 10 at 2 months.

803 **Figure 9**. Electron Microscopy Analysis of Myelinated Axons. **A**. Representative electron
804 microscopy images of axons in the fimbria at 20,000× magnification. Genotypes: +/+, *oTbx1*$^{+/+}$;
805 +/-, *oTbx1*$^{+/-}$. Scale bar = 1,600 nm. **B**. G-ratios plotted against axon diameters for 4,423 and

806 2,317 axons from 5 *oTbx1*$^{+/+}$ mice and 3 *oTbx1*$^{+/-}$ mice, respectively. All axons with closed
807 myelin sheaths were analyzed using MyelTracer. The reciprocal function best fits the data
808 distributions. G-ratios increased as a function of axon diameter (*oTbx1*+/+, R = 0.6268, p <
809 0.001; *oTbx1*+/−, R = 0.6491, p < 0.001). There was no significant difference in the axon
810 diameter range for G-ratios between oTbx1+/+ and oTbx1+/− mice (genotype, p = 0.8131;
811 genotype × axon diameter, p = 0.221). **C**. Average number (± SEM) of axons per image field
812 versus axon diameter. Significant differences were observed between *oTbx1*$^{+/+}$ and *oTbx1*$^{+/-}$
813 mice (χ^2 (27) = 109.7085, p = 6.22 × 10^{-12}), primarily due to a higher number of axons with
814 diameters ≥300 nm and <800 nm and a lower number of axons with diameters ≥1,200 nm and
815 <1,500 nm in *oTbx1*$^{+/-}$ compared to *oTbx1*$^{+/+}$ mice, as determined by Mann-Whitney U tests
816 applied to this diameter range (*, p < 0.05; **, p < 0.01; ***, p < 0.001; ****, p < 0.0001). The shift
817 in axon sizes toward smaller to medium diameters in *oTbx1*$^{+/-}$ compared to *oTbx1*$^{+/+}$ mice
818 resulted in a smaller average axon size for *oTbx1*$^{+/-}$ mice (Mann-Whitney non-parametric tests,
819 p = 7.48 × 10^{-19}). **D**. Differences in the percentage of myelinated axons for *oTbx1*$^{+/-}$ versus
820 oTbx1+/+ mice across axon diameters (Kolmogorov-Smirnov, p = 3.59 × 10^{-16}).

821

822

823 **Table S1. Primers used for genotyping**.

Mouse line	Forward (5' → 3')	Reverse (5' → 3')	Purpose
Pdgfrα-Cre	olMR1084 (GCGGTCTGGCAGTAAAAACTATC)	olMR1085 (GTGAAACAGCATTGCTGTCACTT)	Generic cre - transgene
Pdgfrα-Cre	olMR7338 (CTAGGCCACAGAATTGAAAGATCT)	olMR7339 (GTAGGTGGAAATTCTAGCATCATCC)	Generic cre – internal positive control
ROSA-CAG-tdTomato	olMR9020 (AAGGGAGCTGCAGTGGAGTA)	olMR9021 (CCGAAAATCTGTGGGAAGTC)	tdTomato wild-type control
ROSA-CAG-tdTomato	olMR9103 (GGCATTAAAGCAGCGTATCC)	olMR9105 (CTGTTCCTGTACGGCATGG)	tdTomato mutant
Tbx1$^{+/flox}$	2g 1F (TCTTCTTGGGGCTGTAGACT)	Tbx1 1R (TGACTGTGCTGAAGTGCATC)	LoxP site
Tbx1$^{+/-}$	KO1F (TTGGTGACGATCATCTCGGT)	KO1R (ATGATCTCCGCCGTGTCTAG) Mut2R (AGGTCCCTCGAAGAGGTTCA)	*Tbx1*$^{+/+}$ *Tbx1*$^{+/-}$

824

825 **Table S2. Primers for qRT-PCR**

Gene	**Assay ID**
Tbx1	Mm00448949_m1
Cspg4	Mm00507257_m1
Mag	Mm00487538_m1
Mbp	Mm01266402_m1
Mog	Mm01279062_m1
Plp1	Mm01297210_m1

826

827

References

1. Hiroi N, Yamauchi T. Modeling and Predicting Developmental Trajectories of Neuropsychiatric Dimensions Associated With Copy Number Variations. Int J Neuropsychopharmacol. 2019;22(8):488–500.
2. Michelini G, Carlisi CO, Eaton NR, Elison JT, Haltigan JD, Kotov R, et al. Where do neurodevelopmental conditions fit in transdiagnostic psychiatric frameworks? Incorporating a new neurodevelopmental spectrum. World Psychiatry. 2024;23(3):333–57.
3. Ozonoff S, Iosif AM, Baguio F, Cook IC, Hill MM, Hutman T, et al. A prospective study of the emergence of early behavioral signs of autism. J Am Acad Child Adolesc Psychiatry. 2010;49(3):256–66.
4. Ozonoff S, Young GS, Belding A, Hill M, Hill A, Hutman T, et al. The broader autism phenotype in infancy: when does it emerge? J Am Acad Child Adolesc Psychiatry. 2014;53(4):398–407.
5. Esposito G, Hiroi N, Scattoni ML. Cry, baby, cry: Expression of Distress as a Biomarker and Modulator in Autism Spectrum Disorder. Int J Neuropsychopharmacol. 2017;20(6):498–503.
6. Sung S, Fenoglio A, Wolff JJ, Schultz RT, Botteron KN, Dager SR, et al. Examining the factor structure and discriminative utility of the Infant Behavior Questionnaire-Revised in infant siblings of autistic children. Child Dev. 2022;93(5):1398–413.
7. Northrup JB, Leezenbaum NB, Campbell SB. Observed Social Emotional Behavior at 22 Months Predicts a Later ASD Diagnosis in High-Risk Siblings. J Autism Dev Disord. 2021;51(9):3187–98.
8. Miller M, Sun S, Iosif AM, Young GS, Belding A, Tubbs A, et al. Repetitive behavior with objects in infants developing autism predicts diagnosis and later social behavior as early as 9 months. J Abnorm Psychol. 2021;130(6):665–75.
9. Di Giorgio E, Rosa-Salva O, Frasnelli E, Calcagni A, Lunghi M, Scattoni ML, et al. Abnormal visual attention to simple social stimuli in 4-month-old infants at high risk for Autism. Sci Rep. 2021;11(1):15785.
10. Miller M, Iosif AM, Hill M, Young GS, Schwichtenberg AJ, Ozonoff S. Response to Name in Infants Developing Autism Spectrum Disorder: A Prospective Study. J Pediatr. 2017;183:141–6 e1.
11. Caravella KE, Roberts JE. Adaptive Skill Trajectories in Infants with Fragile X Syndrome Contrasted to Typical Controls and Infants at High Risk for Autism. Res Autism Spectr Disord. 2017;40:1–12.
12. Gur RC, Calkins ME, Satterthwaite TD, Ruparel K, Bilker WB, Moore TM, et al. Neurocognitive growth charting in psychosis spectrum youths. JAMA Psychiatry. 2014;71(4):366–74.
13. Seidman LJ, Shapiro DI, Stone WS, Woodberry KA, Ronzio A, Cornblatt BA, et al. Association of Neurocognition With Transition to Psychosis: Baseline Functioning in the Second Phase of the North American Prodrome Longitudinal Study. JAMA Psychiatry. 2016;73(12):1239–48.
14. Meier MH, Caspi A, Reichenberg A, Keefe RS, Fisher HL, Harrington H, et al. Neuropsychological decline in schizophrenia from the premorbid to the postonset period: evidence from a population-representative longitudinal study. Am J Psychiatry. 2014;171(1):91–101.
15. Bora E, Lin A, Wood SJ, Yung AR, McGorry PD, Pantelis C. Cognitive deficits in youth with familial and clinical high risk to psychosis: a systematic review and meta-analysis. Acta Psychiatr Scand. 2014;130(1):1–15.
16. Sheffield JM, Karcher NR, Barch DM. Cognitive Deficits in Psychotic Disorders: A Lifespan Perspective. Neuropsychol Rev. 2018;28(4):509–33.
17. Tschentscher N, Woll CFJ, Tafelmaier JC, Kriesche D, Bucher JC, Engel RR, et al. Neurocognitive Deficits in First-Episode and Chronic Psychotic Disorders: A Systematic Review from 2009 to 2022. Brain Sci. 2023;13(2).

18. Johansson M, Hjarthag F, Helldin L. Cognitive markers related to long-term remission status in Schizophrenia Spectrum Disorders. Psychiatry Res. 2020;289:113035.
19. Stefansson H, Meyer-Lindenberg A, Steinberg S, Magnusdottir B, Morgen K, Arnarsdottir S, et al. CNVs conferring risk of autism or schizophrenia affect cognition in controls. Nature. 2014;505(7483):361–6.
20. Kendall KM, Rees E, Escott-Price V, Einon M, Thomas R, Hewitt J, et al. Cognitive Performance Among Carriers of Pathogenic Copy Number Variants: Analysis of 152,000 UK Biobank Subjects. Biol Psychiatry. 2017;82(2):103–10.
21. Malhotra D, Sebat J. CNVs: harbingers of a rare variant revolution in psychiatric genetics. Cell. 2012;148(6):1223–41.
22. Marshall CR, Howrigan DP, Merico D, Thiruvahindrapuram B, Wu W, Greer DS, et al. Contribution of copy number variants to schizophrenia from a genome-wide study of 41,321 subjects. Nat Genet. 2017;49(1):27–35.
23. Goh S, Thiyagarajan L, Dudding-Byth T, Mark P, Kirk EP. A systematic review and pooled analysis of penetrance estimates of copy number variants associated with neurodevelopment. Genet Med. 2024:101227.
24. Gur RE, Yi JJ, Donald-McGinn DM, Tang SX, Calkins ME, Whinna D, et al. Neurocognitive development in 22q11.2 deletion syndrome: comparison with youth having developmental delay and medical comorbidities. Mol Psychiatry. 2014;19(11):1205–11.
25. Morrison S, Chawner S, van Amelsvoort T, Swillen A, Vingerhoets C, Vergaelen E, et al. Cognitive deficits in childhood, adolescence and adulthood in 22q11.2 deletion syndrome and association with psychopathology. Transl Psychiatry. 2020;10(1):53.
26. Chawner S, Owen MJ, Holmans P, Raymond FL, Skuse D, Hall J, et al. Genotype-phenotype associations in children with copy number variants associated with high neuropsychiatric risk in the UK (IMAGINE-ID): a case-control cohort study. Lancet Psychiatry. 2019;6(6):493–505.
27. Zinkstok J, Boot E, Bassett AS, Hiroi N, Butcher NJ, Vingerhoets C, et al. The 22q11.2 deletion syndrome from a neurobiological perspective. Lancet Psychiatry. 2019;6(11):951–60.
28. Schneider M, Debbane M, Bassett AS, Chow EW, Fung WL, van den Bree M, et al. Psychiatric disorders from childhood to adulthood in 22q11.2 deletion syndrome: results from the International Consortium on Brain and Behavior in 22q11.2 Deletion Syndrome. Am J Psychiatry. 2014;171(6):627–39.
29. Ensenauer RE, Adeyinka A, Flynn HC, Michels VV, Lindor NM, Dawson DB, et al. Microduplication 22q11.2, an emerging syndrome: clinical, cytogenetic, and molecular analysis of thirteen patients. American Journal of Human Genetics. 2003;73(5):1027–40.
30. Hassed SJ, Hopcus-Niccum D, Zhang L, Li S, Mulvihill JJ. A new genomic duplication syndrome complementary to the velocardiofacial (22q11 deletion) syndrome. Clinical Genetics. 2004;65(5):400–4.
31. Portnoi MF, Lebas F, Gruchy N, Ardalan A, Biran-Mucignat V, Malan V, et al. 22q11.2 duplication syndrome: two new familial cases with some overlapping features with DiGeorge/velocardiofacial syndromes. American Journal of Medical Genetics A. 2005;137(1):47–51.
32. Yobb TM, Somerville MJ, Willatt L, Firth HV, Harrison K, MacKenzie J, et al. Microduplication and triplication of 22q11.2: a highly variable syndrome. American Journal of Human Genetics. 2005;76(5):865–76.
33. de La Rochebrochard C, Joly-Helas G, Goldenberg A, Durand I, Laquerriere A, Ickowicz V, et al. The intrafamilial variability of the 22q11.2 microduplication encompasses a spectrum from minor cognitive deficits to severe congenital anomalies. Am J Med Genet A. 2006;140(14):1608–13.
34. Alberti A, Romano C, Falco M, Cali F, Schinocca P, Galesi O, et al. 1.5 Mb de novo 22q11.21 microduplication in a patient with cognitive deficits and dysmorphic facial features. Clin Genet. 2007;71(2):177–82.

35. Engels H, Brockschmidt A, Hoischen A, Landwehr C, Bosse K, Walldorf C, et al. DNA microarray analysis identifies candidate regions and genes in unexplained mental retardation. Neurology. 2007;68(10):743–50.
36. Mukaddes NM, Herguner S. Autistic disorder and 22q11.2 duplication. World J Biol Psychiatry. 2007;8(2):127–30.
37. Torres-Juan L, Rosell J, Morla M, Vidal-Pou C, Garcia-Algas F, de la Fuente MA, et al. Mutations in TBX1 genocopy the 22q11.2 deletion and duplication syndromes: a new susceptibility factor for mental retardation. Eur J Hum Genet. 2007;15(6):658–63.
38. Descartes M, Franklin J, de Stahl TD, Piotrowski A, Bruder CE, Dumanski JP, et al. Distal 22q11.2 microduplication encompassing the BCR gene. Am J Med Genet A. 2008;146A(23):3075–81.
39. Ramelli GP, Silacci C, Ferrarini A, Cattaneo C, Visconti P, Pescia G. Microduplication 22q11.2 in a child with autism spectrum disorder: clinical and genetic study. Dev Med Child Neurol. 2008;50(12):953–5.
40. Wentzel C, Fernstrom M, Ohrner Y, Anneren G, Thuresson AC. Clinical variability of the 22q11.2 duplication syndrome. Eur J Med Genet. 2008;51(6):501–10.
41. Yu S, Cox K, Friend K, Smith S, Buchheim R, Bain S, et al. Familial 22q11.2 duplication: a three-generation family with a 3-Mb duplication and a familial 1.5-Mb duplication. Clin Genet. 2008;73(2):160–4.
42. Lo-Castro A, Galasso C, Cerminara C, El-Malhany N, Benedetti S, Nardone AM, et al. Association of syndromic mental retardation and autism with 22q11.2 duplication. Neuropediatrics. 2009;40(3):137–40.
43. Portnoi MF. Microduplication 22q11.2: a new chromosomal syndrome. Eur J Med Genet. 2009;52(2-3):88–93.
44. Soysal Y, Vermeesch J, Davani NA, Sensoy N, Hekimler K, Imirzalioglu N. Molecular characterization of microduplication 22q11.2 in a girl with hypernasal speech. Genet Mol Res. 2011;10(3):2148–54.
45. Wenger TL, Miller JS, DePolo LM, de Marchena AB, Clements CC, Emanuel BS, et al. 22q11.2 duplication syndrome: elevated rate of autism spectrum disorder and need for medical screening. Mol Autism. 2016;7:27.
46. Singh T, Poterba T, Curtis D, Akil H, Al Eissa M, Barchas JD, et al. Rare coding variants in ten genes confer substantial risk for schizophrenia. Nature. 2022;604(7906):509–16.
47. Alhazmi S, Alzahrani M, Farsi R, Alharbi M, Algothmi K, Alburae N, et al. Multiple Recurrent Copy Number Variations (CNVs) in Chromosome 22 Including 22q11.2 Associated with Autism Spectrum Disorder. Pharmgenomics Pers Med. 2022;15:705–20.
48. Alghamdi M, Al Khalifah R, Al Homyani DK, Alkhamis WH, Arold ST, Ekhzaimy A, et al. A Novel TBX1 Variant Causing Hypoparathyroidism and Deafness. J Endocr Soc. 2020;4(2):bvz028.
49. Ogata T, Niihori T, Tanaka N, Kawai M, Nagashima T, Funayama R, et al. TBX1 mutation identified by exome sequencing in a Japanese family with 22q11.2 deletion syndrome-like craniofacial features and hypocalcemia. PLoS One. 2014;9(3):e91598.
50. Paylor R, Glaser B, Mupo A, Ataliotis P, Spencer C, Sobotka A, et al. Tbx1 haploinsufficiency is linked to behavioral disorders in mice and humans: implications for 22q11 deletion syndrome. Proc Natl Acad Sci U S A. 2006;103(20):7729–34.
51. Gong W, Gottlieb S, Collins J, Blescia A, Dietz H, Goldmuntz E, et al. Mutation analysis of TBX1 in non-deleted patients with features of DGS/VCFS or isolated cardiovascular defects. J Med Genet. 2001;38(12):E45.
52. Hiroi N, Zhu H, Lee M, Funke B, Arai M, Itokawa M, et al. A 200-kb region of human chromosome 22q11.2 confers antipsychotic-responsive behavioral abnormalities in mice.

973 Proceedings of the National Academy of Sciences of the United States of America.
974 2005;102(52):19132–7.
975 53. Hiroi N, Hiramoto T, Harper KM, Suzuki G, Boku S. Mouse models of 22q11.2-associated
976 autism spectrum disorder. Autism. 2012;S1(001):1–9.
977 54. Hiroi N, Takahashi T, Hishimoto A, Izumi T, Boku S, Hiramoto T. Copy Number Variation at
978 22q11.2: from rare variants to common mechanisms of developmental neuropsychiatric disorders.
979 Mol Psychiatry. 2013;18:1153–65.
980 55. Hiroi N, Nishi A. Dimensional deconstruction and reconstruction of CNV-associated
981 neuropsychiatric disorders. In: Pletnikov MV, Waddington JL, editors. Modeling the
982 Psychopathological Dimensions of Schizophrenia: From Molecules to Behavior. Handbook of
983 Behavioral Neuroscience. 23. London, UK2015. p. 285–302.
984 56. Nishi A, Hiroi N. Genetic Mechanisms Emerging from Mouse Models of CNV-Associated
985 Neuropsychiatric Disorders. In: Abel T, Nickl-Jockschat T, editors. *The Neurobiology of*
986 *Schizophrenia*. New York: Academic Press/Elsevier; 2016. p. 397–417.
987 57. Suzuki G, Harper KM, Hiramoto T, Funke B, Lee M, Kang G, et al. Over-expression of a human
988 chromosome 22q11.2 segment including TXNRD2, COMT and ARVCF developmentally affects
989 incentive learning and working memory in mice. Human Molecular Genetics. 2009;18(20):3914–25.
990 58. Hiramoto T, Kang G, Suzuki G, Satoh Y, Kucherlapati R, Watanabe Y, et al. Tbx1:
991 identification of a 22q11.2 gene as a risk factor for autism spectrum disorder in a mouse model.
992 Hum Mol Genet. 2011;20(24):4775–85.
993 59. Takahashi T, Okabe S, Broin PO, Nishi A, Ye K, Beckert MV, et al. Structure and function of
994 neonatal social communication in a genetic mouse model of autism. Mol Psychiatry.
995 2016;21(9):1208–14.
996 60. Kato R, Machida A, Nomoto K, Kang G, Hiramoto T, Tanigaki K, et al. Maternal approach
997 behaviors toward neonatal calls are impaired by mother's experiences of raising pups with a risk
998 gene variant for autism. Dev Psychobiol. 2021;63(1):108–13.
999 61. Hiramoto T, Sumiyoshi A, Kato R, Yamauchi T, Takano T, Kang G, et al. Highly demarcated
1000 structural alterations in the brain and impaired social incentive learning in Tbx1 heterozygous mice.
1001 Molecular Psychiatry. 2025;30(5):1876–86.
1002 62. Hiramoto T, Sumiyoshi A, Yamauchi T, Tanigaki K, Shi Q, Kang G, et al. Tbx1, a gene encoded
1003 in 22q11.2 copy number variant, is a link between alterations in fimbria myelination and cognitive
1004 speed in mice. Mol Psychiatry. 2022;27(2):929–38.
1005 63. Nieder A, Mooney R. The neurobiology of innate, volitional and learned vocalizations in
1006 mammals and birds. Philos Trans R Soc Lond B Biol Sci. 2020;375(1789):20190054.
1007 64. Boku S, Izumi T, Abe S, Takahashi T, Nishi A, Nomaru H, et al. Copy number elevation of
1008 22q11.2 genes arrests the developmental maturation of working memory capacity and adult
1009 neurogenesis. Molecular Psychiatry. 2018;23(4):985–92.
1010 65. Marques S, van Bruggen D, Vanichkina DP, Floriddia EM, Munguba H, Varemo L, et al.
1011 Transcriptional Convergence of Oligodendrocyte Lineage Progenitors during Development. Dev
1012 Cell. 2018;46(4):504–17 e7.
1013 66. Kessaris N, Fogarty M, Iannarelli P, Grist M, Wegner M, Richardson WD. Competing waves of
1014 oligodendrocytes in the forebrain and postnatal elimination of an embryonic lineage. Nat Neurosci.
1015 2006;9(2):173–9.
1016 67. Menn B, Garcia-Verdugo JM, Yaschine C, Gonzalez-Perez O, Rowitch D, Alvarez-Buylla A.
1017 Origin of oligodendrocytes in the subventricular zone of the adult brain. J Neurosci.
1018 2006;26(30):7907–18.
1019 68. Rushing G, Ihrie RA. Neural stem cell heterogeneity through time and space in the
1020 ventricular-subventricular zone. Front Biol (Beijing). 2016;11(4):261–84.

1021 69. Fuentealba LC, Rompani SB, Parraguez JI, Obernier K, Romero R, Cepko CL, et al.
1022 Embryonic Origin of Postnatal Neural Stem Cells. Cell. 2015;161(7):1644–55.
1023 70. Wang R, Zhang P, Wang J, Ma L, E W, Suo S, et al. Construction of a cross-species cell
1024 landscape at single-cell level. Nucleic Acids Res. 2023;51(2):501–16.
1025 71. Cao J, Spielmann M, Qiu X, Huang X, Ibrahim DM, Hill AJ, et al. The single-cell
1026 transcriptional landscape of mammalian organogenesis. Nature. 2019;566(7745):496–502.
1027 72. Hiramoto T, Boku S, Kang G, Abe S, Nagashima M, Barbachan e Silva M, et al.
1028 Transcriptional regulation of neonatal neural stem cells is a determinant of social behavior. BioRxiv.
1029 2023;11(12):468452.
1030 73. Nishiyama A, Lin XH, Giese N, Heldin CH, Stallcup WB. Co-localization of NG2
1031 proteoglycan and PDGF alpha-receptor on O2A progenitor cells in the developing rat brain. J
1032 Neurosci Res. 1996;43(3):299–314.
1033 74. Rivers LE, Young KM, Rizzi M, Jamen F, Psachoulia K, Wade A, et al. PDGFRA/NG2 glia
1034 generate myelinating oligodendrocytes and piriform projection neurons in adult mice. Nat
1035 Neurosci. 2008;11(12):1392–401.
1036 75. Sil S, Periyasamy P, Thangaraj A, Chivero ET, Buch S. PDGF/PDGFR axis in the neural
1037 systems. Mol Aspects Med. 2018;62:63–74.
1038 76. Brandebura AN, Morehead M, Heller DT, Holcomb P, Kolson DR, Jones G, et al. Glial Cell
1039 Expansion Coincides with Neural Circuit Formation in the Developing Auditory Brainstem. Dev
1040 Neurobiol. 2018;78(11):1097–116.
1041 77. Beiter RM, Rivet-Noor C, Merchak AR, Bai R, Johanson DM, Slogar E, et al. Evidence for
1042 oligodendrocyte progenitor cell heterogeneity in the adult mouse brain. Sci Rep. 2022;12(1):12921.
1043 78. Arnold JS, Werling U, Braunstein EM, Liao J, Nowotschin S, Edelmann W, et al. Inactivation
1044 of Tbx1 in the pharyngeal endoderm results in 22q11DS malformations. Development.
1045 2006;133(5):977–87.
1046 79. Matsuo N, Takao K, Nakanishi K, Yamasaki N, Tanda K, Miyakawa T. Behavioral profiles of
1047 three C57BL/6 substrains. Front Behav Neurosci. 2010;4:29.
1048 80. Hiroi N. Critical Reappraisal of Mechanistic Links of Copy Number Variants to Dimensional
1049 Constructs of Neuropsychiatric Disorders in Mouse Models. Psychiatry and Clinical
1050 Neurosciences. 2018;72(5):301–21.
1051 81. Yang D, Wang Y, Qi T, Zhang X, Shen L, Ma J, et al. Phosphorylation of pyruvate
1052 dehydrogenase inversely associates with neuronal activity. Neuron. 2024;112(6):959–71 e8.
1053 82. Readhead C, Popko B, Takahashi N, Shine HD, Saavedra RA, Sidman RL, et al. Expression of
1054 a myelin basic protein gene in transgenic shiverer mice: correction of the dysmyelinating
1055 phenotype. Cell. 1987;48(4):703–12.
1056 83. Meschkat M, Steyer AM, Weil MT, Kusch K, Jahn O, Piepkorn L, et al. White matter integrity in
1057 mice requires continuous myelin synthesis at the inner tongue. Nat Commun. 2022;13(1):1163.
1058 84. Arellano JI, Duque A, Rakic P. A coming-of-age story: adult neurogenesis or adolescent
1059 neurogenesis in rodents? Front Neurosci. 2024;18:1383728.
1060 85. Bronson FH, Dagg CP, Snell GD. Reproduction. In: Green EL, editor. Biology of the
1061 Laboratory Mouse. Second Edition ed. New York: Dover Publications, Inc.; 2007. p. Oneline
1062 publication.
1063 86. Nakamura M, Ye K, MB ES, Yamauchi T, Hoeppner DJ, Fayyazuddin A, et al. Computational
1064 identification of variables in neonatal vocalizations predictive for postpubertal social behaviors in a
1065 mouse model of 16p11.2 deletion. Mol Psychiatry. 2021;26(11):6578–88.
1066 87. Gao Z, Daquinag AC, Su F, Snyder B, Kolonin MG. PDGFRalpha/PDGFRbeta signaling
1067 balance modulates progenitor cell differentiation into white and beige adipocytes. Development.
1068 2018;145(1).

1069 88. Marcelin G, Ferreira A, Liu Y, Atlan M, Aron-Wisnewsky J, Pelloux V, et al. A PDGFRalpha-
1070 Mediated Switch toward CD9(high) Adipocyte Progenitors Controls Obesity-Induced Adipose Tissue
1071 Fibrosis. Cell Metab. 2017;25(3):673–85.
1072 89. Harper KM, Hiramoto T, Tanigaki K, Kang G, Suzuki G, Trimble W, et al. Alterations of social
1073 interaction through genetic and environmental manipulation of the 22q11.2 gene Sept5 in the
1074 mouse brain. Human Molecular Genetics. 2012;21(15):3489–99.
1075 90. Suzuki G, Harper KM, Hiramoto T, Sawamura T, Lee M, Kang G, et al. Sept5 deficiency exerts
1076 pleiotropic influence on affective behaviors and cognitive functions in mice. Human Molecular
1077 Genetics. 2009;18(9):1652–60.
1078 91. Yamauchi T, Kang G, Hiroi N. Heterozygosity of murine Crkl does not recapitulate behavioral
1079 dimensions of human 22q11.2 hemizygosity. Genes Brain and Behavior. 2020;20(5):e12719.
1080 92. Paylor R, Spencer CM, Yuva-Paylor LA, Pieke-Dahl S. The use of behavioral test batteries, II:
1081 effect of test interval. Physiol Behav. 2006;87(1):95–102.
1082 93. Fonseca AH, Santana GM, Bosque Ortiz GM, Bampi S, Dietrich MO. Analysis of ultrasonic
1083 vocalizations from mice using computer vision and machine learning. Elife. 2021;10.
1084 94. Sakamoto Y, Takano T, Shimoyama S, Hiramoto T, Hiroi N, Nakamura K. Prepartum
1085 bumetanide treatment reverses altered neonatal social communication but non-specifically
1086 reduces post-pubertal social behavior in a mouse model of fragile X syndrome. Genomic
1087 Psychiatry. 2025;1(1):61–72.
1088 95. Kaiser T, Allen HM, Kwon O, Barak B, Wang J, He Z, et al. MyelTracer: A Semi-Automated
1089 Software for Myelin g-Ratio Quantification. eNeuro. 2021;8(4).
1090 96. Allen Brain Atlas. Mouse Brain. http://wwwbrain-maporg. 2017.
1091 97. Nait Oumesmar B, Vignais L, Baron-Van Evercooren A. Developmental expression of
1092 platelet-derived growth factor alpha-receptor in neurons and glial cells of the mouse CNS. J
1093 Neurosci. 1997;17(1):125–39.
1094 98. Zhu X, Bergles DE, Nishiyama A. NG2 cells generate both oligodendrocytes and gray matter
1095 astrocytes. Development. 2008;135(1):145–57.
1096 99. Marques S, Zeisel A, Codeluppi S, van Bruggen D, Mendanha Falcao A, Xiao L, et al.
1097 Oligodendrocyte heterogeneity in the mouse juvenile and adult central nervous system. Science.
1098 2016;352(6291):1326–9.
1099 100. Ozarkar SS, Patel RKR, Vulli T, Friar CA, Burette AC, Philpot BD. Regional analysis of myelin
1100 basic protein across postnatal brain development of C57BL/6J mice. Front Neuroanat.
1101 2025;19:1535745.
1102 101. Bastedo WE, Scott RW, Arostegui M, Underhill TM. Single-cell analysis of mesenchymal
1103 cells in permeable neural vasculature reveals novel diverse subpopulations of fibroblasts. Fluids
1104 Barriers CNS. 2024;21(1):31.
1105 102. Takeuchi A, Takahashi Y, Iida K, Hosokawa M, Irie K, Ito M, et al. Identification of Qk as a
1106 Glial Precursor Cell Marker that Governs the Fate Specification of Neural Stem Cells to a Glial Cell
1107 Lineage. Stem Cell Reports. 2020;15(4):883–97.
1108 103. Dani N, Herbst RH, McCabe C, Green GS, Kaiser K, Head JP, et al. A cellular and spatial map
1109 of the choroid plexus across brain ventricles and ages. Cell. 2021;184(11):3056–74 e21.
1110 104. Downes N, Mullins P. The development of myelin in the brain of the juvenile rat. Toxicol
1111 Pathol. 2014;42(5):913–22.
1112 105. Thompson CL, Ng L, Menon V, Martinez S, Lee CK, Glattfelder K, et al. A high-resolution
1113 spatiotemporal atlas of gene expression of the developing mouse brain. Neuron. 2014;83(2):309–
1114 23.
1115 106. Redmond SA, Figueres-Onate M, Obernier K, Nascimento MA, Parraguez JI, Lopez-
1116 Mascaraque L, et al. Development of Ependymal and Postnatal Neural Stem Cells and Their Origin
1117 from a Common Embryonic Progenitor. Cell Rep. 2019;27(2):429–41 e3.

107. Kang SH, Fukaya M, Yang JK, Rothstein JD, Bergles DE. NG2+ CNS glial progenitors remain committed to the oligodendrocyte lineage in postnatal life and following neurodegeneration. Neuron. 2010;68(4):668–81.
108. Komitova M, Zhu X, Serwanski DR, Nishiyama A. NG2 cells are distinct from neurogenic cells in the postnatal mouse subventricular zone. J Comp Neurol. 2009;512(5):702–16.
109. Rosenberg AB, Roco CM, Muscat RA, Kuchina A, Sample P, Yao Z, et al. Single-cell profiling of the developing mouse brain and spinal cord with split-pool barcoding. Science. 2018;360(6385):176–82.
110. Yao Z, Liu H, Xie F, Fischer S, Adkins RS, Aldridge AI, et al. A transcriptomic and epigenomic cell atlas of the mouse primary motor cortex. Nature. 2021;598(7879):103–10.
111. O'Rourke M, Cullen CL, Auderset L, Pitman KA, Achatz D, Gasperini R, et al. Evaluating Tissue-Specific Recombination in a Pdgfralpha-CreERT2 Transgenic Mouse Line. PLoS One. 2016;11(9):e0162858.
112. Tripathi RB, Rivers LE, Young KM, Jamen F, Richardson WD. NG2 glia generate new oligodendrocytes but few astrocytes in a murine experimental autoimmune encephalomyelitis model of demyelinating disease. J Neurosci. 2010;30(48):16383–90.
113. Thompson PM, Jahanshad N, Ching CRK, Salminen LE, Thomopoulos SI, Bright J, et al. ENIGMA and global neuroscience: A decade of large-scale studies of the brain in health and disease across more than 40 countries. Transl Psychiatry. 2020;10(1):100.
114. Kochunov P, Hong LE, Dennis EL, Morey RA, Tate DF, Wilde EA, et al. ENIGMA-DTI: Translating reproducible white matter deficits into personalized vulnerability metrics in cross-diagnostic psychiatric research. Hum Brain Mapp. 2020;43(1):194–206.
115. Koshiyama D, Fukunaga M, Okada N, Morita K, Nemoto K, Usui K, et al. White matter microstructural alterations across four major psychiatric disorders: mega-analysis study in 2937 individuals. Mol Psychiatry. 2020;25(4):883–95.
116. Kelly S, Jahanshad N, Zalesky A, Kochunov P, Agartz I, Alloza C, et al. Widespread white matter microstructural differences in schizophrenia across 4322 individuals: results from the ENIGMA Schizophrenia DTI Working Group. Mol Psychiatry. 2018;23(5):1261–9.
117. Villalon-Reina JE, Martinez K, Qu X, Ching CRK, Nir TM, Kothapalli D, et al. Altered white matter microstructure in 22q11.2 deletion syndrome: a multisite diffusion tensor imaging study. Mol Psychiatry. 2020;25(11):2818–31.
118. Ching CRK, Gutman BA, Sun D, Villalon Reina J, Ragothaman A, Isaev D, et al. Mapping Subcortical Brain Alterations in 22q11.2 Deletion Syndrome: Effects of Deletion Size and Convergence With Idiopathic Neuropsychiatric Illness. Am J Psychiatry. 2020;177(7):589–600.
119. Sun D, Ching CRK, Lin A, Forsyth JK, Kushan L, Vajdi A, et al. Large-scale mapping of cortical alterations in 22q11.2 deletion syndrome: Convergence with idiopathic psychosis and effects of deletion size. Mol Psychiatry. 2020;25(8):1822–34.
120. Sonderby IE, Ching CRK, Thomopoulos SI, van der Meer D, Sun D, Villalon-Reina JE, et al. Effects of copy number variations on brain structure and risk for psychiatric illness: Large-scale studies from the ENIGMA working groups on CNVs. Hum Brain Mapp. 2021.

1160

1161 **Figure 1**

1162

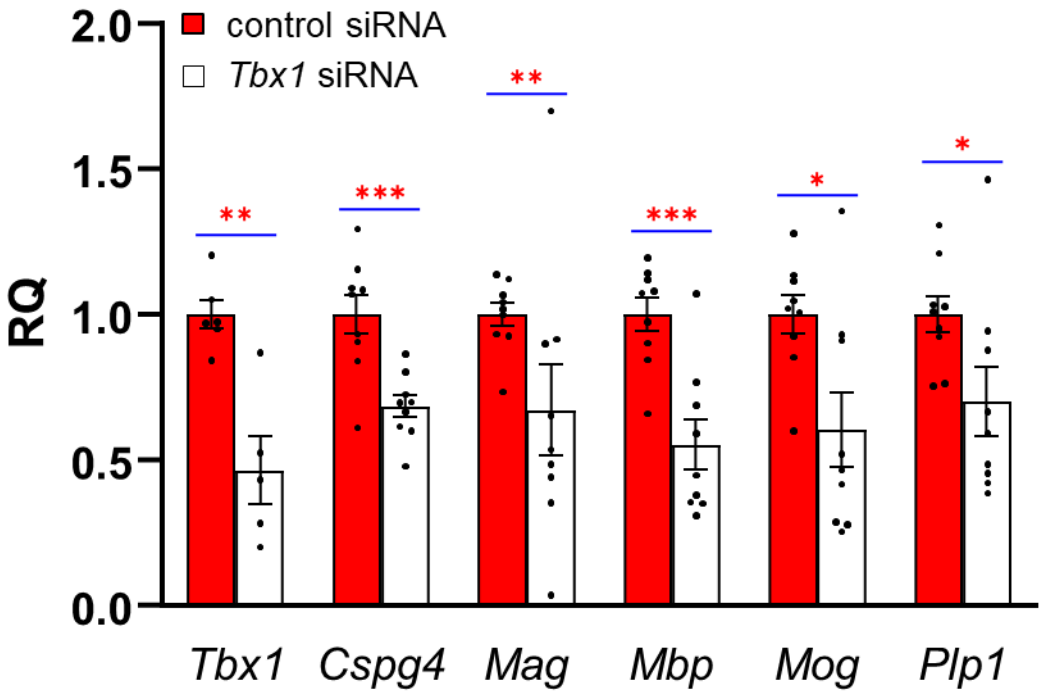

1163

1164

1165 **Figure 2**

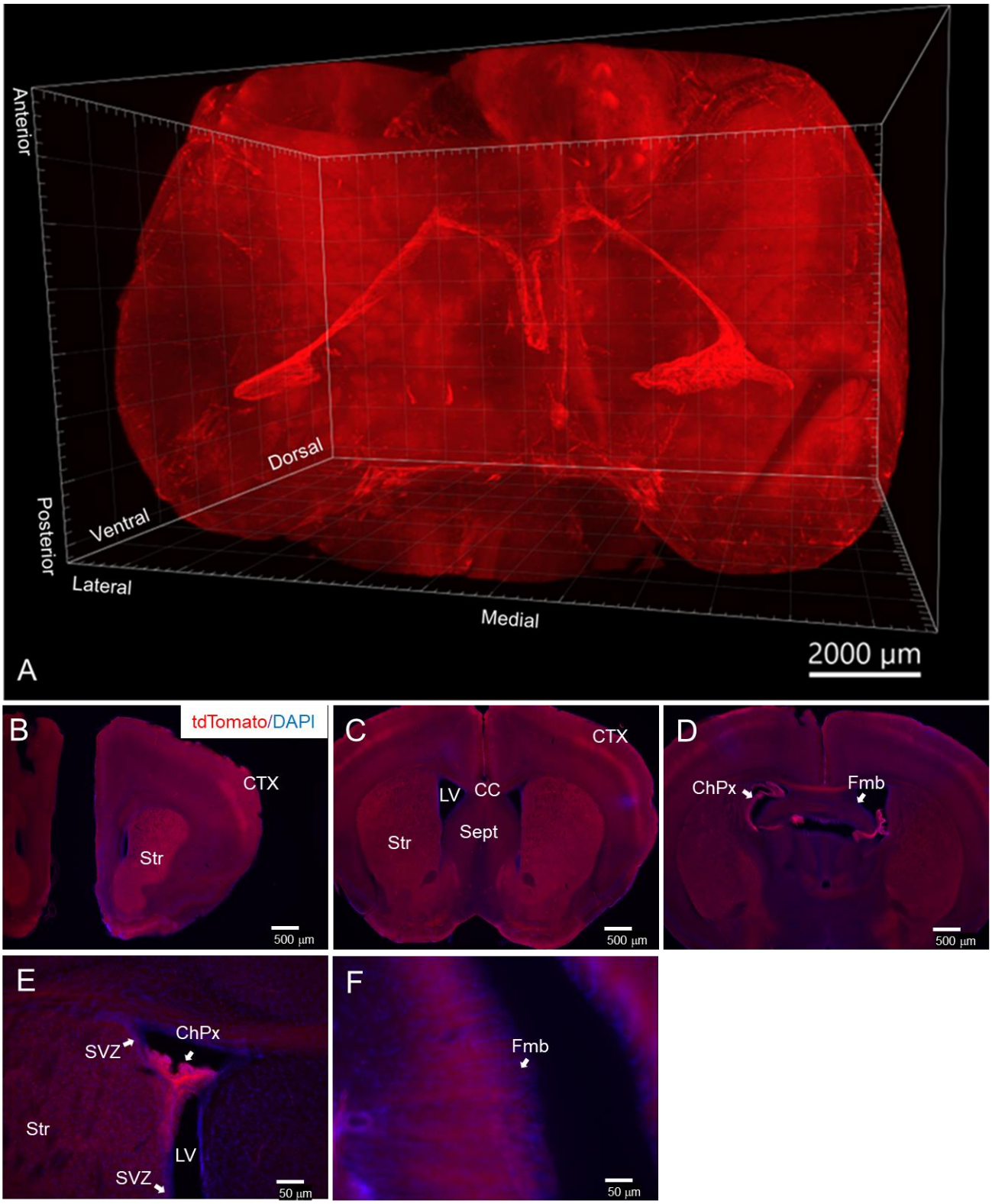

1166

1167

1168

Figure 3

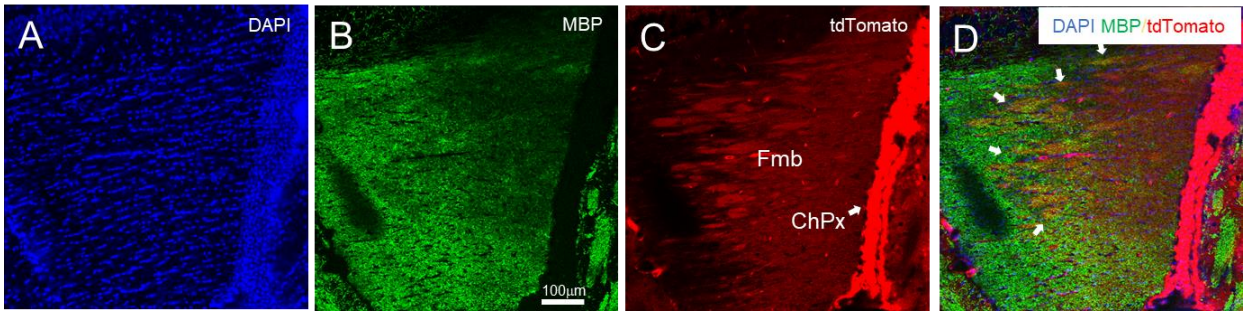

1194 **Figure 4**

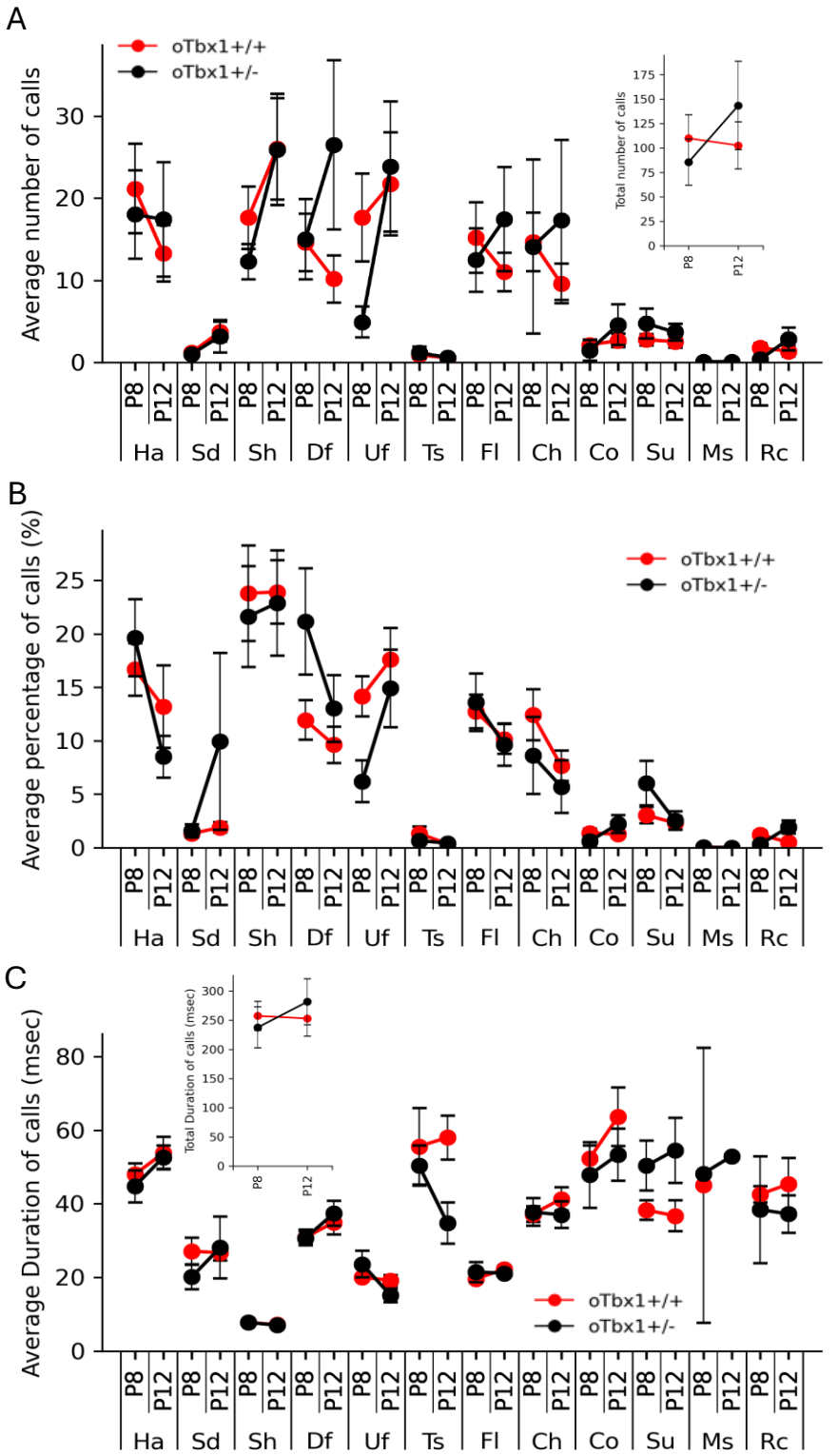

Figure 5

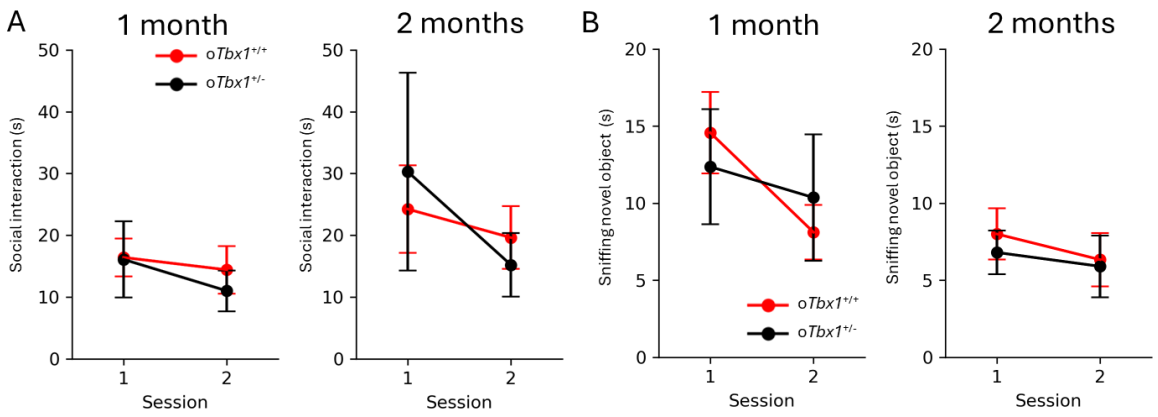

Figure 6

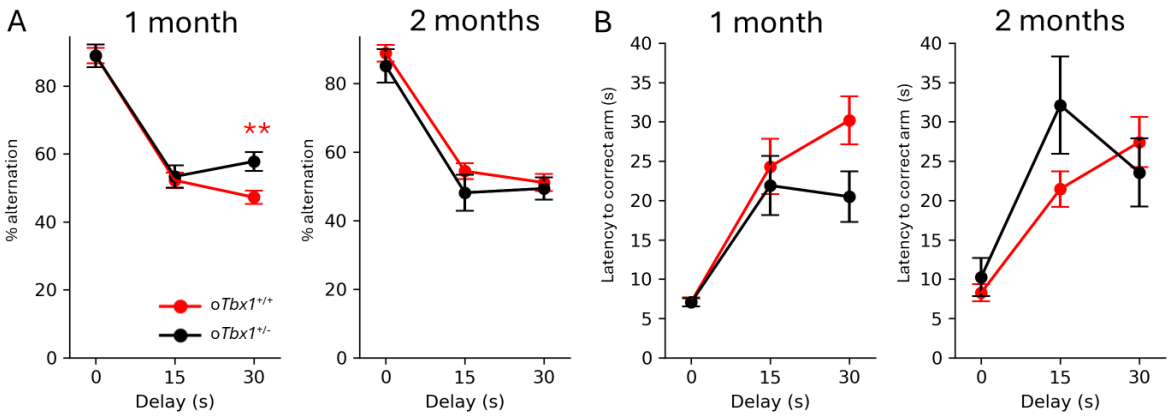

Figure 7

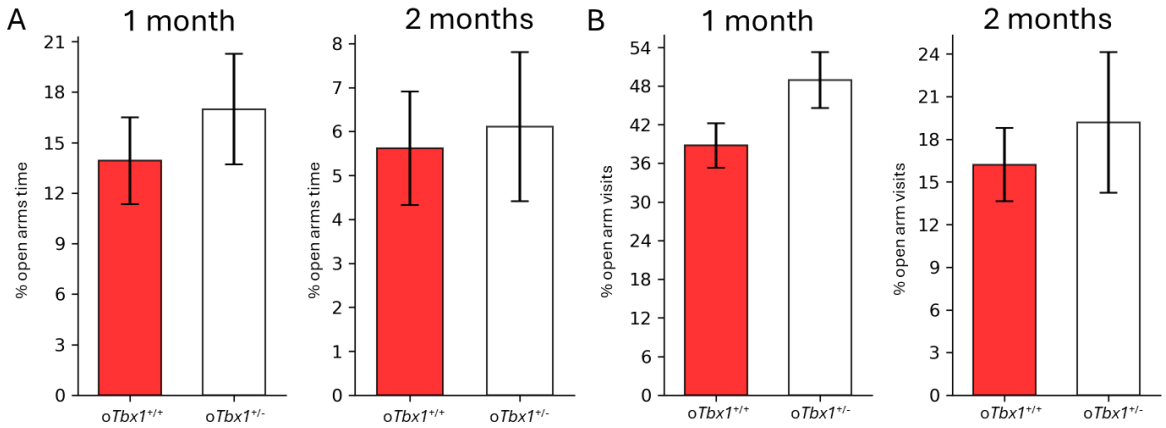

1204 **Figure 8**

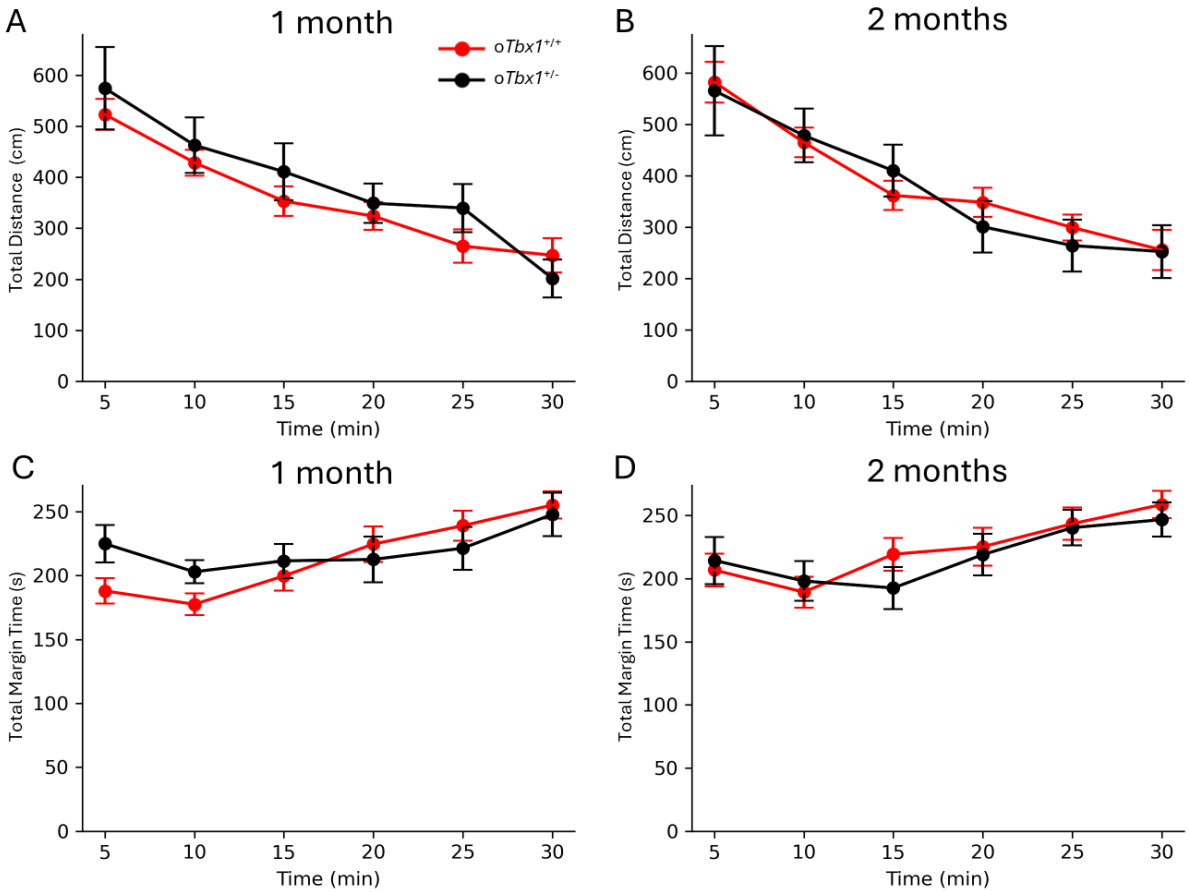

1205

1206

1207

1208

1209

1210

1211

1212

1213

1214

1215

1216

1217

1218

1219 **Figure 9**

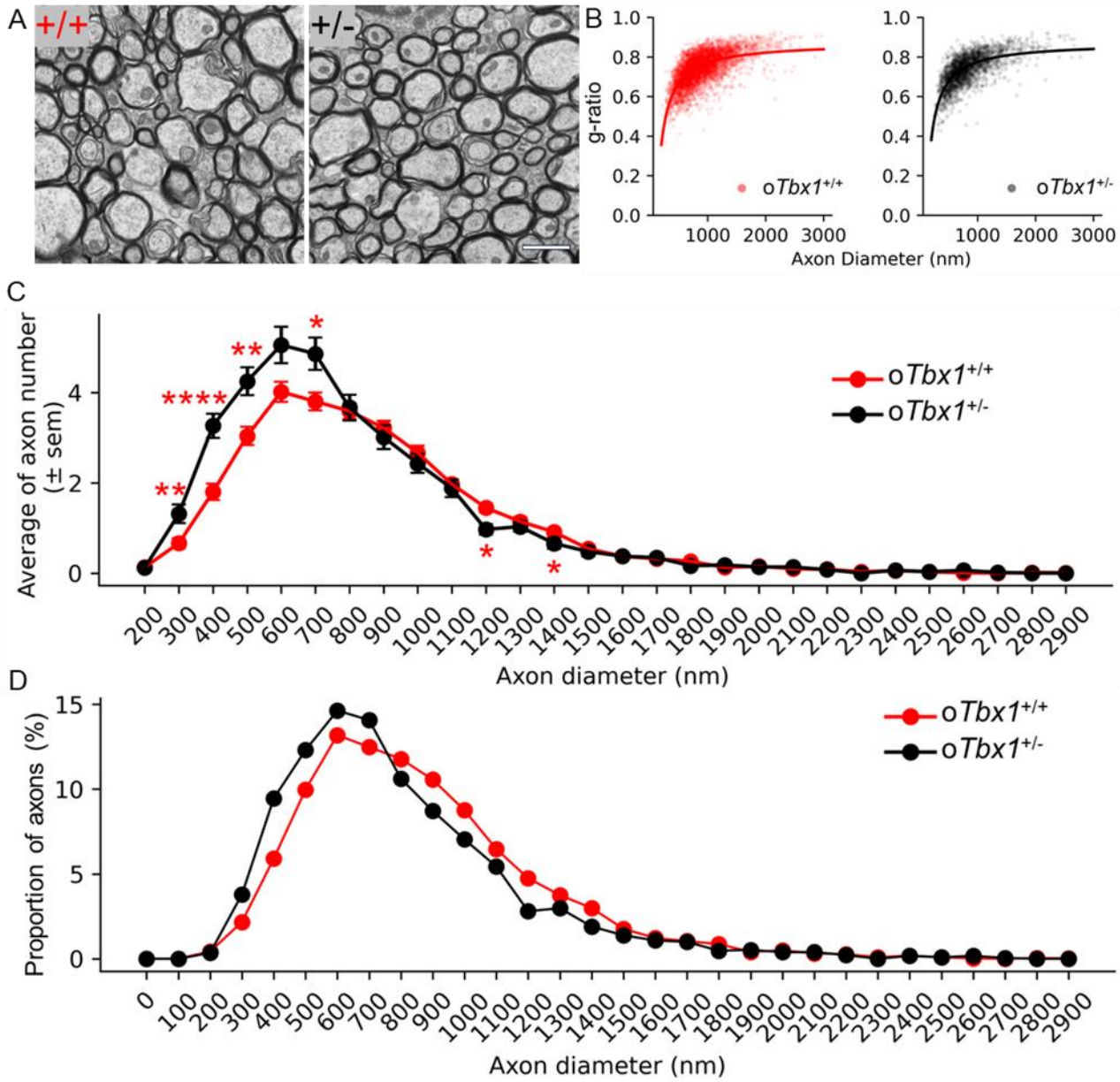

1220

1221

1222 **Supplementary Information**

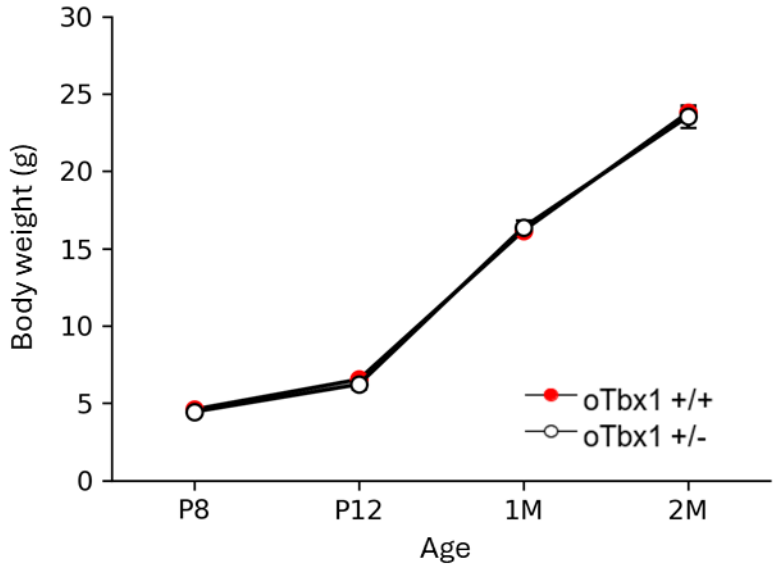

1223

1224 **Figure S1.** Body weights o*Tbx1*$^{+/+}$ and o*Tbx1*$^{+/-}$ mice. o*Tbx1*$^{+/+}$ and o*Tbx1*$^{+/-}$ mice had
1225 indistinguishable body weight increases from P8 to 2 months of age (P8, U = 140, p = 0.800;
1226 P12, U = 153, p = 0.466; 1 month, U = 135.5, p = 0.7035; 2 months, U = 102, p = 0.917).
1227 o*Tbx1*$^{+/+}$ P8, N = 27, P12; N = 30; 1M, 1 month, N = 27; 2M, 2 months, N = 21: o*Tbx1*$^{+/-}$: P8, N
1228 = 11, P12, N = 12; 1M, N = 11; 2M, N = 10.

1229

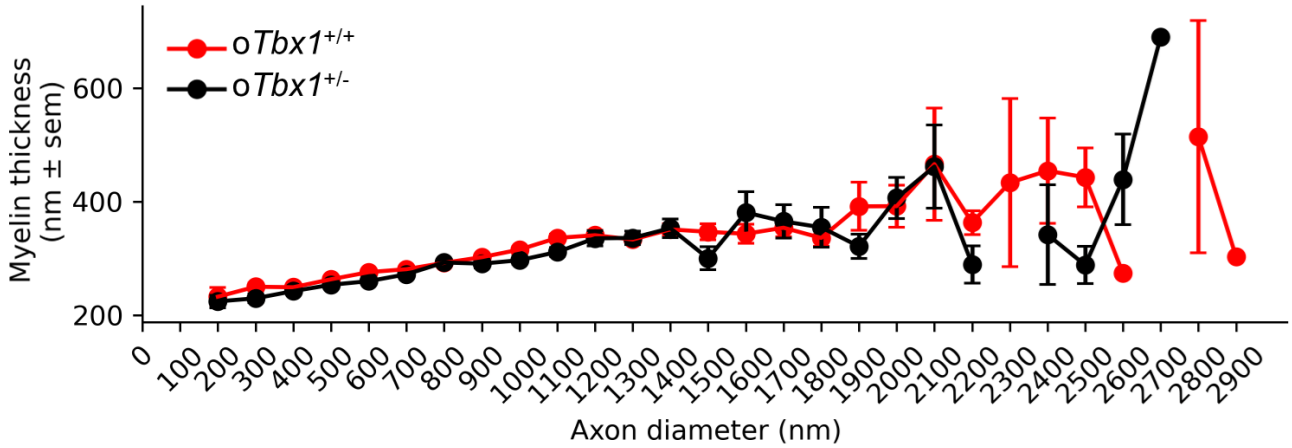

1230
1231 **Supplementary Figure S2.** The myelin thickness of axons for o*Tbx1*$^{+/-}$ versus o*Tbx1*$^{+/+}$ mice
1232 versus axon diameter was similar along the axon diameter range (genotype, p = 0.931;
1233 genotype × axon diameter, p = 0.814).
1234

							Shapiro-Wilk Test				Levene's Test			
Figure	Control Gene	Gene	Treatment	# of Samples	Average	s.e.m	Statistic	p_value	p_adj (FDR BH)	Reject (FDR5%)	Statistic	p_value	p_adj (FDR BH)	Reject (FDR5%)
Figure 1	Pgk1	Tbx1	control siRNA	6	1	0.049186162	0.93572346	0.624966577	0.805579616	FALSE	1.758766194	0.21744683	0.297607562	FALSE
			Tbx1 siRNA	5	0.464725499	0.116052639	0.932068851	0.610545167	0.805579616	FALSE				
		Cspg4	control siRNA	9	1	0.066746189	0.960660226	0.805205712	0.878406231	FALSE	1.522725608	0.235026707	0.297607562	FALSE
			Tbx1 siRNA	9	0.685034037	0.037803054	0.980712867	0.967840714	0.967840714	FALSE				
		MAG	control siRNA	9	1	0.041029197	0.908420558	0.304976014	0.731942433	FALSE	3.473378198	0.080821307	0.297607562	FALSE
			Tbx1 siRNA	9	0.670998004	0.157173093	0.903392871	0.272326671	0.731942433	FALSE				
		MBP	control siRNA	9	1	0.056959774	0.921773656	0.40712653	0.805579616	FALSE	0.679262555	0.421957432	0.421957432	FALSE
			Tbx1 siRNA	9	0.553891554	0.084308916	0.872112121	0.129519549	0.518078195	FALSE				
		MOG	control siRNA	9	1	0.064281655	0.948291674	0.671316347	0.805579616	FALSE	1.89729647	0.18734571	0.297607562	FALSE
			Tbx1 siRNA	9	0.60385684	0.126671201	0.85412067	0.082708168	0.496249006	FALSE				
		Plp1	control siRNA	9	1	0.06060843	0.939293908	0.574485759	0.805579616	FALSE	1.437463429	0.248006301	0.297607562	FALSE
			Tbx1 siRNA	9	0.700871358	0.116118855	0.84502056	0.065659769	0.496249006	FALSE				
	18S	Tbx1	control siRNA	6	1	0.078568382	0.92617953	0.550937859	0.734583812	FALSE	0.009347636	0.925096749	0.925096749	FALSE
			Tbx1 siRNA	5	0.440976588	0.066877094	0.97650378	0.915107555	0.915107555	FALSE				
		Cspg4	control siRNA	9	1	0.044646855	0.916096471	0.360902781	0.662239178	FALSE	0.016880314	0.898245734	0.925096749	FALSE
			Tbx1 siRNA	9	0.687687722	0.045939538	0.919279302	0.386306187	0.662239178	FALSE				
		MAG	control siRNA	9	1	0.055152176	0.966495138	0.863205301	0.915107555	FALSE	1.450912436	0.24589768	0.643468053	FALSE
			Tbx1 siRNA	9	0.642342516	0.157925591	0.844966625	0.065569561	0.242978818	FALSE				
		MBP	control siRNA	9	1	0.053726606	0.931315789	0.493974756	0.734583812	FALSE	0.206705208	0.655469861	0.925096749	FALSE
			Tbx1 siRNA	9	0.544403139	0.082596116	0.85329064	0.080992939	0.242978818	FALSE				
		MOG	control siRNA	9	1	0.06650766	0.957538993	0.772242353	0.915107555	FALSE	1.178141059	0.293818671	0.643468053	FALSE
			Tbx1 siRNA	9	0.588913841	0.123648773	0.841639086	0.060228776	0.242978818	FALSE				
		Plp1	control siRNA	9	1	0.04046838	0.874188469	0.136290611	0.327097466	FALSE	1.045606567	0.321734027	0.643468053	FALSE
			Tbx1 siRNA	9	0.692323814	0.117369849	0.755073552	0.00620775	0.074492996	FALSE				

Linear Mixed Model				
Source	F	df1	df2	Sig.
Corrected Model	2.006348255	11	89	0.03681448
Gene	0.843979959	5	89	0.52216149
Treatment	14.66501979	1	89	0.00023857
Gene * Treatment	0.843979957	5	89	0.522161492
Corrected Model	2.450555968	11	89	0.010091634
Gene	1.101427491	5	89	0.365404553
Treatment	17.51187144	1	89	6.68502E-05
Gene * Treatment	1.101427494	5	89	0.365404552

Mann Whitney U Test						
Sample 1	Sample 2	Statistic	R (Z score)	p_value	p_adj (FDR BH)	Reject (FDR5%)
control siRNA	Tbx1 siRNA	7	0.50847518	0.008658009	0.012987013	TRUE
control siRNA	Tbx1 siRNA	8	0.676423086	0.002756067	0.008268202	TRUE
control siRNA	Tbx1 siRNA	11	0.613984032	0.007774578	0.012987013	TRUE
control siRNA	Tbx1 siRNA	6	0.718049122	0.00123406	0.00740436	TRUE
control siRNA	Tbx1 siRNA	14	0.551544978	0.018757713	0.018757713	TRUE
control siRNA	Tbx1 siRNA	14	0.551544978	0.018757713	0.018757713	TRUE
control siRNA	Tbx1 siRNA	6	0.554700196	0.004329004	0.007774578	TRUE
control siRNA	Tbx1 siRNA	4	0.759675158	0.000493624	0.002961744	TRUE
control siRNA	Tbx1 siRNA	11	0.613984032	0.007774578	0.007774578	TRUE
control siRNA	Tbx1 siRNA	7	0.697236104	0.00185109	0.00555327	TRUE
control siRNA	Tbx1 siRNA	11	0.613984032	0.007774578	0.007774578	TRUE
control siRNA	Tbx1 siRNA	11	0.613984032	0.007774578	0.007774578	TRUE

Figure	Measurement	Call type	PND	Genotype	# of Samples	Average	s.e.m	Shapiro-Wilk test Statistic	p_value	p_adj(FDR BH)	Rejects(FDR 5%)	Levene test Statistic	df1	df2	p_value	p_adj(FDR BH)	Rejects(FDR 5%)
Figure 4A	Number	Harmonics	P8	oTbx1+/+	27	25.44444444	6.455928465	0.734571278	1.2196E-05	2.54525E-05	TRUE	0.588767426	1	36	0.447899604	0.866000524	FALSE
				oTbx1+/-	11	18	5.412107639	0.869194567	0.075694919	0.082576275	FALSE						
			P12	oTbx1+/+	30	18.53333333	4.41620145	0.769232988	1.89257E-05	3.63374E-05	TRUE	0.080099472	1	40	0.778622211	0.866000524	FALSE
				oTbx1+/-	12	17.41666667	6.962516888	0.741135657	0.002162845	0.002883793	TRUE						
		step_down	P8	oTbx1+/+	27	1.518518519	0.424902772	0.641833842	6.62769E-07	2.65108E-06	TRUE	0.588478181	1	36	0.448010251	0.866000524	FALSE
				oTbx1+/-	11	1	0.301511345	0.863411665	0.063748829	0.071161484	FALSE						
			P12	oTbx1+/+	30	3.866666667	1.062131162	0.71998024	3.08876E-06	8.23669E-06	TRUE	0.194362482	1	40	0.661683974	0.866000524	FALSE
				oTbx1+/-	12	3.166666667	1.953370565	0.517821491	2.3982E-05	4.42745E-05	TRUE						
		short	P8	oTbx1+/+	27	19.92592593	3.665472193	0.834571779	0.000578805	0.000817137	TRUE	3.769928996	1	36	0.060039818	0.866000524	FALSE
				oTbx1+/-	11	12.27272727	2.157822594	0.916108012	0.287544787	0.287544787	FALSE						
			P12	oTbx1+/+	30	27.53333333	5.654971027	0.831702948	0.000262676	0.000394014	TRUE	0.789588022	1	40	0.379537318	0.866000524	FALSE
				oTbx1+/-	12	25.91666667	6.770544866	0.883340597	0.096735299	0.098793496	FALSE						
		down_fm	P8	oTbx1+/+	27	17.40740741	3.629280755	0.831780851	0.000512651	0.000745674	TRUE	0.289267018	1	36	0.594000243	0.866000524	FALSE
				oTbx1+/-	11	15	4.872930796	0.815746427	0.01516132	0.017749838	TRUE						
			P12	oTbx1+/+	30	14.46666667	3.822418243	0.713233709	2.44507E-06	6.90372E-06	TRUE	1.591281097	1	40	0.214450379	0.866000524	FALSE
				oTbx1+/-	12	26.5	10.29599805	0.770105839	0.004369121	0.005242945	TRUE						
		up_fm	P8	oTbx1+/+	27	17.7037037	4.965641153	0.629247069	4.62791E-07	2.46822E-06	TRUE	2.477639992	1	36	0.124223918	0.866000524	FALSE
				oTbx1+/-	11	4.909090909	1.889947308	0.722703338	0.000918243	0.001259304	TRUE						
			P12	oTbx1+/+	30	27.83333333	7.521934719	0.702088237	1.6735E-06	5.35522E-06	TRUE	0.168045902	1	40	0.684041632	0.866000524	FALSE
				oTbx1+/-	12	23.83333333	7.906492665	0.838153899	0.026294718	0.030051106	TRUE						
		two_steps	P8	oTbx1+/+	27	1	0.301940542	0.694654405	3.26996E-06	8.26094E-06	TRUE	0.0764692	1	36	0.783722016	0.866000524	FALSE
				oTbx1+/-	11	1.181818182	0.723855609	0.571349978	1.12326E-05	2.45076E-05	TRUE						
			P12	oTbx1+/+	30	0.7	0.215225089	0.653556228	3.51824E-07	2.12738E-06	TRUE	0.113222806	1	40	0.7382634	0.866000524	FALSE
				oTbx1+/-	12	0.583333333	0.192996049	0.768340707	0.004181752	0.005146772	TRUE						
		flat	P8	oTbx1+/+	27	17.7037037	4.250294045	0.742479801	1.6037E-05	3.20739E-05	TRUE	0.680374459	1	36	0.414890086	0.866000524	FALSE
				oTbx1+/-	11	12.45454545	3.866790157	0.875244677	0.090499207	0.094433956	FALSE						
			P12	oTbx1+/+	30	14.86666667	3.159635267	0.817323029	0.000137908	0.000228261	TRUE	0.063139102	1	40	0.802887963	0.866000524	FALSE
				oTbx1+/-	12	17.41666667	6.344239016	0.755882382	0.003080417	0.003891054	TRUE						
		chevron	P8	oTbx1+/+	27	18.11111111	5.570407498	0.636691451	5.71795E-07	2.65108E-06	TRUE	0.0673775	1	36	0.796672834	0.866000524	FALSE
				oTbx1+/-	11	14.09090909	10.5833957	0.4472633	3.54563E-07	2.12738E-06	TRUE						
			P12	oTbx1+/+	30	13.56666667	3.444363489	0.749773264	9.03E-06	2.064E-05	TRUE	0.345282084	1	40	0.560098838	0.866000524	FALSE
				oTbx1+/-	12	17.33333333	9.726045424	0.573818922	6.544E-05	0.000112183	TRUE						
		complex	P8	oTbx1+/+	27	2.592592593	0.879100906	0.63989383	6.26769E-07	2.65108E-06	TRUE	0.506662225	1	36	0.481174865	0.866000524	FALSE
				oTbx1+/-	11	1.454545455	1.267521822	0.409144521	1.25664E-07	1.20637E-06	TRUE						
			P12	oTbx1+/+	30	3.833333333	1.213983027	0.638445973	2.22498E-07	1.77998E-06	TRUE	0.031412363	1	40	0.860217983	0.866000524	FALSE
				oTbx1+/-	12	4.583333333	2.496841439	0.560712337	5.1415E-05	9.14045E-05	TRUE						
		step_up	P8	oTbx1+/+	27	3.703703704	0.802089179	0.813462734	0.000236307	0.000365895	TRUE	0.406675225	1	36	0.527697447	0.866000524	FALSE
				oTbx1+/-	11	4.727272727	1.839421397	0.762873292	0.003061853	0.003891054	TRUE						
			P12	oTbx1+/+	30	3.2	0.848799016	0.710336447	2.21376E-06	6.64128E-06	TRUE	0.034791252	1	40	0.852976553	0.866000524	FALSE
				oTbx1+/-	12	3.666666667	1.0396192	0.877785325	0.082109146	0.087583089	FALSE						
		mult_steps	P8	oTbx1+/+	27	0.074074074	0.051361129	0.29382658	2.32643E-10	5.58344E-09	TRUE	0.028883184	1	36	0.866000524	0.866000524	FALSE
				oTbx1+/-	11	0.090909091	0.090909091	0.344991028	2.2434E-08	2.69208E-07	TRUE						
			P12	oTbx1+/+	30	0.066666667	0.046320556	0.275375307	4.40171E-11	2.11282E-09	TRUE	0.03421728	1	40	0.854180142	0.866000524	FALSE
				oTbx1+/-	12	0.083333333	0.083333333	0.326927483	1.20728E-06	4.13925E-06	TRUE						
		rev_chevron	P8	oTbx1+/+	27	1.592592593	0.475194545	0.708100617	5.03586E-06	1.20861E-05	TRUE	2.543697003	1	36	0.119478121	0.866000524	FALSE
				oTbx1+/-	11	0.363636364	0.278721995	0.47351861	7.28965E-07	2.69156E-06	TRUE						
			P12	oTbx1+/+	30	2.133333333	0.97052342	0.474628329	2.91922E-09	4.67076E-08	TRUE	0.044048453	1	40	0.834828853	0.866000524	FALSE
				oTbx1+/-	12	2.833333333	1.407950011	0.621079922	0.000161712	0.000258739	TRUE						

Linear Mixed Model

Source	F	df1	df2	Sig.
Corrected Model	6.94053254	47	912	0
Genotype	0.196622137	1	912	0.657566457
PND	6.147480911	1	912	0.013339656
Call type	19.63969375	11	912	0
Genotype * PND	4.835206967	1	912	0.028134731
PND * Call type	1.728524601	11	912	0.062712426
Call type * Genotype	0.707710242	11	912	0.731986987
Genotype * PND * Call type	0.368631844	11	912	0.967949606

Mann-Witney U test

Sample1	Sample2	Statistic	R (Z score)	p_value	p_adj(FDR BH)	Rejects(FDR 5%)
oTbx1+/+	oTbx1+/-	139	0.049603452	0.775387862	0.990742675	FALSE
oTbx1+/+	oTbx1+/-	180	0	1	1	FALSE
oTbx1+/+	oTbx1+/-	140	0.044382036	0.799797921	0.990742675	FALSE
oTbx1+/+	oTbx1+/-	174	0.025776963	0.879981095	0.990742675	FALSE
oTbx1+/+	oTbx1+/-	121	0.14358894	0.390409044	0.990742675	FALSE
oTbx1+/+	oTbx1+/-	168.5	-0.049405846	0.773086018	0.990742675	FALSE
oTbx1+/+	oTbx1+/-	145.5	0.015664248	0.949461731	0.990742675	FALSE
oTbx1+/+	oTbx1+/-	148.5	-0.135329056	0.400911456	0.990742675	FALSE
oTbx1+/+	oTbx1+/-	87	0.321117085	0.048527629	0.990742675	FALSE
oTbx1+/+	oTbx1+/-	175	-0.021480803	0.901682953	0.990742675	FALSE
oTbx1+/+	oTbx1+/-	141.5	0.036549912	0.849168654	0.990742675	FALSE
oTbx1+/+	oTbx1+/-	165	-0.064442408	0.690391077	0.990742675	FALSE
oTbx1+/+	oTbx1+/-	133	0.080931948	0.634139425	0.990742675	FALSE
oTbx1+/+	oTbx1+/-	170.5	-0.040813525	0.815460496	0.990742675	FALSE
oTbx1+/+	oTbx1+/-	110.5	0.198413808	0.237616458	0.990742675	FALSE
oTbx1+/+	oTbx1+/-	160	0.08592321	0.591959808	0.990742675	FALSE
oTbx1+/+	oTbx1+/-	112	0.190581684	0.250721045	0.990742675	FALSE
oTbx1+/+	oTbx1+/-	161.5	-0.07947897	0.630588582	0.990742675	FALSE
oTbx1+/+	oTbx1+/-	140	-0.044382036	0.799797921	0.990742675	FALSE
oTbx1+/+	oTbx1+/-	154.5	-0.109552093	0.50033814	0.990742675	FALSE
oTbx1+/+	oTbx1+/-	146	-0.01305354	0.949461731	0.990742675	FALSE
oTbx1+/+	oTbx1+/-	177	-0.012888482	0.945286072	0.990742675	FALSE
oTbx1+/+	oTbx1+/-	104.5	0.229742304	0.168812806	0.990742675	FALSE
oTbx1+/+	oTbx1+/-	123	-0.24488115	0.116641288	0.990742675	FALSE

Figure	Measurement	Call type	PND	Genotype	# of Samples	Average	s.e.m	Shapiro-Wilk test Statistic	p_value	p_adj(FDR BH)	Rejects(FDR 5%)	Levene test Statistic	df1	df2	p_value	p_adj(FDR BH)	Rejects(FDR 5%)
Figure 4A	Number	All	P8	oTbx1+/+	27	126.7777778	26.50132144	0.78554976	7.77043E-05	0.000157208	TRUE	1.121799982	1	36	0.296586227	0.593172454	FALSE
				oTbx1+/-	11	85.54545455	23.66407467	0.834964693	0.027126787	0.027126787	TRUE						
			P12	oTbx1+/+	30	130.6	27.57400075	0.804300725	7.86042E-05	0.000157208	TRUE	0.000269074	1	40	0.98699405	0.98699405	FALSE
				oTbx1+/-	12	143.3333333	45.18922058	0.79983592	0.009328736	0.012438315	TRUE						

Linear Mixed Model

Source	F	df1	df2	Sig.
Corrected Model	0.636064898	3	76	0.59407046
Genotype	0.155970557	1	76	0.693999978
PND	1.419833311	1	76	0.237138636
Genotype * PND	1.103292412	1	76	0.296873255

Mann-Witney U test

Sample1	Sample2	Statistic	R (Z score)	p_value	p_adj(FDR BH)	Rejects(FDR 5%)
oTbx1+/+	oTbx1+/-	126.5	0.114871152	0.504762746	0.73135923	FALSE
oTbx1+/+	oTbx1+/-	166.5	-0.057998167	0.73135923	0.73135923	FALSE

Measurement	Call type	PND	Genotype	# of samples	Average	s.e.m	Shapiro-Wilk test Statistic	p_value	p_adj(FDR BH)	Rejects(FDR 5%)	Levene's test Statistic	df1	df2	p_value	p_adj(FDR BH)	Rejects(FDR 5%)
Number	Harmonics	P8	PdgfraCre;Tbx1+/+	8	9.625	2.672194791	0.919298375	0.42419617	0.449148886	FALSE	1.65961678	2	24	0.211306457	0.559313096	FALSE
			WT;Tbx1+/flox	8	18.125	11.96786993	0.59934529	0.000156224	0.000749877	TRUE						
			WT;Tbx1+/+	11	42.27272727	11.79066727	0.863657084	0.064216294	0.087237229	FALSE						
		P12	PdgfraCre;Tbx1+/+	9	11.22222222	7.025306988	0.600651882	9.73774E-05	0.000539321	TRUE	1.158509452	2	27	0.329073887	0.559313096	FALSE
			WT;Tbx1+/flox	9	11.66666667	5.525194818	0.765487459	0.008192575	0.016093411	TRUE						
			WT;Tbx1+/+	12	29.16666667	8.235946095	0.864345385	0.055433248	0.076753728	FALSE						
		step_down	P8	PdgfraCre;Tbx1+/+	8	0.875	0.295048422	0.835213557	0.067235843	0.08964779	FALSE	1.361546454	2	24	0.275355808	0.559313096	FALSE
			WT;Tbx1+/flox	8	1	0.377964473	0.859949135	0.119934837	0.146361157	FALSE						
			WT;Tbx1+/+	11	2.363636364	0.956059405	0.720871942	0.000869463	0.002504053	TRUE						
		P12	PdgfraCre;Tbx1+/+	9	0.888888889	0.611111111	0.570366044	4.29426E-05	0.000281079	TRUE	2.413977888	2	27	0.108515742	0.559313096	FALSE
			WT;Tbx1+/flox	9	5.111111111	2.6793679	0.695406931	0.001254342	0.003473563	TRUE						
			WT;Tbx1+/+	12	5.166666667	1.565892781	0.863856	0.054652247	0.076753728	FALSE						
		short	P8	PdgfraCre;Tbx1+/+	8	15.125	4.834539053	0.867444039	0.142278889	0.165227097	FALSE	1.622768353	2	24	0.218268212	0.559313096	FALSE
			WT;Tbx1+/flox	8	13.25	4.087218754	0.849020808	0.093116392	0.117620706	FALSE						
			WT;Tbx1+/+	11	28.27272727	7.311374587	0.875466193	0.091090759	0.11711669	FALSE						
		P12	PdgfraCre;Tbx1+/+	9	13	3.905124838	0.914834887	0.351194856	0.383121661	FALSE	2.151774119	2	27	0.135799339	0.559313096	FALSE
			WT;Tbx1+/flox	9	33.33333333	13.89844116	0.807207052	0.024673587	0.039477739	TRUE						
			WT;Tbx1+/+	12	34.08333333	8.745958663	0.909009298	0.207195733	0.22950912	FALSE						
		down_fm	P8	PdgfraCre;Tbx1+/+	8	9.5	3.212698021	0.861074309	0.123069142	0.14768297	FALSE	1.921139644	2	24	0.168297426	0.559313096	FALSE
			WT;Tbx1+/flox	8	11.75	5.456810947	0.738429175	0.006078749	0.012504854	TRUE						
			WT;Tbx1+/+	11	27.27272727	6.85842668	0.884384045	0.118227917	0.146361157	FALSE						
		P12	PdgfraCre;Tbx1+/+	9	12.88888889	9.075982415	0.490677123	4.96662E-06	5.95994E-05	TRUE	0.180736373	2	27	0.835656843	0.911625647	FALSE
			WT;Tbx1+/flox	9	12.22222222	5.484264809	0.778607516	0.011607818	0.021429818	TRUE						
			WT;Tbx1+/+	12	17.33333333	5.805344107	0.805205856	0.010743424	0.020355961	TRUE						
		up_fm	P8	PdgfraCre;Tbx1+/+	8	10.375	4.788145704	0.799663368	0.028388995	0.044238038	TRUE	1.244964464	2	24	0.305890073	0.559313096	FALSE
			WT;Tbx1+/flox	8	9.875	3.026298423	0.916331725	0.400811221	0.430722507	FALSE						
			WT;Tbx1+/+	11	28.72727273	10.97773856	0.713897791	0.000706475	0.002248161	TRUE						
		P12	PdgfraCre;Tbx1+/+	9	10.11111111	7.091552965	0.529781177	1.43217E-05	0.000128896	TRUE	1.093047307	2	27	0.349570685	0.559313096	FALSE
			WT;Tbx1+/flox	9	36.44444444	15.59479179	0.765842027	0.008270225	0.016093411	TRUE						
			WT;Tbx1+/+	12	34.66666667	13.49485499	0.683792344	0.000590864	0.00202582	TRUE						
		two_steps	P8	PdgfraCre;Tbx1+/+	8	0.125	0.125	0.418398447	1.04723E-06	1.88502E-05	TRUE	2.325091481	2	24	0.119400488	0.559313096	FALSE
			WT;Tbx1+/flox	8	0.75	0.411877236	0.724167693	0.004213657	0.009480728	TRUE						
			WT;Tbx1+/+	11	1.818181818	0.600275419	0.82936025	0.022898111	0.037469637	TRUE						
		P12	PdgfraCre;Tbx1+/+	9	0.333333333	0.333333333	0.389841298	3.21749E-07	1.1583E-05	TRUE	0.817105263	2	27	0.452335248	0.603113664	FALSE
			WT;Tbx1+/flox	9	0.666666667	0.333333333	0.710163506	0.001864999	0.00497333	TRUE						
			WT;Tbx1+/+	12	1	0.40824829	0.7517227	0.002785506	0.006907527	TRUE						
		flat	P8	PdgfraCre;Tbx1+/+	8	11.875	3.656879525	0.882816897	0.200332641	0.225374222	FALSE	3.818027267	2	24	0.036336836	0.559313096	FALSE
			WT;Tbx1+/flox	8	6.375	2.744718955	0.801139132	0.029440249	0.044238038	TRUE						
			WT;Tbx1+/+	11	30.18181818	8.790302696	0.855776158	0.050750623	0.073080898	FALSE						
		P12	PdgfraCre;Tbx1+/+	9	9.444444444	5.283914561	0.634351254	0.000241961	0.001024778	TRUE	0.955031557	2	27	0.39741914	0.59612871	FALSE
			WT;Tbx1+/flox	9	12.44444444	4.972454991	0.834538536	0.05019806	0.073080898	FALSE						
			WT;Tbx1+/+	12	20.75	5.615353682	0.900674282	0.161829723	0.184948255	FALSE						
		chevron	P8	PdgfraCre;Tbx1+/+	8	11.375	5.990878483	0.735010786	0.005568815	0.011968073	TRUE	0.858879466	2	24	0.436252017	0.603113664	FALSE
			WT;Tbx1+/flox	8	9	6.059231446	0.550872664	4.19244E-05	0.000281079	TRUE						
			WT;Tbx1+/+	11	29.63636364	11.76610906	0.702313085	0.000500922	0.00180332	TRUE						
		P12	PdgfraCre;Tbx1+/+	9	11.22222222	7.827618088	0.560909917	3.32517E-05	0.000266014	TRUE	0.058536613	2	27	0.943263064	0.984274502	FALSE
			WT;Tbx1+/flox	9	13.22222222	5.340562231	0.814027777	0.029492025	0.044238038	TRUE						
			WT;Tbx1+/+	12	15.58333333	5.334931105	0.817775681	0.015028138	0.025762523	TRUE						
		complex	P8	PdgfraCre;Tbx1+/+	8	1.5	1	0.604228412	0.000178175	0.000801786	TRUE	1.111310057	2	24	0.345479196	0.559313096	FALSE
			WT;Tbx1+/flox	8	1.625	0.80039053	0.783670395	0.019092425	0.031968712	TRUE						
			WT;Tbx1+/+	11	4.090909091	1.928044442	0.714449593	0.000718163	0.002248161	TRUE						
		P12	PdgfraCre;Tbx1+/+	9	3.888888889	3.405242871	0.451702288	1.72645E-06	2.48608E-05	TRUE	0.013210185	2	27	0.986883061	0.986883061	FALSE
			WT;Tbx1+/flox	9	4	1.795054936	0.783337582	0.013157116	0.023682808	TRUE						
			WT;Tbx1+/+	12	3.666666667	1.275250025	0.815437471	0.014110863	0.024780053	TRUE						
		step_up	P8	PdgfraCre;Tbx1+/+	8	3.625	1.450831043	0.863678426	0.130614865	0.154168365	FALSE	0.399734807	2	24	0.674879426	0.809855311	FALSE
			WT;Tbx1+/flox	8	2.75	1.12994943	0.840049789	0.075410948	0.098719786	FALSE						
			WT;Tbx1+/+	11	4.454545455	1.503714409	0.760819461	0.002878136	0.006907527	TRUE						
		P12	PdgfraCre;Tbx1+/+	9	2.555555556	1.415304356	0.615640291	0.00014599	0.000749877	TRUE	1.307144496	2	27	0.287172685	0.559313096	FALSE
			WT;Tbx1+/flox	9	1.333333333	0.600925213	0.724908399	0.002770316	0.006907527	TRUE						
			WT;Tbx1+/+	12	5.083333333	1.694278846	0.780364431	0.00565159	0.011968073	TRUE						
		mult_steps	P8	PdgfraCre;Tbx1+/+	8	0	0	1	1	1	FALSE	1.580246914	2	24	0.226612028	0.559313096	FALSE
			WT;Tbx1+/flox	8	0	0	1	1	1	FALSE						
			WT;Tbx1+/+	11	0.181818182	0.121967344	0.485720309	1.02086E-06	1.88502E-05	TRUE						
		P12	PdgfraCre;Tbx1+/+	9	0	0	1	1	1	FALSE	1.62	2	27	0.216549255	0.559313096	FALSE
			WT;Tbx1+/flox	9	0	0	1	1	1	FALSE						
			WT;Tbx1+/+	12	0.166666667	0.112366644	0.464652258	9.81123E-06	0.000100916	TRUE						
		rev_chevron	P8	PdgfraCre;Tbx1+/+	8	1.125	0.548943791	0.641202	0.000479057	0.00180332	TRUE	0.474061795	2	24	0.628174436	0.793483498	FALSE
			WT;Tbx1+/flox	8	2.25	1.264205001	0.722041682	0.003988818	0.009264352	TRUE						
			WT;Tbx1+/+	11	1.454545455	0.651761757	0.720728359	0.000865751	0.002504053	TRUE						
		P12	PdgfraCre;Tbx1+/+	9	2.777777778	2.777777778	0.389841298	3.21749E-07	1.1583E-05	TRUE	0.284466288	2	27	0.754642872	0.862448996	FALSE
			WT;Tbx1+/flox	9	1	0.666666667	0.59916075	9.35316E-05	0.000539321	TRUE						
			WT;Tbx1+/+	12	2.5	1.276239742	0.646609337	0.000270216	0.001080863	TRUE						

Generalized Linear Mixed Model

Source	F	df1	df2	Sig.
Corrected Model	4.565593657	71	612	0
Genotype	2.526849017	2	612	0.080743877
PND	0.381377322	1	612	0.537096747
Call type	18.61506233	11	612	0
Genotype * PND * Call type	1.47748124	57	612	0.015566306

Mann-Whitney's U test

Sample1	Sample2	Statistic	R (Z score)	p_value	p_adj(FDR BH)	Rejects(FDR 5%)
PdgfraCre;Tbx1+/+	WT;Tbx1+/flox	28.5	0.091893381	0.798445998	0.974374778	FALSE
PdgfraCre;Tbx1+/+	WT;Tbx1+/+	15.5	-0.539886352	0.02034876	0.488370247	FALSE
WT;Tbx1+/flox	WT;Tbx1+/+	19	-0.473584519	0.04088275	0.644874038	FALSE
PdgfraCre;Tbx1+/+	WT;Tbx1+/flox	40	-0.010406509	1	1	FALSE
PdgfraCre;Tbx1+/+	WT;Tbx1+/+	32.5	-0.333423509	0.147939986	0.644874038	FALSE
WT;Tbx1+/flox	WT;Tbx1+/+	35	-0.294653333	0.193005137	0.644874038	FALSE
PdgfraCre;Tbx1+/+	WT;Tbx1+/flox	31	-0.026255252	0.959129759	1	FALSE
PdgfraCre;Tbx1+/+	WT;Tbx1+/+	34.5	-0.179962117	0.49202191	0.906204631	FALSE
WT;Tbx1+/flox	WT;Tbx1+/+	35.5	-0.161018736	0.544759334	0.906204631	FALSE
PdgfraCre;Tbx1+/+	WT;Tbx1+/flox	26.5	-0.291382252	0.258083093	0.743019943	FALSE
PdgfraCre;Tbx1+/+	WT;Tbx1+/+	26.5	-0.42647193	0.058483312	0.644874038	FALSE
WT;Tbx1+/flox	WT;Tbx1+/+	47.5	-0.100802456	0.702085531	0.939137333	FALSE
PdgfraCre;Tbx1+/+	WT;Tbx1+/flox	30.5	0.039382877	0.959129759	1	FALSE
PdgfraCre;Tbx1+/+	WT;Tbx1+/+	27	-0.322037473	0.177370273	0.644874038	FALSE
WT;Tbx1+/flox	WT;Tbx1+/+	27.5	-0.312565783	0.206001429	0.644874038	FALSE
PdgfraCre;Tbx1+/+	WT;Tbx1+/flox	33.5	-0.145691126	0.604812834	0.926521789	FALSE
PdgfraCre;Tbx1+/+	WT;Tbx1+/+	34	-0.310161403	0.169421291	0.644874038	FALSE
WT;Tbx1+/flox	WT;Tbx1+/+	46	-0.124064561	0.60159902	0.926521789	FALSE
PdgfraCre;Tbx1+/+	WT;Tbx1+/flox	32	0	1	1	FALSE
PdgfraCre;Tbx1+/+	WT;Tbx1+/+	22	-0.416754377	0.075414781	0.644874038	FALSE
WT;Tbx1+/flox	WT;Tbx1+/+	24.5	-0.369395925	0.1288402	0.644874038	FALSE
PdgfraCre;Tbx1+/+	WT;Tbx1+/flox	37.5	-0.062439054	0.863307281	1	FALSE
PdgfraCre;Tbx1+/+	WT;Tbx1+/+	46.5	-0.116310526	0.651052972	0.937516279	FALSE
WT;Tbx1+/flox	WT;Tbx1+/+	44	-0.155080702	0.507876025	0.906204631	FALSE
PdgfraCre;Tbx1+/+	WT;Tbx1+/flox	28	-0.105021006	0.720901321	0.939137333	FALSE
PdgfraCre;Tbx1+/+	WT;Tbx1+/+	26	-0.340980854	0.151755709	0.644874038	FALSE
WT;Tbx1+/flox	WT;Tbx1+/+	28	-0.303094092	0.206001429	0.644874038	FALSE
PdgfraCre;Tbx1+/+	WT;Tbx1+/flox	25	-0.32260178	0.190250926	0.644874038	FALSE
PdgfraCre;Tbx1+/+	WT;Tbx1+/+	29	-0.387701754	0.081543225	0.644874038	FALSE
WT;Tbx1+/flox	WT;Tbx1+/+	50.5	-0.054278246	0.8620692	1	FALSE
PdgfraCre;Tbx1+/+	WT;Tbx1+/flox	23	-0.236297264	0.382284382	0.834075016	FALSE
PdgfraCre;Tbx1+/+	WT;Tbx1+/+	15.5	-0.539886352	0.02034876	0.488370247	FALSE
WT;Tbx1+/flox	WT;Tbx1+/+	28	-0.303094092	0.206001429	0.644874038	FALSE
PdgfraCre;Tbx1+/+	WT;Tbx1+/flox	28.5	-0.249756216	0.340106952	0.78989045	FALSE
PdgfraCre;Tbx1+/+	WT;Tbx1+/+	38.5	-0.240375088	0.310026197	0.769720213	FALSE
WT;Tbx1+/flox	WT;Tbx1+/+	50.5	-0.054278246	0.8620692	1	FALSE
PdgfraCre;Tbx1+/+	WT;Tbx1+/flox	20.5	0.301935393

Figure	Measurement	Call type	PND	Genotype	# of Samples	Average	s.e.m	Shapiro-Wilk test Statistic	p_value	p_adj(FDR BH)	Rejects(FDR 5%)	Levene test Statistic	df1	df2	p_value	p_adj(FDR BH)	Rejects(FDR 5%)
Figure 4B	Proportion	Harmonics	P8	oTbx1+/+	27	17.03450018	2.203565508	0.951793015	0.236913264	0.27736187	FALSE	0.007209331	1	36	0.932805151	0.958177206	FALSE
				oTbx1+/-	11	19.61154304	3.599706317	0.960571766	0.778805196	0.79537552	FALSE						
			P12	oTbx1+/+	30	13.16752619	3.364708074	0.59169817	5.78851E-08	3.96926E-07	TRUE	0.873593574	1	40	0.355570832	0.948188885	FALSE
				oTbx1+/-	12	8.505399165	1.955013986	0.873135149	0.07162638	0.090475427	FALSE						
		step_down	P8	oTbx1+/+	27	1.336688279	0.313639637	0.787106931	8.25136E-05	0.000220036	TRUE	0.149229077	1	36	0.701546982	0.958177206	FALSE
				oTbx1+/-	11	1.573785836	0.594457163	0.750182569	0.002090028	0.004180056	TRUE						
			P12	oTbx1+/+	30	1.789236696	0.427419086	0.770336628	1.97568E-05	5.92704E-05	TRUE	2.489159983	1	40	0.122509658	0.586275644	FALSE
				oTbx1+/-	12	9.940976217	8.252655216	0.398949146	3.48338E-06	1.28617E-05	TRUE						
		short	P8	oTbx1+/+	27	23.4473742	4.012502925	0.666321874	1.3633E-06	5.45318E-06	TRUE	0.002788636	1	36	0.958177206	0.958177206	FALSE
				oTbx1+/-	11	21.62772654	4.72041667	0.830675006	0.023827234	0.035740851	TRUE						
			P12	oTbx1+/+	30	23.23444672	2.727284442	0.958858669	0.289563179	0.317734805	FALSE	0.18394001	1	40	0.670309944	0.958177206	FALSE
				oTbx1+/-	12	22.86873026	4.926486399	0.944190502	0.55418241	0.578277298	FALSE						
		down_fm	P8	oTbx1+/+	27	12.75630401	1.76961371	0.920927048	0.041565027	0.058680038	FALSE	4.472020458	1	36	0.041444496	0.497333956	FALSE
				oTbx1+/-	11	21.16328548	4.9646338	0.884678006	0.11924167	0.146758978	FALSE						
			P12	oTbx1+/+	30	10.37298456	1.542082257	0.928056836	0.043611676	0.059699769	FALSE	0.954744089	1	40	0.334387409	0.948188885	FALSE
				oTbx1+/-	12	13.01185528	3.11935555	0.931758583	0.399125427	0.425733789	FALSE						
		up_fm	P8	oTbx1+/+	27	13.05872025	1.780737559	0.92226398	0.044774827	0.059699769	FALSE	5.242724489	1	36	0.028006319	0.497333956	FALSE
				oTbx1+/-	11	6.202009894	1.944137346	0.855210662	0.04989852	0.064733215	FALSE						
			P12	oTbx1+/+	30	17.31720233	2.688345341	0.892989337	0.005683312	0.010103665	TRUE	0.013930753	1	40	0.9066357	0.958177206	FALSE
				oTbx1+/-	12	14.90117688	3.627231491	0.915457904	0.250485063	0.286268643	FALSE						
		two_steps	P8	oTbx1+/+	27	1.22818806	0.583431602	0.439589798	4.31981E-09	6.9117E-08	TRUE	0.367415161	1	36	0.548219905	0.958177206	FALSE
				oTbx1+/-	11	0.657609323	0.30689217	0.709964395	0.000628547	0.001436678	TRUE						
			P12	oTbx1+/+	30	0.376106479	0.140892041	0.56127727	2.53783E-08	2.03026E-07	TRUE	0.031791176	1	40	0.859386723	0.958177206	FALSE
				oTbx1+/-	12	0.420168462	0.189210931	0.706350029	0.000970717	0.002117929	TRUE						
		flat	P8	oTbx1+/+	27	13.18848553	1.439854436	0.955547333	0.291256905	0.317734805	FALSE	0.064044466	1	36	0.801653642	0.958177206	FALSE
				oTbx1+/-	11	13.58957049	2.677180408	0.971073091	0.897150159	0.897150159	FALSE						
			P12	oTbx1+/+	30	10.75966512	1.248052332	0.916827679	0.022208858	0.03438791	TRUE	0.005399042	1	40	0.941791831	0.958177206	FALSE
				oTbx1+/-	12	9.627772862	1.980798048	0.90607655	0.189971969	0.227966362	FALSE						
		chevron	P8	oTbx1+/+	27	11.99601344	2.252797934	0.893206954	0.009383468	0.015531257	TRUE	0.562260857	1	36	0.458223333	0.958177206	FALSE
				oTbx1+/-	11	8.606354313	3.605578163	0.701831937	0.000493834	0.001185202	TRUE						
			P12	oTbx1+/+	30	7.944668927	1.340965584	0.883133352	0.00332987	0.006147453	TRUE	0.121536249	1	40	0.72920259	0.958177206	FALSE
				oTbx1+/-	12	5.704118406	2.467406	0.713398993	0.001137725	0.002374382	TRUE						
		complex	P8	oTbx1+/+	27	1.359067236	0.357237975	0.747017026	1.88041E-05	5.92704E-05	TRUE	1.462744932	1	36	0.234376731	0.803577363	FALSE
				oTbx1+/-	11	0.594390633	0.456151172	0.472920179	7.17045E-07	4.30227E-06	TRUE						
			P12	oTbx1+/+	30	1.444040234	0.348567383	0.776604891	2.52732E-05	7.13597E-05	TRUE	0.463312445	1	40	0.500001335	0.958177206	FALSE
				oTbx1+/-	12	2.213403834	0.819843897	0.755306244	0.003037653	0.005832293	TRUE						
		step_up	P8	oTbx1+/+	27	3.459543469	0.754843072	0.828750014	0.000449811	0.001136364	TRUE	2.986552004	1	36	0.092528851	0.586275644	FALSE
				oTbx1+/-	11	6.030970473	2.091188206	0.792426586	0.007478565	0.012820397	TRUE						
			P12	oTbx1+/+	30	2.930012431	0.802546816	0.690653443	1.14398E-06	5.26814E-06	TRUE	0.337019135	1	40	0.564811412	0.958177206	FALSE
				oTbx1+/-	12	2.522648912	0.867273801	0.814436078	0.013736397	0.021978235	TRUE						
		mult_steps	P8	oTbx1+/+	27	0.053993663	0.038446941	0.300173998	2.61841E-10	6.28418E-09	TRUE	0.119494266	1	36	0.731595596	0.958177206	FALSE
				oTbx1+/-	11	0.031897927	0.031897927	0.344991028	2.2434E-08	2.03026E-07	TRUE						
			P12	oTbx1+/+	30	0.016955782	0.011903467	0.282110274	5.00231E-11	2.40111E-09	TRUE	0.025753757	1	40	0.873310885	0.958177206	FALSE
				oTbx1+/-	12	0.020627063	0.020627063	0.326927483	1.20728E-06	5.26814E-06	TRUE						
		rev_chevron	P8	oTbx1+/+	27	1.081121699	0.315727719	0.719082952	7.22694E-06	2.47781E-05	TRUE	2.201621745	1	36	0.146568911	0.586275644	FALSE
				oTbx1+/-	11	0.31085605	0.230553927	0.488995969	1.11768E-06	5.26814E-06	TRUE						
			P12	oTbx1+/+	30	0.647154535	0.267451787	0.507237554	6.39587E-09	7.67505E-08	TRUE	2.868746639	1	40	0.098089764	0.586275644	FALSE
				oTbx1+/-	12	1.929789318	0.609606267	0.845055282	0.031914786	0.046421506	TRUE						

Source	F	df1	df2	Sig.
Corrected Model	12.69567482	47	912	0
Genotype	0.010709424	1	912	0.917599736
PND	1.295840311	1	912	0.255273381
Call type	39.53182246	11	912	0
Genotype * PND	0.010709424	1	912	0.917599736
PND * Call type	2.796512537	11	912	0.001369316
Call type * Genotype	1.365715759	11	912	0.183698653
Genotype * PND * Call type	0.796636894	11	912	0.643654777

Mann-Witney U test Sample1	Sample2	Statistic	R (Z score)	p_value	p_adj(FDR BH)	Rejects(FDR 5%)
oTbx1+/+	oTbx1+/-	129	-0.101817612	0.546349031	0.974718567	FALSE
oTbx1+/+	oTbx1+/-	157	0.098811692	0.536091044	0.974718567	FALSE
oTbx1+/+	oTbx1+/-	143.5	-0.02610708	0.899119881	0.974718567	FALSE
oTbx1+/+	oTbx1+/-	176.5	-0.015036562	0.945286072	0.974718567	FALSE
oTbx1+/+	oTbx1+/-	142	0.033939204	0.849168654	0.974718567	FALSE
oTbx1+/+	oTbx1+/-	174	-0.025776963	0.879981095	0.974718567	FALSE
oTbx1+/+	oTbx1+/-	105	-0.227131596	0.168812806	0.974718567	FALSE
oTbx1+/+	oTbx1+/-	156.5	-0.100959772	0.536091044	0.974718567	FALSE
oTbx1+/+	oTbx1+/-	84	0.336781333	0.038051176	0.45661411	FALSE
oTbx1+/+	oTbx1+/-	165.5	0.062294328	0.710773696	0.974718567	FALSE
oTbx1+/+	oTbx1+/-	137.5	0.057435576	0.751191124	0.974718567	FALSE
oTbx1+/+	oTbx1+/-	158	-0.094515531	0.5544243	0.974718567	FALSE
oTbx1+/+	oTbx1+/-	146.5	-0.010442832	0.974718567	0.974718567	FALSE
oTbx1+/+	oTbx1+/-	164	0.068738568	0.670224551	0.974718567	FALSE
oTbx1+/+	oTbx1+/-	120	0.148810356	0.372960146	0.974718567	FALSE
oTbx1+/+	oTbx1+/-	149	0.133180976	0.400911456	0.974718567	FALSE
oTbx1+/+	oTbx1+/-	110.5	0.198413808	0.237616458	0.974718567	FALSE
oTbx1+/+	oTbx1+/-	153	-0.115996334	0.465855659	0.974718567	FALSE
oTbx1+/+	oTbx1+/-	128	-0.107039028	0.525351863	0.974718567	FALSE
oTbx1+/+	oTbx1+/-	174	-0.025776963	0.879981095	0.974718567	FALSE
oTbx1+/+	oTbx1+/-	147	-0.007832124	0.974718567	0.974718567	FALSE
oTbx1+/+	oTbx1+/-	177	-0.012888482	0.945286072	0.974718567	FALSE
oTbx1+/+	oTbx1+/-	107	0.216688764	0.189914135	0.974718567	FALSE
oTbx1+/+	oTbx1+/-	99	-0.347989002	0.023533765	0.45661411	FALSE

Measurement	Call type	PND	Genotype	# of samples	Average	s.e.m	Shapiro-Wilk test Statistic	p_value	p_adj(FDR BH)	Rejects(FDR 5%)	Levene's test Statistic	df1	df2	p_value	p_adj(FDR BH)	Rejects(FDR 5%)
Proportion	Harmonics	P8	PdgfraCre;Tbx1+/+	8	14.33386512	3.180619627	0.920521609	0.434110293	0.529761713	FALSE	1.84713931	2	24	0.179413127	0.51429221	FALSE
			WT;Tbx1+/flox	8	13.69827654	5.213100979	0.825142512	0.052831697	0.105663394	FALSE						
			WT;Tbx1+/+	11	21.42494286	2.955550922	0.956472392	0.727051807	0.805349694	FALSE						
		P12	PdgfraCre;Tbx1+/+	9	19.77849016	10.32058624	0.614034689	0.000139793	0.000915012	TRUE	1.199438418	2	27	0.316917223	0.51429221	FALSE
			WT;Tbx1+/flox	9	5.644679288	1.918519292	0.860758774	0.097722904	0.171610953	FALSE						
			WT;Tbx1+/+	12	13.85143838	2.762225592	0.888610048	0.113077876	0.1893397	FALSE						
	step_down	P8	PdgfraCre;Tbx1+/+	8	1.794530722	0.846007146	0.772387788	0.014392817	0.041451314	TRUE	1.151437041	2	24	0.333040024	0.51429221	FALSE
			WT;Tbx1+/flox	8	1.290974418	0.534434464	0.816551909	0.0429211	0.093646035	FALSE						
			WT;Tbx1+/+	11	1.0369584	0.305974108	0.896482842	0.167368171	0.262860212	FALSE						
		P12	PdgfraCre;Tbx1+/+	9	0.512440844	0.392071531	0.528195976	1.37202E-05	0.000142397	TRUE	3.768584833	2	27	0.036019673	0.51429221	FALSE
			WT;Tbx1+/flox	9	2.584253777	0.986144531	0.808525695	0.025540655	0.063411281	FALSE						
			WT;Tbx1+/+	12	2.150570773	0.650897914	0.881745505	0.092280528	0.167826246	FALSE						
	short	P8	PdgfraCre;Tbx1+/+	8	27.79609334	7.835750345	0.802567038	0.030493177	0.073183624	FALSE	1.027435303	2	24	0.373136602	0.51429221	FALSE
			WT;Tbx1+/flox	8	30.52798165	10.4520263	0.674664094	0.001160659	0.004915731	TRUE						
			WT;Tbx1+/+	11	15.13513667	1.98602887	0.910698292	0.248577402	0.357951459	FALSE						
		P12	PdgfraCre;Tbx1+/+	9	29.41714216	6.77204175	0.954397752	0.73826333	0.805378178	FALSE	2.18520834	2	27	0.131943177	0.51429221	FALSE
			WT;Tbx1+/flox	9	21.11850489	4.315377521	0.818225622	0.032903072	0.076420038	FALSE						
			WT;Tbx1+/+	12	20.18438151	3.177084685	0.968703162	0.896753634	0.949503848	FALSE						
	down_fm	P8	PdgfraCre;Tbx1+/+	8	9.902998402	1.798693708	0.925830506	0.478929706	0.574715647	FALSE	1.301310466	2	24	0.290697828	0.51429221	FALSE
			WT;Tbx1+/flox	8	12.95875965	4.301199919	0.91573224	0.396200038	0.509400048	FALSE						
			WT;Tbx1+/+	11	14.68419488	2.820054979	0.931509541	0.426325541	0.529231706	FALSE						
		P12	PdgfraCre;Tbx1+/+	9	15.1261745	3.538818708	0.937379276	0.554598449	0.633826799	FALSE	1.089462096	2	27	0.350732163	0.51429221	FALSE
			WT;Tbx1+/flox	9	6.768936551	2.39904953	0.877183695	0.1466369	0.239951291	FALSE						
			WT;Tbx1+/+	12	9.511128113	1.791519021	0.945887631	0.577853788	0.650085512	FALSE						
	up_fm	P8	PdgfraCre;Tbx1+/+	8	10.52722533	3.589529281	0.898985786	0.282937423	0.399441068	FALSE	0.222556444	2	24	0.802103358	0.875021845	FALSE
			WT;Tbx1+/flox	8	15.51934247	3.299813459	0.929283224	0.509574132	0.594583706	FALSE						
			WT;Tbx1+/+	11	13.11026403	2.688376967	0.960336023	0.775876897	0.833778158	FALSE						
		P12	PdgfraCre;Tbx1+/+	9	10.7373311	3.075778662	0.912907898	0.336760896	0.449014528	FALSE	1.438522228	2	27	0.254889982	0.51429221	FALSE
			WT;Tbx1+/flox	9	24.26204578	6.725552181	0.910146573	0.316901753	0.430508042	FALSE						
			WT;Tbx1+/+	12	17.04347316	3.399092861	0.941065847	0.512002636	0.594583706	FALSE						
	two_steps	P8	PdgfraCre;Tbx1+/+	8	0.102459016	0.102459016	0.418398447	1.04723E-06	2.51336E-05	TRUE	1.00441335	2	24	0.381141088	0.51429221	FALSE
			WT;Tbx1+/flox	8	2.204948931	1.891510087	0.486985371	7.19813E-06	0.000103653	TRUE						
			WT;Tbx1+/+	11	1.33652855	0.427577641	0.831222503	0.024225071	0.063411281	FALSE						
		P12	PdgfraCre;Tbx1+/+	9	0.074906367	0.074906367	0.389841298	3.21749E-07	1.1583E-05	TRUE	1.013541908	2	27	0.376326518	0.51429221	FALSE
			WT;Tbx1+/flox	9	0.455038711	0.205119656	0.782599951	0.012902722	0.038708165	TRUE						
			WT;Tbx1+/+	12	0.542807388	0.309332544	0.587077317	8.38703E-05	0.000670963	TRUE						
	flat	P8	PdgfraCre;Tbx1+/+	8	17.93017709	2.717057881	0.917100523	0.406781173	0.513828851	FALSE	0.524216516	2	24	0.598643331	0.75618105	FALSE
			WT;Tbx1+/flox	8	8.633543264	2.89229413	0.820293101	0.04699594	0.099520814	FALSE						
			WT;Tbx1+/+	11	13.05266786	1.437946293	0.927701172	0.388068488	0.50801693	FALSE						
		P12	PdgfraCre;Tbx1+/+	9	10.49163426	2.2312487	0.893212814	0.215226195	0.322839292	FALSE	0.040346651	2	27	0.960514231	0.960514231	FALSE
			WT;Tbx1+/flox	9	7.38091094	2.106347882	0.89566068	0.22790882	0.33488643	FALSE						
			WT;Tbx1+/+	12	13.4947539	1.915033856	0.923022175	0.311949399	0.430508042	FALSE						
	chevron	P8	PdgfraCre;Tbx1+/+	8	11.11468622	3.975984082	0.839208898	0.073925068	0.143854186	FALSE	0.991480484	2	24	0.385719158	0.51429221	FALSE
			WT;Tbx1+/flox	8	8.28992559	2.59542819	0.854717441	0.106307995	0.182242278	FALSE						
			WT;Tbx1+/+	11	15.33231531	4.329267764	0.896602764	0.167938469	0.262860212	FALSE						
		P12	PdgfraCre;Tbx1+/+	9	8.48801746	3.058254192	0.834102105	0.049637303	0.102111023	FALSE	1.856606996	2	27	0.175598067	0.51429221	FALSE
			WT;Tbx1+/flox	9	6.795574321	1.76969935	0.807793859	0.025055817	0.063411281	FALSE						
			WT;Tbx1+/+	12	8.398978482	2.216508759	0.903793823	0.177537843	0.271972866	FALSE						
	complex	P8	PdgfraCre;Tbx1+/+	8	0.976069158	0.63900965	0.568475715	6.77437E-05	0.000609693	TRUE	0.3998853	2	24	0.674781143	0.771178449	FALSE
			WT;Tbx1+/flox	8	1.68881032	0.777065407	0.807628446	0.034526318	0.077684215	FALSE						
			WT;Tbx1+/+	11	1.397798141	0.529558045	0.775672329	0.004505088	0.017071912	TRUE						
		P12	PdgfraCre;Tbx1+/+	9	1.35985243	0.834393015	0.639968592	0.000281573	0.00153755	TRUE	0.065201783	2	27	0.937025452	0.960514231	FALSE
			WT;Tbx1+/flox	9	1.639512949	0.546565381	0.736084074	0.003737285	0.014949138	TRUE						
			WT;Tbx1+/+	12	1.360576551	0.50435214	0.777657114	0.005278143	0.019001316	TRUE						
	step_up	P8	PdgfraCre;Tbx1+/+	8	4.58948929	1.934601202	0.843751974	0.082294537	0.155926491	FALSE	2.38559384	2	24	0.113511907	0.51429221	FALSE
			WT;Tbx1+/flox	8	3.489325269	1.336233123	0.849076133	0.093236803	0.167826246	FALSE						
			WT;Tbx1+/+	11	2.6161052	0.811090133	0.802232956	0.01006582	0.031589754	TRUE						
		P12	PdgfraCre;Tbx1+/+	9	3.389790988	1.520322048	0.773329537	0.010091172	0.031589754	TRUE	1.256794019	2	27	0.300686319	0.51429221	FALSE
			WT;Tbx1+/flox	9	0.834752633	0.532565223	0.603414342	0.000104925	0.000755456	TRUE						
			WT;Tbx1+/+	12	4.156623362	1.54243506	0.656505111	0.000331387	0.001590656	TRUE						
	mult_steps	P8	PdgfraCre;Tbx1+/+	8	0	0	1	1	1	FALSE	1.488233273	2	24	0.245874864	0.51429221	FALSE
			WT;Tbx1+/flox	8	0	0	1	1	1	FALSE						
			WT;Tbx1+/+	11	0.132529899	0.091610889	0.511703575	2.09968E-06	3.77942E-05	TRUE						
		P12	PdgfraCre;Tbx1+/+	9	0	0	1	1	1	FALSE	1.582954373	2	27	0.223840796	0.51429221	FALSE
			WT;Tbx1+/flox	9	0	0	1	1	1	FALSE						
			WT;Tbx1+/+	12	0.042389454	0.028911445	0.485515454	1.38441E-05	0.000142397	TRUE						
	rev_chevron	P8	PdgfraCre;Tbx1+/+	8	0.932406314	0.485217797	0.736969104	0.005855571	0.020076244	TRUE	0.998042961	2	24	0.383388724	0.51429221	FALSE
			WT;Tbx1+/flox	8	1.698111905	0.810075328	0.792567662	0.02382121	0.063411281	FALSE						
			WT;Tbx1+/+	11	0.740558193	0.375948876	0.684843395	0.000298968	0.00153755	TRUE						
		P12	PdgfraCre;Tbx1+/+	9	0.624219725	0.624219725	0.389841298	3.21749E-07	1.1583E-05	TRUE	0.46841942	2	27	0.630983165	0.757179799	FALSE
			WT;Tbx1+/flox	9	0.29356793	0.173122527	0.653259574	0.000403018	0.001813582	TRUE						
			WT;Tbx1+/+	12	0.929545596	0.476189549	0.644326098	0.000257894	0.00153755	TRUE						

Source	F	df1	df2	Sig.
Corrected Model	7.678337945	71	612	0
Genotype	0.567660277	2	612	0.567148336
PND	1.529321287	1	612	0.216688691
Call type	42.41123303	11	612	0
Genotype * PND	0.567660277	2	612	0.567148336
PND * Call type	0.791648519	11	612	0.648626623
Call type * Genotype	1.940248357	22	612	0.006372406
Genotype * PND * Call type	1.033284006	22	612	0.419829765

Mann-Whitney's U test Sample1	Sample2	Statistic	R (Z score)	p_value	p_adj(FDR BH)	Rejects(FDR 5%)
PdgfraCre;Tbx1+/+	WT;Tbx1+/flox	29.5	0.065638129	0.878477078	1	FALSE
PdgfraCre;Tbx1+/+	WT;Tbx1+/+	25	-0.359924234	0.1288402	0.7730412	FALSE
WT;Tbx1+/flox	WT;Tbx1+/+	32	-0.227320569	0.351062422	0.901457961	FALSE
PdgfraCre;Tbx1+/+	WT;Tbx1+/flox	25	0.32260178	0.190250926	0.901457961	FALSE
PdgfraCre;Tbx1+/+	WT;Tbx1+/+	47	-0.108556491	0.651052972	0.901457961	FALSE
WT;Tbx1+/flox	WT;Tbx1+/+	26.5	-0.42647193	0.058483312	0.701799748	FALSE
PdgfraCre;Tbx1+/+	WT;Tbx1+/flox	29.5	0.065638129	0.878477078	1	FALSE
PdgfraCre;Tbx1+/+	WT;Tbx1+/+	38.5	0.104188594	0.71678442	0.955712559	FALSE
WT;Tbx1+/flox	WT;Tbx1+/+	42.5	0.028415071	0.967849488	1	FALSE
PdgfraCre;Tbx1+/+	WT;Tbx1+/flox	24	-0.343414798	0.161497326	0.89444673	FALSE
PdgfraCre;Tbx1+/+	WT;Tbx1+/+	27	-0.418717895	0.058483312	0.701799748	FALSE
WT;Tbx1+/flox	WT;Tbx1+/+	53	0.01550807	0.97227231	1	FALSE
PdgfraCre;Tbx1+/+	WT;Tbx1+/flox	31	-0.026255252	0.959129759	1	FALSE
PdgfraCre;Tbx1+/+	WT;Tbx1+/+	27.5	0.312565783	0.206001429	0.901457961	FALSE
WT;Tbx1+/flox	WT;Tbx1+/+	24	0.378867615	0.108650208	0.74285928	FALSE
PdgfraCre;Tbx1+/+	WT;Tbx1+/flox	32	0.176910653	0.489428219	0.901457961	FALSE
PdgfraCre;Tbx1+/+	WT;Tbx1+/+	41	0.201604912	0.3824448	0.901457961	FALSE
WT;Tbx1+/flox	WT;Tbx1+/+	47	0.108556491	0.651052972	0.901457961	FALSE
PdgfraCre;Tbx1+/+	WT;Tbx1+/flox	29	-0.078765755	0.798445998	0.974374778	FALSE
PdgfraCre;Tbx1+/+	WT;Tbx1+/+	30	-0.265207331	0.272287052	0.901457961	FALSE
WT;Tbx1+/flox	WT;Tbx1+/+	37	-0.132603665	0.599878278	0.901457961	FALSE
PdgfraCre;Tbx1+/+	WT;Tbx1+/flox	21.5	0.395447343	0.11349239	0.74285928	FALSE
PdgfraCre;Tbx1+/+	WT;Tbx1+/+	37.5	0.255883158	0.277317729	0.901457961	FALSE
WT;Tbx1+/flox	WT;Tbx1+/+	38.5	-0.240375088	0.310026197	0.901457961	FALSE
PdgfraCre;Tbx1+/+	WT;Tbx1+/flox	22	-0.262552516	0.328205128	0.901457961	FALSE
PdgfraCre;Tbx1+/+	WT;Tbx1+/+	36	-0.151547046	0.544759334	0.901457961	FALSE
WT;Tbx1+/flox	WT;Tbx1+/+	38.5	0.104188594	0.71678442	0.955712559	FALSE
PdgfraCre;Tbx1+/+	WT;Tbx1+/flox	22	-0.385040834	0.11349239	0.74285928	FALSE
PdgfraCre;Tbx1+/+	WT;Tbx1+/+	35	-0.294653333	0.193005137	0.901457961	FALSE
WT;Tbx1+/flox	WT;Tbx1+/+	41.5	0.193850877	0.422107304	0.901457961	FALSE
PdgfraCre;Tbx1+/+	WT;Tbx1+/flox	22.5	-0.24942489	0.382284382	0.901457961	FALSE
PdgfraCre;Tbx1+/+	WT;Tbx1+/+	16.5	-0.520942971	0.0259321	0.701799748	FALSE
WT;Tbx1+/flox	WT;Tbx1+/+	32.5	-0.217848879	0.395041147	0.901457961	FALSE
PdgfraCre;Tbx1+/+	WT;Tbx1+/flox	26	-0.301788762	0.222418758	0.901457961	FALSE
PdgfraCre;Tbx1+/+	WT;Tbx1+/+	38	-0.248129123	0.277317729	0.901457961	FALSE
WT;Tbx1+/flox	WT;Tbx1+/+	50.5	0.054278246	0.8620692	1	FALSE
PdgfraCre;Tbx1+/+	WT;Tbx1+/flox	13	0.49884978	0.04988345	0.701799748	FALSE
PdgfraCre;Tbx1+/+	WT;Tbx1+/+	22.5	0.407282686	0.090841735	0.74285928	FALSE
WT;Tbx1+/flox	WT;Tbx1+/+	23	-0.397810996	0.090841735	0.74285928	FALSE
PdgfraCre;Tbx1+/+	WT;Tbx1+/flox	29	0.239349707	0.340106952	0.901457961	FALSE
PdgfraCre;Tbx1+/+	WT;Tbx1+/+	39	-0.232621053	0.310026197	0.901457961	FALSE
WT;Tbx1+/flox	WT;Tbx1+/+	26.5	-0.42647193	0.058483312	0.701799748	FALSE
PdgfraCre;Tbx1+/+	WT;Tbx1+/flox	29	0.078765755	0.798445998	0.974374778	FALSE
PdgfraCre;Tbx1+/+	WT;Tbx1+/+	36	-0.151547046	0.544759334	0.901457961	FALSE
WT;Tbx1+/flox	WT;Tbx1+/+	32	-0.227320569	0.351062422	0.901457961	FALSE
PdgfraCre;Tbx1+/+	WT;Tbx1+/flox	37	0.072845563	0.796174414	0.974374778	FALSE
PdgfraCre;Tbx1+/+	WT;Tbx1+/+	52	-0.03101614	0.917007451	1	FALSE
WT;Tbx1+/flox	WT;Tbx1+/+	48.5	-0.085294386	0.754370088	0.974374778	FALSE
PdgfraCre;Tbx1+/+	WT;Tb

Figure	Measurement	Call type	PND	Genotype	# of Samples	Average	s.e.m	Shapiro-Wilk test Statistic	p_value	p_adj(FDR BH)	Rejects(FDR 5%)	Levene test Statistic	df1	df2	p_value	p_adj(FDR BH)	Rejects(FDR 5%)
Figure 4C	Duration	Harmonics	P8	oTbx1+/+	23	47.92295829	2.699256034	0.979313314	0.8941468	0.989708006	FALSE	0.000929168	1	31	0.975877848	0.985623162	FALSE
				oTbx1+/-	10	44.69960544	4.401566176	0.974668384	0.930436969	0.989708006	FALSE						
			P12	oTbx1+/+	22	54.74005891	3.852574293	0.918354988	0.070288621	0.331429934	FALSE	1.537197377	1	29	0.224974682	0.490853852	FALSE
				oTbx1+/-	9	52.60944711	3.167958994	0.916101158	0.360939831	0.770815088	FALSE						
		step_down	P8	oTbx1+/+	18	27.09201646	3.053456892	0.865561366	0.015047655	0.158000372	FALSE	0.2059045	1	23	0.654249229	0.962256678	FALSE
				oTbx1+/-	7	20.10412698	3.302056133	0.904883921	0.361587048	0.770815088	FALSE						
			P12	oTbx1+/+	15	27.33660106	1.7963783	0.982755959	0.98487395	0.989708006	FALSE	2.068498506	1	20	0.165834425	0.429742989	FALSE
				oTbx1+/-	7	28.09701587	8.430810214	0.715816438	0.005502878	0.077620809	FALSE						
		short	P8	oTbx1+/+	27	7.74224882	0.312538479	0.945187688	0.163532123	0.528334551	FALSE	0.171090279	1	36	0.68159848	0.962256678	FALSE
				oTbx1+/-	11	7.774337147	0.612486858	0.846332788	0.038221501	0.229329005	FALSE						
			P12	oTbx1+/+	26	7.072236643	0.334744164	0.87922591	0.005544343	0.077620809	FALSE	0.00038636	1	34	0.984432657	0.985623162	FALSE
				oTbx1+/-	10	7.017617959	0.485436046	0.96597141	0.851189494	0.989708006	FALSE						
		down_fm	P8	oTbx1+/+	24	30.66279906	1.957850728	0.966806293	0.589142263	0.907498758	FALSE	3.431740525	1	33	0.072916956	0.35000139	FALSE
				oTbx1+/-	11	30.69520938	1.801882739	0.955081701	0.709225118	0.930857968	FALSE						
			P12	oTbx1+/+	25	35.67096042	2.959919864	0.969138086	0.62329185	0.907498758	FALSE	2.160735587	1	32	0.151341379	0.429742989	FALSE
				oTbx1+/-	9	37.35198732	3.365400362	0.94418776	0.626606286	0.907498758	FALSE						
		up_fm	P8	oTbx1+/+	23	19.62332101	0.925405003	0.95598197	0.387208849	0.770815088	FALSE	5.35177982	1	30	0.027737942	0.221903537	FALSE
				oTbx1+/-	9	23.60520165	3.653717179	0.921376705	0.403760284	0.770815088	FALSE						
			P12	oTbx1+/+	24	19.72581213	1.368821557	0.947432995	0.238222212	0.667022192	FALSE	0.058377287	1	32	0.810620958	0.985623162	FALSE
				oTbx1+/-	10	15.11864466	1.853801309	0.986202121	0.989708006	0.989708006	FALSE						
		two_steps	P8	oTbx1+/+	12	56.71407407	8.656626098	0.946003079	0.579481781	0.907498758	FALSE	2.000905298	1	14	0.179059579	0.429742989	FALSE
				oTbx1+/-	4	50.34666667	5.410990188	0.792466283	0.089381523	0.341274908	FALSE						
			P12	oTbx1+/+	10	58.62755556	4.194056899	0.951295912	0.683848679	0.926504662	FALSE	0.000336509	1	14	0.985623162	0.985623162	FALSE
				oTbx1+/-	6	34.70222222	5.58446381	0.918257356	0.492899448	0.840512896	FALSE						
		flat	P8	oTbx1+/+	26	19.78944829	0.81484035	0.984566271	0.953157961	0.989708006	FALSE	1.174282732	1	34	0.286148033	0.572296066	FALSE
				oTbx1+/-	10	21.47446293	2.726545128	0.82753104	0.031245172	0.218716204	FALSE						
			P12	oTbx1+/+	24	22.07510842	0.90491284	0.950715065	0.280761451	0.736998808	FALSE	2.759012943	1	31	0.106790325	0.4271613	FALSE
				oTbx1+/-	9	21.11847067	0.935953023	0.891232073	0.205424145	0.616272435	FALSE						
		chevron	P8	oTbx1+/+	21	36.64371988	2.271811058	0.919187725	0.0835924	0.341274908	FALSE	0.003024766	1	27	0.956545111	0.985623162	FALSE
				oTbx1+/-	8	37.73476406	3.772893681	0.954048574	0.751886845	0.956946893	FALSE						
			P12	oTbx1+/+	20	41.88753169	2.667991417	0.975014746	0.855094075	0.989708006	FALSE	0.204884413	1	25	0.654710508	0.962256678	FALSE
				oTbx1+/-	7	37.00915927	3.607040424	0.965664983	0.865602672	0.989708006	FALSE						
		complex	P8	oTbx1+/+	12	53.79841981	3.593523806	0.928657532	0.366100401	0.770815088	FALSE	0.004785745	1	12	0.945986497	0.985623162	FALSE
				oTbx1+/-	2	47.81714286	8.92952381										
			P12	oTbx1+/+	15	62.12476912	6.394717172	0.939049602	0.370569885	0.770815088	FALSE	0.257959301	1	21	0.616818976	0.962256678	FALSE
				oTbx1+/-	8	53.32536201	7.106570063	0.86379683	0.130967751	0.458387129	FALSE						
		step_up	P8	oTbx1+/+	21	39.52578272	2.436556474	0.955946565	0.43852523	0.800785202	FALSE	2.443787387	1	28	0.129224079	0.429742989	FALSE
				oTbx1+/-	9	50.31356252	6.763535213	0.971306562	0.905666947	0.989708006	FALSE						
			P12	oTbx1+/+	19	36.25782364	3.631192924	0.956213474	0.500305295	0.840512896	FALSE	0.000525987	1	25	0.981884673	0.985623162	FALSE
				oTbx1+/-	8	54.54926984	8.836116188	0.641596675	0.000484111	0.020332659	TRUE						
		mult_steps	P8	oTbx1+/+	2	45.01333333	37.33333333					1.84044E+31	1	1	1.48395E-16	1.78074E-15	TRUE
				oTbx1+/-	1	48.21333333											
			P12	oTbx1+/+	2	13.01333333	5.76					2.80384E+31	1	1	1.20227E-16	1.78074E-15	TRUE
				oTbx1+/-	1	52.90666667											
		rev_chevron	P8	oTbx1+/+	12	42.56651852	2.153044286	0.841997564	0.029282464	0.218716204	FALSE	4.749155614	1	12	0.049960362	0.299762171	FALSE
				oTbx1+/-	2	38.4	14.50666667										
			P12	oTbx1+/+	9	47.50971016	5.892589066	0.94786489	0.666641116	0.926504662	FALSE	0.537574475	1	15	0.474743246	0.87644907	FALSE
				oTbx1+/-	8	37.21680672	5.066803973	0.837518036	0.0710207	0.331429934	FALSE						

Linear Mixed Model

Source	F	df1	df2	Sig.
Corrected Model	20.26123774	47	560	0
Genotype	0.043473793	1	560	0.834911507
PND	0.165222066	1	560	0.684548787
Call type	60.43094494	11	560	0
Genotype * PND	0.105188211	1	560	0.745811343
PND * Call type	1.398862882	11	560	0.169112377
Call type * Genotype	3.360831125	11	560	0.000163775
Genotype * PND * Call type	1.038937083	11	560	0.410076829

Mann-Witney U test

Sample1	Sample2	Statistic	R (Z score)	p_value	p_adj(FDR BH)	Rejects(FDR 5%)
oTbx1+/+	oTbx1+/-	129	-0.101817612	0.602683656	0.911355311	FALSE
oTbx1+/+	oTbx1+/-	97	-0.356581323	0.948931589	0.990189484	FALSE
oTbx1+/+	oTbx1+/-	86	-0.326338501	0.177507801	0.710031204	FALSE
oTbx1+/+	oTbx1+/-	68	-0.481169978	0.298245614	0.911355311	FALSE
oTbx1+/+	oTbx1+/-	132	0.086153364	0.611651952	0.911355311	FALSE
oTbx1+/+	oTbx1+/-	133	-0.201919544	0.930816808	0.990189484	FALSE
oTbx1+/+	oTbx1+/-	137	-0.060046284	0.874932414	0.990189484	FALSE
oTbx1+/+	oTbx1+/-	101	-0.339396681	0.673085541	0.911355311	FALSE
oTbx1+/+	oTbx1+/-	91	-0.300231421	0.62111142	0.911355311	FALSE
oTbx1+/+	oTbx1+/-	165	-0.064442408	0.092918255	0.557509532	FALSE
oTbx1+/+	oTbx1+/-	28	-0.629180629	0.683516484	0.911355311	FALSE
oTbx1+/+	oTbx1+/-	53	-0.545612386	0.010989011	0.263736264	FALSE
oTbx1+/+	oTbx1+/-	113	-0.185360268	0.565958548	0.911355311	FALSE
oTbx1+/+	oTbx1+/-	129	-0.219104186	0.414164975	0.911355311	FALSE
oTbx1+/+	oTbx1+/-	81	-0.352445581	0.904925626	0.990189484	FALSE
oTbx1+/+	oTbx1+/-	87	-0.399542928	0.369771292	0.911355311	FALSE
oTbx1+/+	oTbx1+/-	16	-0.691837621	0.549450549	0.911355311	FALSE
oTbx1+/+	oTbx1+/-	68	-0.481169978	0.635523359	0.911355311	FALSE
oTbx1+/+	oTbx1+/-	52	-0.503866645	0.056277595	0.557509532	FALSE
oTbx1+/+	oTbx1+/-	42	-0.592870152	0.074893866	0.557509532	FALSE
oTbx1+/+	oTbx1+/-	1	-0.770158862	1	1	FALSE
oTbx1+/+	oTbx1+/-	0	-0.773308893	0.666666667	0.911355311	FALSE
oTbx1+/+	oTbx1+/-	13	-0.707501869	0.923076923	0.990189484	FALSE
oTbx1+/+	oTbx1+/-	52	-0.549908546	0.138790621	0.666194981	FALSE

Figure	Measurement	Call type	PND	Genotype	# of Samples	Average	s.e.m	Shapiro-Wilk test Statistic	p_value	p_adj(FDR BH)	Rejects(FDR 5%)	Levene test Statistic	df1	df2	p_value	p_adj(FDR BH)	Rejects(FDR 5%)
Figure 4C	Duration	All	P8	oTbx1+/+	27	260.2677275	23.10002451	0.966685951	0.517069697	0.689426263	FALSE	0.024977278	1	36	0.875306878	0.875306878	FALSE
				oTbx1+/-	11	237.7105327	35.22954873	0.98531574	0.988519132	0.988519132	FALSE						
			P12	oTbx1+/+	27	266.3561112	29.14567445	0.965607464	0.490966678	0.689426263	FALSE	0.933710604	1	36	0.34034749	0.68069498	FALSE
				oTbx1+/-	11	281.6978642	39.45653524	0.85749799	0.053434357	0.213737428	FALSE						

Repeated 2-way ANOVA

Source		Type III Sum of Squares	df	Mean Square	F	Sig.
Within subjects						
PND	Sphericity Assumed	11487.37597	1	11487.37597	0.749626853	0.393039589
PND * Genotype	Sphericity Assumed	5543.314971	1	5543.314971	0.361737769	0.551780088
Error(PND)	Sphericity Assumed	490372.0159	32	15324.1255		
Between Subjects						
Intercept		3819990.943	1	3819990.943	166.4686802	3.16998E-14
Genotype		5.440297392	1	5.440297392	0.000237079	0.987810766
Error		734310.5625	32	22947.20508		

Student t test

Sample1	Sample2	Statistic	dof	cohens_d	p_value	p_adj(FDR BH)	Rejects(FDR 5%)
oTbx1+/+	oTbx1+/-	0.529251423	36	0.189310895	0.599879665	0.770649486	FALSE
oTbx1+/+	oTbx1+/-	-0.293732063	36	-0.105066661	0.770649486	0.770649486	FALSE

Measurement	Call type	PND	Genotype	# of samples	Average	s.e.m	Shapiro-Wilk test Statistic	p_value	p_adj(FDR BH)	Rejects(FDR 5%)	Levene's test Statistic	df1	df2	p_value	p_adj(FDR BH)	Rejects(FDR 5%)
Duration	Harmonics	P8	PdgfraCre;Tbx1+/+	7	40.90886772	4.558427742	0.938468978	0.624970931	0.989653678	FALSE	0.002206996	2	20	0.997795681	0.997795681	FALSE
			WT;Tbx1+/flox	5	42.93581128	5.625100406	0.880300822	0.310676402	0.861420933	FALSE						
			WT;Tbx1+/+	11	54.65335546	3.322269435	0.906698369	0.2227774	0.747542576	FALSE						
		P12	PdgfraCre;Tbx1+/+	7	47.1113757	5.674386478	0.953771049	0.763849974	0.989653678	FALSE	2.463344678	2	19	0.111885654	0.830248368	FALSE
			WT;Tbx1+/flox	6	64.71990508	11.31009545	0.964217505	0.851580079	0.989653678	FALSE						
			WT;Tbx1+/+	9	54.02024841	3.022231296	0.965456458	0.853325402	0.989653678	FALSE						
		step_down	P8	PdgfraCre;Tbx1+/+	5	26.92266667	3.372016607	0.877170705	0.296686073	0.861420933	FALSE	0.430873811	2	15	0.657736097	0.996273433	FALSE
			WT;Tbx1+/flox	5	23.83644444	4.227757401	0.930576706	0.60030857	0.989653678	FALSE						
			WT;Tbx1+/+	8	29.23259259	6.236899193	0.834931578	0.066786083	0.493875425	FALSE						
		P12	PdgfraCre;Tbx1+/+	2	27.97511111	1.379555556					1.403826013	2	12	0.283250233	0.890215017	FALSE
			WT;Tbx1+/flox	5	27.04863492	4.662940802	0.93123362	0.604806917	0.989653678	FALSE						
			WT;Tbx1+/+	8	27.35695238	2.060533643	0.942444012	0.635276389	0.989653678	FALSE						
		short	P8	PdgfraCre;Tbx1+/+	8	7.917815937	0.530604626	0.831355391	0.061324236	0.493875425	FALSE	0.02965329	2	24	0.970817565	0.997795681	FALSE
			WT;Tbx1+/flox	8	7.81333203	0.768281296	0.655720075	0.00070415	0.042953152	TRUE						
			WT;Tbx1+/+	11	7.562866763	0.416805441	0.985154377	0.988045907	0.989653678	FALSE						
		P12	PdgfraCre;Tbx1+/+	8	7.224727273	0.302944896	0.892752792	0.248184669	0.756963239	FALSE	0.62103357	2	23	0.54615906	0.996273433	FALSE
			WT;Tbx1+/flox	7	6.733424679	0.691876485	0.83817731	0.095540452	0.58279676	FALSE						
			WT;Tbx1+/+	11	7.176941981	0.650036053	0.89527921	0.161741928	0.686425775	FALSE						
		down_fm	P8	PdgfraCre;Tbx1+/+	7	31.22903484	2.618699941	0.966327518	0.870816941	0.989653678	FALSE	2.420919834	2	21	0.113215687	0.830248368	FALSE
			WT;Tbx1+/flox	6	24.00876305	5.033714095	0.858242658	0.183218167	0.698519264	FALSE						
			WT;Tbx1+/+	11	33.93194139	2.490502409	0.977074081	0.947711079	0.989653678	FALSE						
		P12	PdgfraCre;Tbx1+/+	8	35.27615686	5.281399559	0.962996667	0.838114522	0.989653678	FALSE	0.086686621	2	22	0.917276034	0.997795681	FALSE
			WT;Tbx1+/flox	6	40.01672804	7.675950561	0.963961751	0.849691462	0.989653678	FALSE						
			WT;Tbx1+/+	11	33.58767159	4.005392441	0.958638001	0.754588316	0.989653678	FALSE						
		up_fm	P8	PdgfraCre;Tbx1+/+	6	22.08635809	1.767895755	0.979031784	0.94664488	0.989653678	FALSE	0.803986224	2	20	0.46148733	0.996273433	FALSE
			WT;Tbx1+/flox	7	17.68497536	1.231492248	0.778875725	0.025161975	0.383720116	FALSE						
			WT;Tbx1+/+	10	19.50234072	1.538468802	0.88695579	0.156663332	0.686425775	FALSE						
		P12	PdgfraCre;Tbx1+/+	7	18.25207174	1.882487619	0.881423279	0.23284113	0.747542576	FALSE	0.393935778	2	21	0.679277341	0.996273433	FALSE
			WT;Tbx1+/flox	7	19.37050535	2.449587654	0.952865475	0.755690423	0.989653678	FALSE						
			WT;Tbx1+/+	10	21.00614516	2.58398818	0.900295495	0.220738544	0.747542576	FALSE						
		two_steps	P8	PdgfraCre;Tbx1+/+	1	56.74666667						0.756333907	2	9	0.497030518	0.996273433	FALSE
			WT;Tbx1+/flox	3	39.37185185	14.56837035	0.765693459	0.034986854	0.426839615	FALSE						
			WT;Tbx1+/+	8	63.21333333	11.47831855	0.944422712	0.655048847	0.989653678	FALSE						
		P12	PdgfraCre;Tbx1+/+	1	59.59111111						1.718803649	2	7	0.247024372	0.890215017	FALSE
			WT;Tbx1+/flox	4	63.89333333	5.261381314	0.948534927	0.706977093	0.989653678	FALSE						
			WT;Tbx1+/+	5	54.22222222	7.218198127	0.955559829	0.776776713	0.989653678	FALSE						
		flat	P8	PdgfraCre;Tbx1+/+	8	19.38285418	2.161523708	0.938127232	0.592752901	0.989653678	FALSE	1.88909965	2	23	0.173933952	0.890215017	FALSE
			WT;Tbx1+/flox	7	20.03418318	1.026599508	0.918007443	0.45407321	0.989653678	FALSE						
			WT;Tbx1+/+	11	19.92941271	1.060503268	0.930035527	0.411213037	0.989653678	FALSE						
		P12	PdgfraCre;Tbx1+/+	7	22.06660313	2.099649318	0.855242162	0.137169031	0.686425775	FALSE	0.661867473	2	21	0.526320871	0.996273433	FALSE
			WT;Tbx1+/flox	6	23.32211358	1.547504437	0.833187707	0.114362185	0.6341903	FALSE						
			WT;Tbx1+/+	11	21.40033624	1.281598243	0.985002754	0.987590136	0.989653678	FALSE						
		chevron	P8	PdgfraCre;Tbx1+/+	6	36.00005604	4.652989959	0.795458709	0.053475915	0.493875425	FALSE	0.059069292	2	18	0.942823397	0.997795681	FALSE
			WT;Tbx1+/flox	6	32.45211329	4.474684324	0.990198852	0.989653678	0.989653678	FALSE						
			WT;Tbx1+/+	9	39.86723351	3.153606108	0.913333661	0.33990915	0.901498181	FALSE						
		P12	PdgfraCre;Tbx1+/+	5	35.15140741	5.45098299	0.794380663	0.072866866	0.493875425	FALSE	0.724169595	2	17	0.499090145	0.996273433	FALSE
			WT;Tbx1+/flox	6	43.83518788	3.031502235	0.981537083	0.958938137	0.989653678	FALSE						
			WT;Tbx1+/+	9	44.33138549	4.612113275	0.930351025	0.484695498	0.989653678	FALSE						
		complex	P8	PdgfraCre;Tbx1+/+	2	52.06552381	5.47352381					4.243778405	2	9	0.050328058	0.830248368	FALSE
			WT;Tbx1+/flox	4	50.53333333	2.727266981	0.983042133	0.919621758	0.989653678	FALSE						
			WT;Tbx1+/+	6	56.55277613	6.979082855	0.944235993	0.693480606	0.989653678	FALSE						
		P12	PdgfraCre;Tbx1+/+	3	56.86289128	15.15889488	0.98798584	0.790240544	0.989653678	FALSE	0.007045782	2	12	0.992983086	0.997795681	FALSE
			WT;Tbx1+/flox	5	68.77497258	12.75070208	0.964095962	0.836176977	0.989653678	FALSE						
			WT;Tbx1+/+	7	59.62971429	9.27012584	0.944156119	0.676391711	0.989653678	FALSE						
		step_up	P8	PdgfraCre;Tbx1+/+	5	40.9686811	3.783911882	0.84138729	0.168793223	0.686425775	FALSE	1.646688998	2	18	0.220420241	0.890215017	FALSE
			WT;Tbx1+/flox	6	43.3817284	3.877075903	0.690721619	0.00492818	0.150309498	FALSE						
			WT;Tbx1+/+	10	36.49076612	4.16921906	0.943592325	0.593632891	0.989653678	FALSE						
		P12	PdgfraCre;Tbx1+/+	5	32.81066667	8.360663706	0.944022431	0.694498426	0.989653678	FALSE	0.168774818	2	16	0.8461834	0.997795681	FALSE
			WT;Tbx1+/flox	4	28.91555556	8.444243272	0.92068423	0.540789471	0.989653678	FALSE						
			WT;Tbx1+/+	10	40.91830937	4.426603923	0.969189671	0.883231963	0.989653678	FALSE						
		mult_steps	P8	PdgfraCre;Tbx1+/+	0											
			WT;Tbx1+/flox	0												
			WT;Tbx1+/+	2	45.01333333	37.33333333										
		P12	PdgfraCre;Tbx1+/+	0												
			WT;Tbx1+/flox	0												
			WT;Tbx1+/+	2	13.01333333	5.76										
		rev_chevron	P8	PdgfraCre;Tbx1+/+	3	43.94666667	3.205526093	0.998031496	0.91523587	0.989653678	FALSE	0.132365162	2	9	0.877695297	0.997795681	FALSE
			WT;Tbx1+/flox	4	41.984	2.412836781	0.991194337	0.963506274	0.989653678	FALSE						
			WT;Tbx1+/+	5	42.20444444	4.861369009	0.690556819	0.007608686	0.154709958	FALSE						
		P12	PdgfraCre;Tbx1+/+	1	43.6224						0.468689127	2	6	0.646945397	0.996273433	FALSE
			WT;Tbx1+/flox	3	58.64296296	12.13379604	0.982868766	0.749306217	0.989653678	FALSE						
			WT;Tbx1+/+	5	41.60722051	7.264631898	0.944978233	0.701312904	0.989653678	FALSE						

Generalized Linear Mixed Model

Source	F	df1	df2	Sig.
Corrected Model	11.02882805	67	364	0
Genotype	0.347190073	2	364	0.706904756
PND	1.596530724	1	364	0.207204201
Call type	52.1277172	11	364	0
Genotype * PND	5.022025307	2	364	0.007055228
PND * Call type	1.821393368	11	364	0.048996774
Call type * Genotype	0.536675492	20	364	0.950317556
Genotype * PND * Call type	0.998274051	20	364	0.463368195

Student's t-test

Sample1	Sample2	Statistic	dof	Cohen's d	p_value	p_adj(FDR BH)	Rejects(FDR 5%)
PdgfraCre;Tbx1+/+	WT;Tbx1+/flox	-0.282121004	10	-0.165193145	0.783603353	0.968298081	FALSE
PdgfraCre;Tbx1+/+	WT;Tbx1+/+	-2.489154851	16	-1.203490884	0.024196155	0.968298081	FALSE
WT;Tbx1+/flox	WT;Tbx1+/+	-1.891444267	14	-1.020169172	0.079436704	0.968298081	FALSE
PdgfraCre;Tbx1+/+	WT;Tbx1+/flox	-1.457113075	11	-0.810662878	0.173032593	0.968298081	FALSE
PdgfraCre;Tbx1+/+	WT;Tbx1+/+	-1.144156066	14	-0.576600459	0.271744981	0.968298081	FALSE
WT;Tbx1+/flox	WT;Tbx1+/+	1.091739122	13	0.57539704	0.294768343	0.968298081	FALSE
PdgfraCre;Tbx1+/+	WT;Tbx1+/flox	0.570697045	8	0.360940503	0.583874953	0.968298081	FALSE
PdgfraCre;Tbx1+/+	WT;Tbx1+/+	-0.15619576	11	-0.15619576	0.789172445	0.968298081	FALSE
WT;Tbx1+/flox	WT;Tbx1+/+	-0.623418251	11	-0.355403084	0.545719109	0.968298081	FALSE
PdgfraCre;Tbx1+/+	WT;Tbx1+/flox	0.118223257	5	0.098912673	0.910493384	0.968298081	FALSE
PdgfraCre;Tbx1+/+	WT;Tbx1+/+	0.142292666	8	0.11249223	0.890367177	0.968298081	FALSE
WT;Tbx1+/flox	WT;Tbx1+/+	-0.069161795	11	-0.039428289	0.94610209	0.968298081	FALSE
PdgfraCre;Tbx1+/+	WT;Tbx1+/flox	0.11190297	14	0.055951485	0.912488936	0.968298081	FALSE
PdgfraCre;Tbx1+/+	WT;Tbx1+/+	0.533322905	17	0.247813921	0.600713923	0.968298081	FALSE
WT;Tbx1+/flox	WT;Tbx1+/+	0.307715843	17	0.142983302	0.762036619	0.968298081	FALSE
PdgfraCre;Tbx1+/+	WT;Tbx1+/flox	0.681216815	13	0.352563197	0.507688111	0.968298081	FALSE
PdgfraCre;Tbx1+/+	WT;Tbx1+/+	0.059016841	17	0.027422777	0.953626898	0.968298081	FALSE
WT;Tbx1+/flox	WT;Tbx1+/+	-0.449666572	16	-0.21741099	0.658982876	0.968298081	FALSE
PdgfraCre;Tbx1+/+	WT;Tbx1+/flox	1.329497727	11	0.739664253	0.210596869	0.968298081	FALSE
PdgfraCre;Tbx1+/+	WT;Tbx1+/+	-0.717870319	16	-0.347085833	0.483188151	0.968298081	FALSE
WT;Tbx1+/flox	WT;Tbx1+/+	-1.993865557	15	-1.01192509	0.064675183	0.968298081	FALSE
PdgfraCre;Tbx1+/+	WT;Tbx1+/flox	-0.526963161	12	-0.284592634	0.607823392	0.968298081	FALSE
PdgfraCre;Tbx1+/+	WT;Tbx1+/+	0.25976169	17	0.120700916	0.79816736	0.968298081	FALSE
WT;Tbx1+/flox	WT;Tbx1+/+	0.825483127	15	0.418948552	0.422032461	0.968298081	FALSE
PdgfraCre;Tbx1+/+	WT;Tbx1+/flox	2.090998344	11	1.163324085	0.060536036	0.968298081	FALSE
PdgfraCre;Tbx1+/+	WT;Tbx1+/+	1.06895429	14	0.552005622	0.303175501	0.968298081	FALSE
WT;Tbx1+/flox	WT;Tbx1+/+	-0.858608983	15	-0.423127126	0.404068462	0.968298081	FALSE
PdgfraCre;Tbx1+/+	WT;Tbx1+/flox	-0.362025824	12	-0.193510942	0.723627738	0.968298081	FALSE
PdgfraCre;Tbx1+/+	WT;Tbx1+/+	-0.790464576	15	-0.389545196	0.441575344	0.968298081	FALSE
WT;Tbx1+/flox	WT;Tbx1+/+	-0.440145385	15	-0.216906014	0.666107981	0.968298081	FALSE
PdgfraCre;Tbx1+/+	WT;Tbx1+/flox	0.596319781	2		0.6114663	0.968298081	FALSE
PdgfraCre;Tbx1+/+	WT;Tbx1+/+	-0.187793669	7		0.856366123	0.968298081	FALSE
WT;Tbx1+/flox	WT;Tbx1+/+	-1.135840723	9	-0.768967804	0.285363816	0.968298081	FALSE
PdgfraCre;Tbx1+/+	WT;Tbx1+/flox	-0.365685768	3		0.738863479	0.968298081	FALSE
PdgfraCre;Tbx1+/+	WT;Tbx1+/+	0.303654689	4		0.776530465	0.968298081	FALSE
WT;Tbx1+/flox	WT;Tbx1+/+	1.028937284	7	0.690232114	0.337744317	0.968298081	FALSE
PdgfraCre;Tbx1+/+	WT;Tbx1+/flox

Figure	Measurement	Month	Session	Genotype	# of samples	Average	s.e.m	Shapiro-Wilk test Statistic	Shapiro-Wilk test p_value	Shapiro-Wilk test p_adj(FDR BH)	Shapiro-Wilk test Rejects(FDR 5%)	Levene test Statistic	Levene test df1	Levene test df2	Levene test p_value	Levene test p_adj(FDR BH)	Levene test Rejects(FDR 5%)	Linear Mixed Model Source	Linear Mixed Model F	Linear Mixed Model df1	Linear Mixed Model df2	Linear Mixed Model Sig.	Mann-Whitney U test Sample1	Mann-Whitney U test Sample2	Mann-Whitney U test Statistic	Mann-Whitney U test R (Z score)	Mann-Whitney U test p_value	Mann-Whitney U test p_adj(FDR BH)	Mann-Whitney U test Rejects(FDR 5%)
Figure 5A	Social Interaction (s)	1	1	oTbx1+/+	27	16.40740741	3.092707745	0.822716916	0.000347817	0.000695635	TRUE	0.0722396	1	36	0.789637762	0.789637762	FALSE	Corrected Model	0.497244222	3	72	0.685351082	oTbx1+/-	oTbx1+/+	138.5	-0.05221416	0.775387862	0.849168654	FALSE
				oTbx1+/-	11	16.09090909	6.185693972	0.732690896	0.001237266	0.001649687	TRUE							Genotype	0.111765542	1	72	0.739114848							
			2	oTbx1+/+	27	14.40740741	3.858708012	0.644196044	7.09586E-07	2.83834E-06	TRUE	0.344949992	1	36	0.56065175	0.789637762	FALSE	Session	1.379597591	1	72	0.244039836	oTbx1+/-	oTbx1+/+	142	-0.033939204	0.849168654	0.849168654	FALSE
				oTbx1+/-	11	11	3.311138228	0.855904878	0.050946602	0.050946602	FALSE							Genotype * Session	0.262132613	1	72	0.610225677							
		2	1	oTbx1+/+	21	24.23809524	7.075411737	0.65323431	7.59541E-06	1.51908E-05	TRUE	0.093406833	1	29	0.762073072	0.762073072	FALSE	Corrected Model	1.489687533	3	58	0.226836385	oTbx1+/-	oTbx1+/+	93.5	0.087281656	0.662541772	0.723978187	FALSE
				oTbx1+/-	10	30.3	16.01808006	0.521146224	6.44244E-06	1.51908E-05	TRUE							Genotype	0.005469838	1	58	0.941298006							
			2	oTbx1+/+	21	19.61904762	5.080061956	0.764962029	0.000200312	0.000267082	TRUE	0.24965746	1	29	0.621086413	0.762073072	FALSE	Session	4.309691377	1	58	0.042338451	oTbx1+/-	oTbx1+/+	95.5	-0.072102238	0.723978187	0.723978187	FALSE
				oTbx1+/-	10	15.2	5.133333333	0.841080498	0.045458931	0.045458931	TRUE							Genotype * Session	1.217519133	1	58	0.274405205							

Measurement	Month	Session	Genotype	# of samples	Average	s.e.m	Shapiro-Wilk test Statistic	Shapiro-Wilk test p_value	Shapiro-Wilk test p_adj(FDR BH)	Shapiro-Wilk test Rejects(FDR 5%)	Levene test Statistic	Levene test df1	Levene test df2	Levene test p_value	Levene test p_adj(FDR BH)	Levene test Rejects(FDR 5%)	Linear Mixed Model Source	Linear Mixed Model F	Linear Mixed Model df1	Linear Mixed Model df2	Linear Mixed Model Sig.	Mann-Whitney U test Sample1	Mann-Whitney U test Sample2	Mann-Whitney U test Statistic	Mann-Whitney U test R (Z score)	Mann-Whitney U test p_value	Mann-Whitney U test p_adj(FDR BH)	Mann-Whitney U test Rejects(FDR 5%)
Social Interaction (s)	1	1	PdgfraCre;Tbx1+/+	8	19	6.450359901	0.852384539	0.100707919	0.151061878	FALSE	1.333074967	2	24	0.282495218	0.282495218	FALSE	Corrected Model	1.081487416	5	48	0.382584793	PdgfraCre;Tbx1+/+	WT;Tbx1+/flox	25.5	0.245049015	0.370382559	0.745047522	FALSE
			WT;Tbx1+/+	10	20	6.151783842	0.853382418	0.063721582	0.151061878	FALSE							Genotype	1.686430667	2	48	0.195965476	PdgfraCre;Tbx1+/+	WT;Tbx1+/+	37	0.062828086	0.828557064	0.828557064	FALSE
			WT;Tbx1+/flox	9	10.11111111	2.468942894	0.870970279	0.125930494	0.151116593	FALSE							Session	0.495285736	1	48	0.484979032	WT;Tbx1+/flox	WT;Tbx1+/+	35.5	-0.177951304	0.496698348	0.745047522	FALSE
		2	PdgfraCre;Tbx1+/+	8	11.625	4.37907973	0.852137342	0.100130923	0.151061878	FALSE	1.941945267	2	24	0.165308228	0.282495218	FALSE	Genotype*Session	0.843209591	2	48	0.436601196	PdgfraCre;Tbx1+/+	WT;Tbx1+/flox	31	0.116690007	0.672974085	0.807568902	FALSE
			WT;Tbx1+/+	10	23.3	9.316711389	0.746606164	0.003244757	0.01946854	TRUE												PdgfraCre;Tbx1+/+	WT;Tbx1+/+	29.5	-0.219898302	0.408245349	0.745047522	FALSE
			WT;Tbx1+/flox	9	7	1.748014747	0.925306341	0.437971545	0.437971545	FALSE												WT;Tbx1+/flox	WT;Tbx1+/+	29	-0.29970746	0.21102427	0.745047522	FALSE
	2	1	PdgfraCre;Tbx1+/+	8	25.375	10.82480204	0.646705991	0.000554496	0.001663489	TRUE	0.105027705	2	18	0.900847215	0.972131	FALSE	Corrected Model	0.499425251	5	36	0.774566604	PdgfraCre;Tbx1+/+	WT;Tbx1+/flox	27	0.029880715	0.955089355	0.955089355	FALSE
			WT;Tbx1+/+	6	26.16666667	19.80642432	0.554416353	0.000124267	0.000745601	TRUE							Genotype	0.03924997	2	36	0.961551418	PdgfraCre;Tbx1+/+	WT;Tbx1+/+	13.5	0.362284419	0.228438228	0.89044289	FALSE
			WT;Tbx1+/flox	7	21.28571429	7.870119155	0.815067345	0.057543741	0.067157791	FALSE							Session	1.75456665	1	36	0.193651322	WT;Tbx1+/flox	WT;Tbx1+/+	14.5	0.257539377	0.445221445	0.89044289	FALSE
		2	PdgfraCre;Tbx1+/+	8	17.875	6.418270517	0.835164751	0.067157791	0.067157791	FALSE	0.028309139	2	18	0.972131	0.972131	FALSE	Genotype*Session	0.238208993	2	36	0.789270203	PdgfraCre;Tbx1+/+	WT;Tbx1+/flox	26	0.05976143	0.866511267	0.955089355	FALSE
			WT;Tbx1+/+	6	22.83333333	12.78910126	0.642868731	0.00146069	0.002921381	TRUE												PdgfraCre;Tbx1+/+	WT;Tbx1+/+	20.5	-0.120761473	0.754578755	0.955089355	FALSE
			WT;Tbx1+/flox	7	18.85714286	9.174053919	0.752239945	0.013389431	0.020084147	TRUE												WT;Tbx1+/flox	WT;Tbx1+/+	15	-0.237728656	0.445221445	0.89044289	FALSE

Figure	Measurement	Month	Session	Genotype	# of samples	Average	s.e.m	Shapiro-Wilk test Statistic	Shapiro-Wilk test p_value	Shapiro-Wilk test p_adj(FDR BH)	Shapiro-Wilk test Rejects(FDR 5%)	Levene test Statistic	Levene test df1	Levene test df2	Levene test p_value	Levene test p_adj(FDR BH)	Levene test Rejects(FDR 5%)	Linear Mixed Model Source	F	df1	df2	Sig.	Mann-Whitney U test Sample1	Sample2	Statistic	R (Z score)	p_value	p_adj(FDR BH)	Rejects(FDR 5%)
Figure 5B	Sniffing novel object (s)	1	1	oTbx1+/+	26	14.57692308	2.634781017	0.846840904	0.001236135	0.00247227	TRUE	0.08242971	1	35	0.775724316	0.775724316	FALSE	Corrected Model	2.521664315	3	70	0.064800787	oTbx1+/-	oTbx1+/+	129	-0.076479138	0.65844134	0.934817788	FALSE
				oTbx1+/-	11	12.36363636	3.739889953	0.818474025	0.016467715	0.016467715	TRUE							Genotype	2.25065E-05	1	70	0.996228266							
			2	oTbx1+/+	26	8.115384615	1.778786901	0.802681024	0.000195641	0.000782565	TRUE	1.057934255	1	35	0.310742865	0.621485731	FALSE	Session	3.706544227	1	70	0.05826308	oTbx1+/-	oTbx1+/+	140	-0.016388387	0.934817788	0.934817788	FALSE
				oTbx1+/-	11	10.36363636	4.101602186	0.789282155	0.006799356	0.009065808	TRUE							Genotype * Session	1.03048056	1	70	0.31354175							
		2	1	oTbx1+/+	21	8	1.657594356	0.868273317	0.008915895	0.01783179	TRUE	2.542177104	1	29	0.12168399	0.243367981	FALSE	Corrected Model	0.495546864	3	58	0.686790912	oTbx1+/-	oTbx1+/+	104	0.007589709	0.983438982	0.983438982	FALSE
				oTbx1+/-	10	6.8	1.41264134	0.911900064	0.294299164	0.294299164	FALSE							Genotype	0.116338641	1	58	0.734272506							
			2	oTbx1+/+	21	6.333333333	1.731134136	0.786296484	0.000408019	0.001632078	TRUE	0.028910762	1	29	0.86616589	0.86616589	FALSE	Session	0.920506319	1	58	0.341324669	oTbx1+/-	oTbx1+/+	99	0.045538256	0.81932528	0.983438982	FALSE
				oTbx1+/-	10	5.9	2.008039398	0.823579501	0.027996164	0.037328218	TRUE							Genotype * Session	0.082129844	1	58	0.775452844							

Measurement	Month	Session	Genotype	# of samples	Average	s.e.m	Shapiro-Wilk test Statistic	Shapiro-Wilk test p_value	Shapiro-Wilk test p_adj(FDR BH)	Shapiro-Wilk test Rejects(FDR 5%)	Levene test Statistic	Levene test df1	Levene test df2	Levene test p_value	Levene test p_adj(FDR BH)	Levene test Rejects(FDR 5%)	Generalized Linear Mixed Model Source	F	df1	df2	Sig.	Mann-Whitney U test Sample1	Sample2	Statistic	R (Z score)	p_value	p_adj(FDR BH)	Rejects(FDR 5%)
Sniffing novel object (s)	1	1	PdgfraCre;Tbx1+/+	8	12	3.9551052	0.861423719	0.124057733	0.148869279	FALSE	0.476633313	2	23	0.626867139	0.952913718	FALSE	Corrected Model	3.093385391	5	46	0.017260974	PdgfraCre;Tbx1+/+	WT;Tbx1+/flox	30.5	-0.128359008	0.672974085	0.931427396	FALSE
			WT;Tbx1+/+	9	14	3.989569735	0.818691778	0.033304831	0.066609661	FALSE							Genotype	0.177160277	2	46	0.838214318	PdgfraCre;Tbx1+/+	WT;Tbx1+/+	30	-0.140028008	0.605841218	0.931427396	FALSE
			WT;Tbx1+/flox	9	17.44444444	5.725457554	0.864838833	0.10819449	0.148869279	FALSE							Session	12.98794535	1	46	0.000767292	WT;Tbx1+/flox	WT;Tbx1+/+	37	0.072845563	0.796174414	0.931427396	FALSE
		2	PdgfraCre;Tbx1+/+	8	7	3.5152728	0.759035249	0.010275376	0.030826129	TRUE	0.048332199	2	23	0.952913718	0.952913718	FALSE	Genotype*Session	0.931759073	2	46	0.401165818	PdgfraCre;Tbx1+/+	WT;Tbx1+/flox	28	-0.186704011	0.480707528	0.931427396	FALSE
			WT;Tbx1+/+	9	9.555555556	3.667087518	0.721553597	0.00253196	0.01519176	TRUE												PdgfraCre;Tbx1+/+	WT;Tbx1+/+	26	-0.233380014	0.370382559	0.931427396	FALSE
			WT;Tbx1+/flox	9	7.666666667	2.254624876	0.919315229	0.386600395	0.386600395	FALSE												WT;Tbx1+/flox	WT;Tbx1+/+	39	-0.031219527	0.931427396	0.931427396	FALSE
	2	1	PdgfraCre;Tbx1+/+	8	7.5	2.692582404	0.907626652	0.337653424	0.37778911	FALSE	0.627763682	2	18	0.545071894	0.545071894	FALSE	Corrected Model	0.477274668	5	36	0.790748408	PdgfraCre;Tbx1+/+	WT;Tbx1+/flox	27	-0.029880715	0.955089355	1	FALSE
			WT;Tbx1+/+	6	8	2.695675549	0.87228892	0.23548219	0.353223285	FALSE							Genotype	0.057987693	2	36	0.943749519	PdgfraCre;Tbx1+/+	WT;Tbx1+/+	23.5	-0.017251639	1	1	FALSE
			WT;Tbx1+/flox	7	8.571428571	3.537938214	0.813275039	0.055283937	0.110567873	FALSE							Session	1.061158579	1	36	0.309822637	WT;Tbx1+/flox	WT;Tbx1+/+	19	-0.079242885	0.835664336	1	FALSE
		2	PdgfraCre;Tbx1+/+	8	8	4.110092109	0.764055086	0.011666808	0.070000849	FALSE	1.298312466	2	18	0.297363734	0.545071894	FALSE	Genotype*Session	0.658142803	2	36	0.523930478	PdgfraCre;Tbx1+/+	WT;Tbx1+/flox	27	0.029880715	0.955089355	1	FALSE
			WT;Tbx1+/+	6	6.333333333	1.452966315	0.90065047	0.37778911	0.37778911	FALSE												PdgfraCre;Tbx1+/+	WT;Tbx1+/+	19.5	-0.155264751	0.662004662	1	FALSE
			WT;Tbx1+/flox	7	4.428571429	2.191511143	0.796592563	0.037898712	0.110567873	FALSE												WT;Tbx1+/flox	WT;Tbx1+/+	14	-0.277350098	0.365967366	1	FALSE

Figure	Measurement	Month	Delay (s)	Genotype	# of samples	Average	s.e.m	Shapiro-Wilk test Statistic	p_value	p_adj(FDR BH)	Rejects(FDR 5%)	Levene test Statistic	df1	df2	p_value	p_adj(FDR BH)	Rejects(FDR 5%)
Figure 6A	% alternation	1	0	oTbx1+/+	24	87.96296296	2.209774585	0.817882433	0.000586058	0.001758173	TRUE	1.26349718	1	32	0.269351926	0.808055777	FALSE
				oTbx1+/-	10	88.88888889	3.3126933	0.84073699	0.04503041	0.054036492	FALSE						
			15	oTbx1+/+	24	51.85185185	2.184325276	0.813035203	0.000484908	0.001758173	TRUE	0.003101076	1	32	0.955937164	0.955937164	FALSE
				oTbx1+/-	10	53.33333333	3.228814032	0.884986306	0.14879822	0.14879822	FALSE						
			30	oTbx1+/+	24	44.90740741	2.059150213	0.905249105	0.027853786	0.041780679	TRUE	0.011740247	1	32	0.914392707	0.955937164	FALSE
				oTbx1+/-	10	57.77777778	2.771598064	0.819704545	0.025134415	0.041780679	TRUE						
		2	0	oTbx1+/+	20	88.88888889	2.418254167	0.832136365	0.002714676	0.008144029	TRUE	0.005608641	1	27	0.940853676	0.940853676	FALSE
				oTbx1+/-	9	85.18518519	4.899539465	0.790885567	0.016062009	0.032124018	TRUE						
			15	oTbx1+/+	20	54.44444444	2.265657383	0.898171934	0.038114561	0.057171842	FALSE	2.474961012	1	27	0.127318695	0.381956086	FALSE
				oTbx1+/-	9	48.14814815	5.237828009	0.911520399	0.326661423	0.337937343	FALSE						
			30	oTbx1+/+	20	51.11111111	2.47140896	0.800994201	0.000893986	0.005363913	TRUE	0.039618489	1	27	0.843719703	0.940853676	FALSE
				oTbx1+/-	9	49.38271605	3.266359643	0.913067364	0.337937343	0.337937343	FALSE						

Linear Mixed Model Source	F	df1	df2	Sig.
Corrected Model	66.06011981	5	96	0
Genotype	4.660889678	1	96	0.033349839
Delay	122.9828701	2	96	0
Genotype * Delay	3.150937861	2	96	0.04727228
Corrected Model	38.5469499	5	81	0
Genotype	2.046863951	1	81	0.156366686
Delay	81.56087251	2	81	0
Genotype * Delay	0.243946056	2	81	0.784103458

Mann-Whitney U test Sample1	Sample2	Statistic	R (Z score)	p_value	p_adj(FDR BH)	Rejects(FDR 5%)
oTbx1+/-	oTbx1+/+	113	0.045374261	0.809114032	0.809114032	FALSE
oTbx1+/-	oTbx1+/+	113	0.045374261	0.809114032	0.809114032	FALSE
oTbx1+/-	oTbx1+/+	43	0.499116867	0.002700336	0.008101007	TRUE
oTbx1+/-	oTbx1+/+	80	-0.087537622	0.660118692	0.660118692	FALSE
oTbx1+/-	oTbx1+/+	72.5	-0.153190838	0.443859589	0.660118692	FALSE
oTbx1+/-	oTbx1+/+	75	-0.131306433	0.501389665	0.660118692	FALSE

Measurement	Month	Delay (s)	Genotype	# of samples	Average	s.e.m	Shapiro-Wilk test Statistic	p_value	p_adj(FDR BH)	Rejects(FDR 5%)	Levene test Statistic	df1	df2	p_value	p_adj(FDR BH)	Rejects(FDR 5%)
% alternation	1	0	PdgfraCre;Tbx1+/+	8	86.11111111	2.777777778	0.827205306	0.05551859	0.124916827	FALSE	0.400924437	2	21	0.674718601	0.961718489	FALSE
			WT;Tbx1+/+	7	87.3015873	4.489566865	0.664435629	0.001497441	0.006738486	TRUE						
			WT;Tbx1+/flox	9	90.12345679	4.320987654	0.775541227	0.01070126	0.032103779	TRUE						
		15	PdgfraCre;Tbx1+/+	8	50	4.199605256	0.567903737	6.66981E-05	0.000600283	TRUE	0.122464503	2	21	0.885364514	0.961718489	FALSE
			WT;Tbx1+/+	7	53.96825397	4.489566865	0.893581377	0.293870591	0.293870591	FALSE						
			WT;Tbx1+/flox	9	51.85185185	3.207501495	0.872821722	0.131797654	0.175446148	FALSE						
		30	PdgfraCre;Tbx1+/+	8	45.83333333	3.893138268	0.871515193	0.155952131	0.175446148	FALSE	0.039106145	2	21	0.961718489	0.961718489	FALSE
			WT;Tbx1+/+	7	44.44444444	3.428963332	0.8577129	0.144397137	0.175446148	FALSE						
			WT;Tbx1+/flox	9	44.44444444	3.703703704	0.853289618	0.080990849	0.145783528	FALSE						
	2	0	PdgfraCre;Tbx1+/+	8	87.5	3.893138268	0.735991362	0.005710635	0.019119856	TRUE	0.205732484	2	17	0.816047931	0.925960593	FALSE
			WT;Tbx1+/+	6	90.74074074	5.30289669	0.772718964	0.032937266	0.074108848	FALSE						
			WT;Tbx1+/flox	6	88.88888889	4.05720413	0.853191607	0.167002833	0.214717928	FALSE						
		15	PdgfraCre;Tbx1+/+	8	55.55555556	2.969569355	0.848910992	0.092877818	0.139316727	FALSE	0.476	2	17	0.629298498	0.925960593	FALSE
			WT;Tbx1+/+	6	57.40740741	5.30289669	0.907578534	0.420658529	0.473240845	FALSE						
			WT;Tbx1+/flox	6	50	3.79516695	0.701259348	0.006373285	0.019119856	TRUE						
		30	PdgfraCre;Tbx1+/+	8	52.77777778	3.482128725	0.826041799	0.053987435	0.097177383	FALSE	0.077272727	2	17	0.925960593	0.925960593	FALSE
			WT;Tbx1+/+	6	48.14814815	5.493480361	0.665788341	0.002641354	0.019119856	TRUE						
			WT;Tbx1+/flox	6	51.85185185	4.684855793	0.915458969	0.473270921	0.473270921	FALSE						

Generalized Linear Mixed Model Source	F	df1	df2	Sig.
Corrected Model	31.01103484	8	63	0
Genotype	0.104620037	2	63	0.900822824
Delay	121.2150635	2	63	0
Genotype*Delay	0.26479949	4	63	0.899485819
Corrected Model	22.23991673	8	51	3.94129E-14
Genotype	0.119696984	2	51	0.887437723
Delay	87.4546486	2	51	0
Genotype*Delay	0.640087093	4	51	0.636335206

Mann-Whitney U test Sample1	Sample2	Statistic	R (Z score)	p_value	p_adj(FDR BH)	Rejects(FDR 5%)
PdgfraCre;Tbx1+/+	WT;Tbx1+/flox	26.5	-0.221711013	0.423447141	1	FALSE
PdgfraCre;Tbx1+/+	WT;Tbx1+/+	27.5	-0.014940358	1	1	FALSE
WT;Tbx1+/flox	WT;Tbx1+/+	27.5	0.105851225	0.757692308	1	FALSE
PdgfraCre;Tbx1+/+	WT;Tbx1+/flox	35	-0.023338001	0.962566845	1	FALSE
PdgfraCre;Tbx1+/+	WT;Tbx1+/+	22.5	-0.164343934	0.612587413	1	FALSE
WT;Tbx1+/flox	WT;Tbx1+/+	27	-0.119082628	0.680594406	1	FALSE
PdgfraCre;Tbx1+/+	WT;Tbx1+/flox	35.5	-0.011669001	1	1	FALSE
PdgfraCre;Tbx1+/+	WT;Tbx1+/+	27	0.029880715	0.955089355	1	FALSE
WT;Tbx1+/flox	WT;Tbx1+/+	30	0.039694209	0.918181818	1	FALSE
PdgfraCre;Tbx1+/+	WT;Tbx1+/flox	22	-0.069006556	0.851814852	0.94971695	FALSE
PdgfraCre;Tbx1+/+	WT;Tbx1+/+	19.5	-0.155264751	0.662004662	0.94971695	FALSE
WT;Tbx1+/flox	WT;Tbx1+/+	15	-0.138675049	0.699134199	0.94971695	FALSE
PdgfraCre;Tbx1+/+	WT;Tbx1+/flox	17	0.241522946	0.413586414	0.94971695	FALSE
PdgfraCre;Tbx1+/+	WT;Tbx1+/+	23	-0.034503278	0.94971695	0.94971695	FALSE
WT;Tbx1+/flox	WT;Tbx1+/+	13	-0.231125082	0.484848485	0.94971695	FALSE
PdgfraCre;Tbx1+/+	WT;Tbx1+/flox	23	0.034503278	0.94971695	0.94971695	FALSE
PdgfraCre;Tbx1+/+	WT;Tbx1+/+	19.5	0.155264751	0.662004662	0.94971695	FALSE
WT;Tbx1+/flox	WT;Tbx1+/+	15.5	0.111562541	0.818181818	0.94971695	FALSE

Figure	Measurement	Month	Delay (s)	Genotype	# of samples	Average	s.e.m	Shapiro-Wilk test Statistic	Shapiro-Wilk test p_value	Shapiro-Wilk test p_adj(FDR BH)	Shapiro-Wilk test Rejects(FDR 5%)	Levene test Statistic	Levene test df1	Levene test df2	Levene test p_value	Levene test p_adj(FDR BH)	Levene test Rejects(FDR 5%)
Figure 5B	Latency to correct arm (s)	1	0	oTbx1+/+	24	7.060929233	0.514093404	0.800175638	0.00029653	0.00177918	TRUE	0.277615077	1	32	0.601902435	0.601902435	FALSE
				oTbx1+/-	10	7.045238095	0.530928951	0.926337453	0.412848339	0.476660672	FALSE						
			15	oTbx1+/+	24	23.71111111	3.024286701	0.822986774	0.000717253	0.00215176	TRUE	0.326055759	1	32	0.571979595	0.601902435	FALSE
				oTbx1+/-	10	21.89666667	3.777162368	0.850065677	0.058193748	0.116387496	FALSE						
			30	oTbx1+/+	24	30.76111111	2.763625603	0.951467639	0.29143235	0.437148525	FALSE	1.123976658	1	32	0.297000607	0.601902435	FALSE
				oTbx1+/-	10	20.47833333	3.235213323	0.932865391	0.476660672	0.476660672	FALSE						
		2	0	oTbx1+/+	20	8.249603175	1.084890689	0.650063636	1.01826E-05	6.10959E-05	TRUE	1.416496538	1	27	0.244340874	0.366511312	FALSE
				oTbx1+/-	9	10.25432099	2.448449218	0.825388972	0.039632942	0.118898826	FALSE						
			15	oTbx1+/+	20	21.45690476	2.262232887	0.949405569	0.358157001	0.358157001	FALSE	1.772805112	1	27	0.194168243	0.366511312	FALSE
				oTbx1+/-	9	32.12037037	6.192265298	0.86589138	0.11106244	0.145532979	FALSE						
			30	oTbx1+/+	20	27.41833333	3.194822863	0.924555501	0.121277482	0.145532979	FALSE	0.387060947	1	27	0.539067153	0.539067153	FALSE
				oTbx1+/-	9	23.54814815	4.343311557	0.852295522	0.078981247	0.145532979	FALSE						

Linear Mixed Model Source	F	df1	df2	Sig.
Corrected Model	16.83605715	5	96	6.44695E-12
Genotype	2.181306251	1	96	0.142968861
Delay	27.42527721	2	96	3.79112E-10
Genotype * Delay	2.058495873	2	96	0.13324324

Mann-Whitney U test Sample1	Sample2	Statistic	R (Z score)	p_value	p_adj(FDR BH)	Rejects(FDR 5%)
oTbx1+/-	oTbx1+/+	110	0.064820372	0.723944044	0.896531195	FALSE
oTbx1+/-	oTbx1+/+	116	-0.025928149	0.896531195	0.896531195	FALSE
oTbx1+/-	oTbx1+/+	67	-0.343547973	0.045949085	0.137847254	FALSE
oTbx1+/-	oTbx1+/+	79	0.096291384	0.626843222	0.626843222	FALSE
oTbx1+/-	oTbx1+/+	58	0.28012039	0.13969359	0.419080769	FALSE
oTbx1+/-	oTbx1+/+	71	-0.166321482	0.390153575	0.585230362	FALSE

Measurement	Month	Delay (s)	Genotype	# of samples	Average	s.e.m	Shapiro-Wilk test Statistic	Shapiro-Wilk test p_value	Shapiro-Wilk test p_adj(FDR BH)	Shapiro-Wilk test Rejects(FDR 5%)	Levene test Statistic	Levene test df1	Levene test df2	Levene test p_value	Levene test p_adj(FDR BH)	Levene test Rejects(FDR 5%)
Latency to correct arm (s)	1	0	PdgfraCre;Tbx1+/+	8	6.936507937	1.245302549	0.49801402	9.77951E-06	8.80156E-05	TRUE	0.118489741	2	21	0.888850552	0.888850552	FALSE
			WT;Tbx1+/+	7	7.238095238	0.859979629	0.889504742	0.272090107	0.61220274	FALSE						
			WT;Tbx1+/flox	9	7.033730159	0.619516622	0.953498416	0.728441817	0.964816546	FALSE						
		15	PdgfraCre;Tbx1+/+	8	32.51875	7.148675811	0.867888501	0.143716676	0.61220274	FALSE	1.806979696	2	21	0.188754388	0.283131582	FALSE
			WT;Tbx1+/+	7	13.89285714	1.511419745	0.881281719	0.232198499	0.61220274	FALSE						
			WT;Tbx1+/flox	9	23.51851852	3.323532402	0.936177907	0.542290058	0.964816546	FALSE						
		30	PdgfraCre;Tbx1+/+	8	33.4	5.751512051	0.954254508	0.753939808	0.964816546	FALSE	2.91193178	2	21	0.076529454	0.229588362	FALSE
			WT;Tbx1+/+	7	37.25952381	4.89605426	0.981124342	0.964816546	0.964816546	FALSE						
			WT;Tbx1+/flox	9	23.36111111	2.668082668	0.967019227	0.868103653	0.964816546	FALSE						
	2	0	PdgfraCre;Tbx1+/+	8	7.634672619	0.856014268	0.893506903	0.252187548	0.567421983	FALSE	2.318063852	2	17	0.128762611	0.193143916	FALSE
			WT;Tbx1+/+	6	6.136574074	0.419288306	0.935332466	0.621863247	0.799538461	FALSE						
			WT;Tbx1+/flox	6	11.18253968	3.263533536	0.781374891	0.039698931	0.357290375	FALSE						
		15	PdgfraCre;Tbx1+/+	8	18.46458333	3.639106975	0.925920356	0.479712667	0.799538461	FALSE	3.251300612	2	17	0.063728018	0.191184054	FALSE
			WT;Tbx1+/+	6	20.77301587	2.072925902	0.928919732	0.571785689	0.799538461	FALSE						
			WT;Tbx1+/flox	6	26.13055556	5.381154386	0.960050918	0.820132956	0.820132956	FALSE						
		30	PdgfraCre;Tbx1+/+	8	28.00625	6.083776841	0.851422944	0.0984807	0.44316315	FALSE	0.906736253	2	17	0.422502853	0.422502853	FALSE
			WT;Tbx1+/+	6	30.63333333	6.500957194	0.873464834	0.240368777	0.567421983	FALSE						
			WT;Tbx1+/flox	6	23.41944444	3.546480824	0.954883247	0.779566398	0.820132956	FALSE						

Generalized Linear Mixed Model Source	F	df1	df2	Sig.
Corrected Model	12.80465967	8	63	9.75433E-11
Genotype	1.578749645	2	63	0.214282282
Delay	41.38453208	2	63	3.34022E-12
Genotype*Delay	4.562533663	4	63	0.0026726
Corrected Model	5.716167127	8	51	3.39007E-05
Genotype	0.163060535	2	51	0.849980901
Delay	20.11273606	2	51	3.63144E-07
Genotype*Delay	1.061101788	4	51	0.385349838

Mann-Whitney U test Sample1	Sample2	Statistic	R (Z score)	p_value	p_adj(FDR BH)	Rejects(FDR 5%)
PdgfraCre;Tbx1+/+	WT;Tbx1+/flox	26	-0.233380014	0.370382559	0.666688606	FALSE
PdgfraCre;Tbx1+/+	WT;Tbx1+/+	27	-0.029880715	0.955089355	1	FALSE
WT;Tbx1+/flox	WT;Tbx1+/+	31.5	0	1	1	FALSE
PdgfraCre;Tbx1+/+	WT;Tbx1+/flox	30	0.140028008	0.605841218	0.778938708	FALSE
PdgfraCre;Tbx1+/+	WT;Tbx1+/+	8	0.597614305	0.020512821	0.140034965	FALSE
WT;Tbx1+/flox	WT;Tbx1+/+	14	0.463099109	0.071153846	0.213461538	FALSE
PdgfraCre;Tbx1+/+	WT;Tbx1+/flox	20	0.373408022	0.138790621	0.312278898	FALSE
PdgfraCre;Tbx1+/+	WT;Tbx1+/+	22	-0.179284291	0.535819736	0.778938708	FALSE
WT;Tbx1+/flox	WT;Tbx1+/+	11	-0.542487527	0.031118881	0.140034965	FALSE
PdgfraCre;Tbx1+/+	WT;Tbx1+/flox	20	-0.138013112	0.662004662	0.754578755	FALSE
PdgfraCre;Tbx1+/+	WT;Tbx1+/+	14.5	0.327781141	0.282384282	0.754578755	FALSE
WT;Tbx1+/flox	WT;Tbx1+/+	12.5	0.25423759	0.484848485	0.754578755	FALSE
PdgfraCre;Tbx1+/+	WT;Tbx1+/flox	16	-0.276026224	0.344988345	0.754578755	FALSE
PdgfraCre;Tbx1+/+	WT;Tbx1+/+	18	-0.207019668	0.490842491	0.754578755	FALSE
WT;Tbx1+/flox	WT;Tbx1+/+	15	0.138675049	0.699134199	0.754578755	FALSE
PdgfraCre;Tbx1+/+	WT;Tbx1+/flox	21	0.103509834	0.754578755	0.754578755	FALSE
PdgfraCre;Tbx1+/+	WT;Tbx1+/+	21	-0.103509834	0.754578755	0.754578755	FALSE
WT;Tbx1+/flox	WT;Tbx1+/+	13	-0.231125082	0.484848485	0.754578755	FALSE

Figure	Measurement	Month	Genotype	# of samples	Average	s.e.m	Shapiro-Wilk test Statistic	Shapiro-Wilk test p_value	Shapiro-Wilk test p_adj(FDR BH)	Shapiro-Wilk test Rejects(FDR 5%)	Levene test Statistic	Levene test df1	Levene test df2	Levene test p_value	Levene test p_adj(FDR BH)	Levene test Rejects(FDR 5%)	Mann-Whitney U test Sample1	Mann-Whitney U test Sample2	Statistic	R (Z score)	p_value	p_adj(FDR BH)	Rejects(FDR 5%)
Figure 7A	% open arms time	1	oTbx1+/+	23	13.92453346	2.578767506	0.871431687	0.00682799	0.01365598	TRUE	0.03061532	1	32	0.862203787	0.862203787	FALSE	oTbx1+/-	oTbx1+/+	100	0.167302625	0.343976779	0.343976779	FALSE
			oTbx1+/-	11	16.98607089	3.279767612	0.906204785	0.219762803	0.219762803	FALSE													
		2	oTbx1+/+	20	5.617823791	1.293061822	0.865730567	0.009893527	0.019787054	TRUE	0.129376135	1	28	0.721778502	0.721778502	FALSE	oTbx1+/-	oTbx1+/+	98	0.016064387	0.948316451	0.948316451	FALSE
			oTbx1+/-	10	6.108311403	1.697112495	0.861318188	0.079087694	0.079087694	FALSE													

Measurement	Month	Genotype	# of samples	Average	s.e.m	Shapiro-Wilk test Statistic	Shapiro-Wilk test p_value	Shapiro-Wilk test p_adj(FDR BH)	Shapiro-Wilk test Rejects(FDR 5%)	Levene test Statistic	Levene test df1	Levene test df2	Levene test p_value	Levene test p_adj(FDR BH)	Levene test Rejects(FDR 5%)	One way ANOVA Source	One way ANOVA Type III Sum of Squares	One way ANOVA df	One way ANOVA Mean Square	One way ANOVA F	One way ANOVA Sig.	Student t test Sample1	Student t test Sample2	Student t test Statistic	Student t test dof	Student t test cohens_d	Student t test p_value	Student t test p_adj(FDR BH)	Student t test Rejects(FDR 5%)
% open arms time	1	PdgfraCre;Tbx1+/+	7	12.90725421	4.103497891	0.886610333	0.257444394	0.386166591	FALSE	0.107045624	2	20	0.898995957	0.898995957	FALSE	Intercept	4421.166501	1	4421.166501	26.47361987	4.92643E-05	PdgfraCre;Tbx1+/+	WT;Tbx1+/flox	-0.090770003	14	-0.045743782	0.928961264	0.928961264	FALSE
		WT;Tbx1+/+	7	15.44729701	4.180055074	0.973508997	0.922513345	0.922513345	FALSE							Genotype	24.86679522	2	12.43339761	0.074450271	0.928509658	PdgfraCre;Tbx1+/+	WT;Tbx1+/+	-0.43363151	12	-0.231785792	0.672249124	0.928961264	FALSE
		WT;Tbx1+/flox	9	13.53137901	5.135617804	0.770175921	0.009280317	0.02784095	TRUE							Error	3340.054381	20	167.0027191			WT;Tbx1+/+	WT;Tbx1+/+	-0.277229778	14	-0.139710676	0.785655127	0.928961264	FALSE
	2	PdgfraCre;Tbx1+/+	8	7.962568057	2.541302393	0.9223745	0.449425688	0.674138532	FALSE	1.779086372	2	17	0.19881424	0.19881424	FALSE	Intercept	563.5759562	1	563.5759562	18.85031974	0.000443371	PdgfraCre;Tbx1+/+	WT;Tbx1+/flox	1.934686976	12	1.044850385	0.076951997	0.126596757	FALSE
		WT;Tbx1+/+	6	6.17210563	1.907847722	0.972621635	0.90955982	0.90955982	FALSE							Genotype	127.1072061	2	63.55360307	2.125721876	0.14997335	PdgfraCre;Tbx1+/+	WT;Tbx1+/+	0.529258771	12	0.285832405	0.606278344	0.606278344	FALSE
		WT;Tbx1+/flox	6	1.937216264	1.116534507	0.751259955	0.02049345	0.061480349	FALSE							Error	508.2561668	17	29.89742157			WT;Tbx1+/flox	WT;Tbx1+/+	-1.915762576	10	-1.106066039	0.084397838	0.126596757	FALSE

Figure	Measurement	Month	Genotype	# of samples	Average	s.e.m	Shapiro-Wilk test Statistic	Shapiro-Wilk test p_value	Shapiro-Wilk test p_adj(FDR BH)	Shapiro-Wilk test Rejects(FDR 5%)	Levene test Statistic	Levene test df1	Levene test df2	Levene test p_value	Levene test p_adj(FDR BH)	Levene test Rejects(FDR 5%)	Student t test Sample1	Student t test Sample2	Student t test Statistic	Student t test dof	Student t test cohens_d	Student t test p_value	Student t test p_adj(FDR BH)	Student t test Rejects(FDR 5%)
Figure 7B	% open arm visits	1	oTbx1+/+	23	38.76689665	3.457186322	0.959194931	0.447303171	0.472928936	FALSE	0.034575631	1	32	0.853661423	0.853661423	FALSE	oTbx1+/-	oTbx1+/+	1.741236711	32	0.638317885	0.091249849	0.091249849	FALSE
			oTbx1+/-	11	48.92821047	4.328945934	0.935843176	0.472928936	0.472928936	FALSE														
		2	oTbx1+/+	20	16.20798761	2.580004845	0.933143261	0.177461607	0.339087396	FALSE	0.734877731	1	28	0.398584802	0.398584802	FALSE	oTbx1+/-	oTbx1+/+	0.59246246	28	0.229459724	0.558295668	0.558295668	FALSE
			oTbx1+/-	10	19.18868564	4.938885044	0.91781454	0.339087396	0.339087396	FALSE														

Measurement	Month	Genotype	# of samples	Average	s.e.m	Shapiro-Wilk test Statistic	Shapiro-Wilk test p_value	Shapiro-Wilk test p_adj(FDR BH)	Shapiro-Wilk test Rejects(FDR 5%)	Levene test Statistic	Levene test df1	Levene test df2	Levene test p_value	Levene test p_adj(FDR BH)	Levene test Rejects(FDR 5%)	One way ANOVA Source	One way ANOVA Type III Sum of Squares	One way ANOVA df	One way ANOVA Mean Square	One way ANOVA F	One way ANOVA Sig.	Student t test Sample1	Student t test Sample2	Student t test Statistic	Student t test dof	Student t test cohens_d	Student t test p_value	Student t test p_adj(FDR BH)	Student t test Rejects(FDR 5%)
% open arm visits	1	PdgfraCre;Tbx1+/+	7	35.6769162	4.664325787	0.928344033	0.536905413	0.536905413	FALSE	0.54245905	2	20	0.589631629	0.589631629	FALSE	Intercept	33992.03738	1	33992.03738	114.4766364	1.00324E-09	PdgfraCre;Tbx1+/+	WT;Tbx1+/flox	-0.38767913	14	-0.195371917	0.704083822	0.851686321	FALSE
		WT;Tbx1+/+	7	41.14160143	5.028883164	0.831111044	0.081981393	0.219437109	FALSE							Genotype	109.0958965	2	54.54794824	0.183703776	0.833570659	PdgfraCre;Tbx1+/+	WT;Tbx1+/+	-0.796719857	12	-0.425864677	0.441092294	0.851686321	FALSE
		WT;Tbx1+/flox	9	39.32322217	7.418792132	0.877086869	0.146291406	0.219437109	FALSE							Error	5938.685561	20	296.934278			WT;Tbx1+/flox	WT;Tbx1+/+	-0.190455488	14	-0.095980544	0.851686321	0.851686321	FALSE
	2	PdgfraCre;Tbx1+/+	8	20.47904805	3.951856074	0.921801353	0.444650175	0.666975262	FALSE	0.062288917	2	17	0.939824807	0.939824807	FALSE	Intercept	4860.798667	1	4860.798667	38.36512241	9.80937E-06	PdgfraCre;Tbx1+/+	WT;Tbx1+/flox	1.794257938	12	0.969010037	0.097985827	0.293957482	FALSE
		WT;Tbx1+/+	6	16.68154542	5.036940952	0.970955927	0.898793324	0.898793324	FALSE							Genotype	375.5691249	2	187.7845625	1.482138681	0.255070525	PdgfraCre;Tbx1+/+	WT;Tbx1+/+	0.602275965	12	0.325266196	0.558199622	0.558199622	FALSE
		WT;Tbx1+/flox	6	10.03968254	4.156071184	0.906492643	0.413726943	0.666975262	FALSE							Error	2153.872376	17	126.698375			WT;Tbx1+/flox	WT;Tbx1+/+	-1.017097195	10	-0.587221339	0.33308331	0.499624965	FALSE

Figure	Measurement	Month	Time (min)	Genotype	# of samples	Average	s.e.m	Shapiro-Wilk test Statistic	Shapiro-Wilk test p_value	Shapiro-Wilk test p_adj(FDR BH)	Shapiro-Wilk test Rejects(FDR 5%)	Levene test Statistic	Levene test df1	Levene test df2	Levene test p_value	Levene test p_adj(FDR BH)	Levene test Rejects(FDR 5%)
Figure 8A	Total Margin Time (s)	1	5	oTbx1+/+	24	187.9541667	9.818642574	0.989732318	0.995574805	0.995574805	FALSE	0.044942279	1	33	0.833414161	0.88610226	FALSE
				oTbx1+/-	11	224.8954545	14.69387698	0.929218262	0.402999507	0.592165394	FALSE						
			10	oTbx1+/+	24	177.46875	8.621859233	0.960282408	0.444124046	0.592165394	FALSE	1.749233955	1	33	0.195066221	0.88610226	FALSE
				oTbx1+/-	11	202.8863636	9.029917675	0.968324319	0.869129208	0.948140954	FALSE						
			15	oTbx1+/+	24	199.6520833	11.65783522	0.959487016	0.428203171	0.592165394	FALSE	0.97523234	1	33	0.330564543	0.88610226	FALSE
				oTbx1+/-	11	211.4636364	13.35909988	0.948946345	0.630518333	0.756622	FALSE						
			20	oTbx1+/+	24	224.575	13.89428188	0.864461767	0.004105455	0.012316364	TRUE	0.073888102	1	33	0.787451039	0.88610226	FALSE
				oTbx1+/-	11	212.5727273	18.03323745	0.905116019	0.213240511	0.426481022	FALSE						
			25	oTbx1+/+	24	238.9916667	11.76924598	0.78965836	0.000200552	0.001244162	TRUE	0.459512459	1	33	0.502577518	0.88610226	FALSE
				oTbx1+/-	11	221.3590909	16.82044727	0.889299635	0.136293398	0.327104154	FALSE						
			30	oTbx1+/+	24	255.1479167	10.74757408	0.790566413	0.00020736	0.001244162	TRUE	0.020836853	1	33	0.88610226	0.88610226	FALSE
				oTbx1+/-	11	247.8272727	16.96605483	0.755966079	0.002486921	0.009947684	TRUE						

Linear Mixed Model Source	F	df1	df2	Sig.
Corrected Model	6.693346578	11	198	1.67687E-09
Genotype	0.200852805	1	198	0.654523373
Time	8.251156703	5	198	4.22922E-07
Genotype * Time	2.151693449	5	198	0.06094955

Mann-Whitney U test Sample1	Sample2	Statistic	R (Z score)	p_value	p_adj(FDR BH)	Rejects(FDR 5%)
oTbx1+/-	oTbx1+/+	79	0.318331237	0.061404045	0.200151386	FALSE
oTbx1+/-	oTbx1+/+	80	0.312324987	0.066717129	0.200151386	FALSE
oTbx1+/-	oTbx1+/+	118	0.084087497	0.63644326	0.63644326	FALSE
oTbx1+/-	oTbx1+/+	105	-0.162168743	0.351863535	0.540916088	FALSE
oTbx1+/-	oTbx1+/+	109.5	-0.135140619	0.450763407	0.540916088	FALSE
oTbx1+/-	oTbx1+/+	109	-0.138143744	0.429851852	0.540916088	FALSE

Measurement	Month	Time (min)	Genotype	# of samples	Average	s.e.m	Shapiro-Wilk test Statistic	Shapiro-Wilk test p_value	Shapiro-Wilk test p_adj(FDR BH)	Shapiro-Wilk test Rejects(FDR 5%)	Levene test Statistic	Levene test df1	Levene test df2	Levene test p_value	Levene test p_adj(FDR BH)	Levene test Rejects(FDR 5%)
Total Margin Time (s)	1	5	PdgfraCre;Tbx1+/+	8	192.4	19.42002142	0.940119442	0.612255906	0.795951402	FALSE	0.155922633	2	21	0.856606813	0.96116231	FALSE
			WT;Tbx1+/+	7	183.6142857	18.45076045	0.951934955	0.747275189	0.836773791	FALSE						
			WT;Tbx1+/flox	9	187.3777778	15.59257549	0.878358778	0.150890078	0.388003057	FALSE						
		10	PdgfraCre;Tbx1+/+	8	176.525	17.77269173	0.852568912	0.10114029	0.303420871	FALSE	0.275926248	2	21	0.761577722	0.96116231	FALSE
			WT;Tbx1+/+	7	178.4642857	12.14288305	0.937809188	0.619073312	0.795951402	FALSE						
			WT;Tbx1+/flox	9	177.5333333	15.42819389	0.958946118	0.787226042	0.836773791	FALSE						
		15	PdgfraCre;Tbx1+/+	8	190.74375	21.81628945	0.976457289	0.943303265	0.943303265	FALSE	0.039686801	2	21	0.96116231	0.96116231	FALSE
			WT;Tbx1+/+	7	207.3857143	23.9748646	0.793291374	0.035136728	0.128541595	FALSE						
			WT;Tbx1+/flox	9	201.5555556	17.9268991	0.939932071	0.581183632	0.795951402	FALSE						
		20	PdgfraCre;Tbx1+/+	8	217.70625	22.27686468	0.930651593	0.522025005	0.795951402	FALSE	1.011932031	2	21	0.380567208	0.96116231	FALSE
			WT;Tbx1+/+	7	262.8928571	13.23386002	0.882178317	0.236294206	0.531661963	FALSE						
			WT;Tbx1+/flox	9	200.8777778	27.81605266	0.821368373	0.035705999	0.128541595	FALSE						
		25	PdgfraCre;Tbx1+/+	8	241.09375	16.03556994	0.932714563	0.541105179	0.795951402	FALSE	1.824164579	2	21	0.186009019	0.96116231	FALSE
			WT;Tbx1+/+	7	260.0642857	6.701019061	0.956735323	0.790286358	0.836773791	FALSE						
			WT;Tbx1+/flox	9	220.7333333	27.39387604	0.785658445	0.013990261	0.106253968	FALSE						
		30	PdgfraCre;Tbx1+/+	8	266.31875	13.4645697	0.780658686	0.017708995	0.106253968	FALSE	0.45938567	2	21	0.637870373	0.96116231	FALSE
			WT;Tbx1+/+	7	249.7428571	17.73063138	0.907420109	0.378299157	0.756598315	FALSE						
			WT;Tbx1+/flox	9	249.4222222	23.24614531	0.741618208	0.004333717	0.078006906	FALSE						

Repeated Measures ANOVA		Type III Sum of Squares	df	Mean Square	F	Sig.
Within subjects						
Time	Greenhouse-Geisser	113778.7452	2.742258347	41490.89212	12.81272325	3.10589E-06
Time * Genotype	Greenhouse-Geisser	17553.4018	5.484516693	3200.537582	0.988351906	0.437454084
Error(Time)	Greenhouse-Geisser	186482.8892	57.58742528	3238.257107		
Between subjects						
Intercept		6567827.009	1	6567827.009	673.365646	1.94254E-17
Genotype		7190.956262	2	3595.478131	0.368625948	0.696071568
Error		204828.3396	21	9753.730455		

Student t test Sample1	Sample2	Statistic	dof	cohens_d	p_value	p_adj(FDR BH)	Rejects(FDR 5%)
PdgfraCre;Tbx1+/+	WT;Tbx1+/flox	0.203680516	15	0.098970941	0.841340647	0.991826617	FALSE
PdgfraCre;Tbx1+/+	WT;Tbx1+/+	0.325226959	13	0.168320942	0.750184167	0.991826617	FALSE
WT;Tbx1+/flox	WT;Tbx1+/+	0.156685574	14	0.078962107	0.877729762	0.991826617	FALSE
PdgfraCre;Tbx1+/+	WT;Tbx1+/flox	-0.043066059	15	-0.020926343	0.96621693	0.991826617	FALSE
PdgfraCre;Tbx1+/+	WT;Tbx1+/+	-0.087424034	13	-0.045246236	0.931666773	0.991826617	FALSE
WT;Tbx1+/flox	WT;Tbx1+/+	-0.045251736	14	-0.022804731	0.964545789	0.991826617	FALSE
PdgfraCre;Tbx1+/+	WT;Tbx1+/flox	-0.386193777	15	-0.187656445	0.704775853	0.991826617	FALSE
PdgfraCre;Tbx1+/+	WT;Tbx1+/+	-0.514417762	13	-0.266236486	0.615593079	0.991826617	FALSE
WT;Tbx1+/flox	WT;Tbx1+/+	-0.199074094	14	-0.100323913	0.845066999	0.991826617	FALSE
PdgfraCre;Tbx1+/+	WT;Tbx1+/flox	0.464184705	15	0.225553224	0.649180802	0.991826617	FALSE
PdgfraCre;Tbx1+/+	WT;Tbx1+/+	-1.67915527	13	-0.869045415	0.116981237	0.991826617	FALSE
WT;Tbx1+/flox	WT;Tbx1+/+	-1.833493431	14	-0.923993838	0.088073727	0.991826617	FALSE
PdgfraCre;Tbx1+/+	WT;Tbx1+/flox	0.620368342	15	0.30144483	0.544326164	0.991826617	FALSE
PdgfraCre;Tbx1+/+	WT;Tbx1+/+	-1.035608398	13	-0.535978266	0.319265725	0.991826617	FALSE
WT;Tbx1+/flox	WT;Tbx1+/+	-1.234919708	14	-0.622341035	0.23718542	0.991826617	FALSE
PdgfraCre;Tbx1+/+	WT;Tbx1+/flox	0.608023955	15	0.295446536	0.552267228	0.991826617	FALSE
PdgfraCre;Tbx1+/+	WT;Tbx1+/+	0.755605871	13	0.391063191	0.463357322	0.991826617	FALSE
WT;Tbx1+/flox	WT;Tbx1+/+	-0.01042843	14	-0.005255435	0.991826617	0.991826617	FALSE

Figure	Measurement	Month	Time (min)	Genotype	# of samples	Average	s.e.m	Shapiro-Wilk test Statistic	Shapiro-Wilk test p_value	Shapiro-Wilk test p_adj(FDR BH)	Shapiro-Wilk test Rejects(FDR 5%)	Levene test Statistic	Levene test df1	Levene test df2	Levene test p_value	Levene test p_adj(FDR BH)	Levene test Rejects(FDR 5%)
Figure 8B	Total Margin Time (s)	2	5	oTbx1+/+	20	206.8325	12.85423966	0.930050585	0.154763372	0.371432094	FALSE	0.018345627	1	28	0.893228286	0.893228286	FALSE
				oTbx1+/-	10	214.465	18.6721823	0.924244799	0.393721373	0.472465648	FALSE						
			10	oTbx1+/+	20	189.3575	12.22481583	0.94401407	0.285201157	0.427801736	FALSE	0.528505896	1	28	0.473270499	0.893228286	FALSE
				oTbx1+/-	10	198.145	15.69639635	0.863931639	0.08488746	0.25466238	FALSE						
			15	oTbx1+/+	20	219.36	12.95180672	0.943204905	0.275461326	0.427801736	FALSE	0.293845397	1	28	0.59205509	0.893228286	FALSE
				oTbx1+/-	10	192.6	16.68604041	0.922021218	0.374121624	0.472465648	FALSE						
			20	oTbx1+/+	20	225.285	15.17396884	0.870559134	0.012018056	0.048072225	TRUE	0.875553509	1	28	0.357423105	0.893228286	FALSE
				oTbx1+/-	10	219.055	16.35034395	0.973597897	0.922052465	0.922052465	FALSE						
			25	oTbx1+/+	20	243.54	12.86533725	0.847368866	0.004817268	0.028903611	TRUE	0.13461714	1	28	0.716450392	0.893228286	FALSE
				oTbx1+/-	10	240.37	14.0183693	0.908087267	0.268109319	0.427801736	FALSE						
			30	oTbx1+/+	20	258.69	10.77157297	0.763194126	0.000256532	0.003078381	TRUE	0.021812291	1	28	0.883645943	0.893228286	FALSE
				oTbx1+/-	10	246.795	13.5509685	0.941920819	0.574578388	0.626812787	FALSE						

Linear Mixed Model Source	F	df1	df2	Sig.
Corrected Model	6.617692766	11	168	3.86918E-09
Genotype	0.089121278	1	168	0.765666179
Time	11.39367746	5	168	1.76945E-09
Genotype * Time	0.987985386	5	168	0.426725453

Mann-Whitney U test Sample1	Sample2	Statistic	R (Z score)	p_value	p_adj(FDR BH)	Rejects(FDR 5%)
oTbx1+/-	oTbx1+/+	95	0.040160966	0.845778642	0.845778642	FALSE
oTbx1+/-	oTbx1+/+	91	0.07228974	0.713163831	0.845778642	FALSE
oTbx1+/-	oTbx1+/+	64	-0.289158958	0.11962883	0.717772982	FALSE
oTbx1+/-	oTbx1+/+	87	-0.104418513	0.588437383	0.845778642	FALSE
oTbx1+/-	oTbx1+/+	85	-0.120482899	0.529969714	0.845778642	FALSE
oTbx1+/-	oTbx1+/+	77	-0.184740446	0.328175706	0.845778642	FALSE

Measurement	Month	Time (min)	Genotype	# of samples	Average	s.e.m	Shapiro-Wilk test Statistic	Shapiro-Wilk test p_value	Shapiro-Wilk test p_adj(FDR BH)	Shapiro-Wilk test Rejects(FDR 5%)	Levene test Statistic	Levene test df1	Levene test df2	Levene test p_value	Levene test p_adj(FDR BH)	Levene test Rejects(FDR 5%)
Total Margin Time (s)	2	5	PdgfraCre;Tbx1+/+	8	215.05	20.7141213	0.914114559	0.383949912	0.589193044	FALSE	2.353529985	2	17	0.125229683	0.324892303	FALSE
			WT;Tbx1+/+	6	155.8916667	13.65221238	0.920982548	0.512465635	0.658884388	FALSE						
			WT;Tbx1+/flox	6	246.8166667	15.77535549	0.902472395	0.388750333	0.589193044	FALSE						
		10	PdgfraCre;Tbx1+/+	8	192.06875	20.35318275	0.869602244	0.149385243	0.537786875	FALSE	0.703121363	2	17	0.508876155	0.610651385	FALSE
			WT;Tbx1+/+	6	149.775	19.35028747	0.957394761	0.799454028	0.899385782	FALSE						
			WT;Tbx1+/flox	6	225.325	13.08559482	0.903135512	0.392795363	0.589193044	FALSE						
		15	PdgfraCre;Tbx1+/+	8	210.59375	24.92307171	0.904635296	0.317826456	0.589193044	FALSE	2.176534062	2	17	0.144013566	0.324892303	FALSE
			WT;Tbx1+/+	6	186.4166667	12.48941997	0.975341879	0.926200355	0.96371726	FALSE						
			WT;Tbx1+/flox	6	263.9916667	13.16809539	0.926026806	0.549786816	0.659744179	FALSE						
		20	PdgfraCre;Tbx1+/+	8	214.0375	28.49870415	0.834033939	0.065373269	0.392239615	FALSE	1.521800567	2	17	0.246616393	0.36992459	FALSE
			WT;Tbx1+/+	6	189.425	21.96758123	0.982597585	0.96371726	0.96371726	FALSE						
			WT;Tbx1+/flox	6	276.1416667	10.47147249	0.752640586	0.021139106	0.190251956	FALSE						
		25	PdgfraCre;Tbx1+/+	8	231.325	19.64722127	0.925406735	0.47524764	0.658035195	FALSE	2.026321741	2	17	0.162446151	0.324892303	FALSE
			WT;Tbx1+/+	6	218.1083333	28.53045863	0.887468781	0.305136927	0.589193044	FALSE						
			WT;Tbx1+/flox	6	285.2583333	6.691492318	0.829589393	0.106631799	0.479843093	FALSE						
		30	PdgfraCre;Tbx1+/+	8	258.3625	18.83312467	0.716307697	0.00343956	0.061912072	FALSE	0.476100124	2	17	0.629238835	0.629238835	FALSE
			WT;Tbx1+/+	6	232.4333333	21.96380229	0.884449517	0.290118872	0.589193044	FALSE						
			WT;Tbx1+/flox	6	285.3833333	6.690623621	0.871648175	0.232854122	0.589193044	FALSE						

Repeated Measures ANOVA		Type III Sum of Squares	df	Mean Square	F	Sig.
Within subjects						
Time	Greenhouse-Geisser	63034.55554	2.524553611	24968.59455	12.07218449	2.00728E-05
Time * Genotype	Greenhouse-Geisser	7497.715639	5.049107223	1484.958688	0.717969736	0.61474568
Error(Time)	Greenhouse-Geisser	88764.99903	42.9174114	2068.274766		
Between subjects						
Intercept		5924566.762	1	5924566.762	563.1055124	1.79933E-14
Genotype		102679.8172	2	51339.90862	4.879645501	0.021148604
Error		178861.0353	17	10521.23737		

Student t test Sample1	Sample2	Statistic	dof	cohens_d	p_value	p_adj(FDR BH)	Rejects(FDR 5%)
PdgfraCre;Tbx1+/+	WT;Tbx1+/flox	-1.14816594	12	-0.620080478	0.273274002	0.351352288	FALSE
PdgfraCre;Tbx1+/+	WT;Tbx1+/+	2.204819261	12	1.190738493	0.047722279	0.107375127	FALSE
WT;Tbx1+/flox	WT;Tbx1+/+	4.358294506	10	2.516262506	0.00142495	0.014632215	TRUE
PdgfraCre;Tbx1+/+	WT;Tbx1+/flox	-1.267237854	12	-0.684386661	0.229111121	0.343666681	FALSE
PdgfraCre;Tbx1+/+	WT;Tbx1+/+	1.46200151	12	0.789571057	0.169430463	0.277249849	FALSE
WT;Tbx1+/flox	WT;Tbx1+/+	3.234229662	10	1.867283366	0.008956536	0.040304412	TRUE
PdgfraCre;Tbx1+/+	WT;Tbx1+/flox	-1.712823843	12	-0.925030599	0.1124384	0.20238912	FALSE
PdgfraCre;Tbx1+/+	WT;Tbx1+/+	0.780634653	12	0.421590897	0.450142746	0.506410589	FALSE
WT;Tbx1+/flox	WT;Tbx1+/+	4.274352212	10	2.4677984	0.001625802	0.014632215	TRUE
PdgfraCre;Tbx1+/+	WT;Tbx1+/flox	-1.803787117	12	-0.974156382	0.09640862	0.192817241	FALSE
PdgfraCre;Tbx1+/+	WT;Tbx1+/+	0.644726307	12	0.348192001	0.531236864	0.562486091	FALSE
WT;Tbx1+/flox	WT;Tbx1+/+	3.563351857	10	2.057302154	0.005152424	0.030914546	TRUE
PdgfraCre;Tbx1+/+	WT;Tbx1+/flox	-2.283065064	12	-1.232996056	0.041448022	0.107375127	FALSE
PdgfraCre;Tbx1+/+	WT;Tbx1+/+	0.395110604	12	0.213384114	0.699694601	0.699694601	FALSE
WT;Tbx1+/flox	WT;Tbx1+/+	2.291444377	10	1.322966028	0.044903228	0.107375127	FALSE
PdgfraCre;Tbx1+/+	WT;Tbx1+/flox	-1.190208127	12	-0.642785854	0.256978702	0.351352288	FALSE
PdgfraCre;Tbx1+/+	WT;Tbx1+/+	0.897571615	12	0.484744074	0.387067972	0.464481566	FALSE
WT;Tbx1+/flox	WT;Tbx1+/+	2.306159612	10	1.331461873	0.043792782	0.107375127	FALSE

Figure	Measurement	Month	Time (min)	Genotype	# of samples	Average	s.e.m	Shapiro-Wilk test Statistic	Shapiro-Wilk test p_value	Shapiro-Wilk test p_adj(FDR BH)	Shapiro-Wilk test Rejects(FDR 5%)	Levene test Statistic	Levene test df1	Levene test df2	Levene test p_value	Levene test p_adj(FDR BH)	Levene test Rejects(FDR 5%)
Figure 8C	Total Distance (cm)	1	5	oTbx1+/+	24	523.3911589	30.20140117	0.975883028	0.809668571	0.809668571	FALSE	4.130581659	1	33	0.050226926	0.301361554	FALSE
				oTbx1+/-	11	575.0133513	81.09884483	0.924914551	0.361718736	0.569470319	FALSE						
			10	oTbx1+/+	24	428.858175	25.3219597	0.947354113	0.237276704	0.569470319	FALSE	1.663209327	1	33	0.206136149	0.412272297	FALSE
				oTbx1+/-	11	463.1100966	54.68330524	0.916262967	0.288732783	0.569470319	FALSE						
			15	oTbx1+/+	24	353.2098723	29.23769273	0.966833314	0.589787776	0.707745332	FALSE	0.140317736	1	33	0.710361842	0.896645927	FALSE
				oTbx1+/-	11	411.012008	55.7960521	0.755590857	0.002459007	0.029508078	TRUE						
			20	oTbx1+/+	24	323.8313083	27.24334579	0.975754462	0.806709631	0.809668571	FALSE	0.017135892	1	33	0.896645927	0.896645927	FALSE
				oTbx1+/-	11	349.0746296	38.67701388	0.902850991	0.200221378	0.569470319	FALSE						
			25	oTbx1+/+	24	264.9099236	32.94277932	0.903535486	0.02559625	0.153577498	FALSE	0.040522424	1	33	0.841698265	0.896645927	FALSE
				oTbx1+/-	11	339.7488583	47.44333904	0.940451418	0.525819716	0.701092954	FALSE						
			30	oTbx1+/+	24	246.8655593	33.32994361	0.947492768	0.238941106	0.569470319	FALSE	2.249666174	1	33	0.143150583	0.412272297	FALSE
				oTbx1+/-	11	201.5505166	37.02036109	0.926826438	0.37964688	0.569470319	FALSE						

Linear Mixed Model

Source	F	df1	df2	Sig.
Corrected Model	14.18810262	11	198	0
Genotype	0.631374662	1	198	0.4278029
Time	27.84739692	5	198	0
Genotype * Time	0.955127959	5	198	0.446565974

Mann-Whitney U test

Sample1	Sample2	Statistic	R (Z score)	p_value	p_adj(FDR BH)	Rejects(FDR 5%)
oTbx1+/-	oTbx1+/+	125	0.042043748	0.82012655	0.902572012	FALSE
oTbx1+/-	oTbx1+/+	126	0.036037499	0.84744042	0.902572012	FALSE
oTbx1+/-	oTbx1+/+	128	0.024024999	0.902572012	0.902572012	FALSE
oTbx1+/-	oTbx1+/+	120	0.072074997	0.687299671	0.902572012	FALSE
oTbx1+/-	oTbx1+/+	93	0.23424374	0.173954599	0.902572012	FALSE
oTbx1+/-	oTbx1+/+	111	-0.126131245	0.472220258	0.902572012	FALSE

Measurement	Month	Time (min)	Genotype	# of samples	Average	s.e.m	Shapiro-Wilk test Statistic	Shapiro-Wilk test p_value	Shapiro-Wilk test p_adj(FDR BH)	Shapiro-Wilk test Rejects(FDR 5%)	Levene test Statistic	Levene test df1	Levene test df2	Levene test p_value	Levene test p_adj(FDR BH)	Levene test Rejects(FDR 5%)
Total Distance (cm)	1	5	PdgfraCre;Tbx1+/+	8	620.0439824	61.18380332	0.896772958	0.270160506	0.686126804	FALSE	0.78676576	2	21	0.468282323	0.702423485	FALSE
			WT;Tbx1+/+	7	441.6039626	47.42794277	0.93556056	0.599115546	0.898673318	FALSE						
			WT;Tbx1+/flox	9	501.0898018	31.91778323	0.918522745	0.380149455	0.760298911	FALSE						
		10	PdgfraCre;Tbx1+/+	8	528.1841483	47.57087669	0.949171774	0.702877111	0.973214461	FALSE	1.114125751	2	21	0.346839968	0.693679937	FALSE
			WT;Tbx1+/+	7	384.9748501	26.01161759	0.970333	0.900838417	0.980892361	FALSE						
			WT;Tbx1+/flox	9	374.699896	33.33231151	0.977856565	0.952350694	0.980892361	FALSE						
		15	PdgfraCre;Tbx1+/+	8	435.548186	56.01819145	0.984272937	0.980892361	0.980892361	FALSE	2.264993593	2	21	0.12860899	0.678212575	FALSE
			WT;Tbx1+/+	7	331.29903	29.99137947	0.789411464	0.03213434	0.431236082	FALSE						
			WT;Tbx1+/flox	9	297.0620262	48.93223185	0.905661169	0.286676525	0.686126804	FALSE						
		20	PdgfraCre;Tbx1+/+	8	411.8585995	57.63072458	0.973883362	0.926616722	0.980892361	FALSE	1.597337999	2	21	0.226070858	0.678212575	FALSE
			WT;Tbx1+/+	7	260.7565684	42.47375038	0.889114132	0.270074414	0.686126804	FALSE						
			WT;Tbx1+/flox	9	294.6429583	26.46424959	0.856295547	0.087368002	0.524208011	FALSE						
		25	PdgfraCre;Tbx1+/+	8	337.0979663	67.94142154	0.902611055	0.304945246	0.686126804	FALSE	0.479360415	2	21	0.62579012	0.750948144	FALSE
			WT;Tbx1+/+	7	280.8983661	57.58848895	0.918866143	0.460635174	0.763439422	FALSE						
			WT;Tbx1+/flox	9	188.3073192	38.18211176	0.832731267	0.04791512	0.431236082	FALSE						
		30	PdgfraCre;Tbx1+/+	8	285.4238129	54.60920401	0.924397037	0.466546314	0.763439422	FALSE	0.105755822	2	21	0.900120365	0.900120365	FALSE
			WT;Tbx1+/+	7	310.8749546	62.46942788	0.966178335	0.869648503	0.980892361	FALSE						
			WT;Tbx1+/flox	9	162.8064708	49.74066212	0.878647793	0.15195339	0.683790257	FALSE						

Repeated Measures ANOVA

		Type III Sum of Squares	df	Mean Square	F	Sig.
Within subjects						
Time	Greenhouse-Geisser	1232066.871	3.551512016	346913.3331	18.43930669	6.42253E-10
Time * Genotype	Greenhouse-Geisser	149400.5872	7.103024031	21033.37769	1.11797635	0.361061454
Error(Time)	Greenhouse-Geisser	1403165.787	74.58175233	18813.79484		
Between subjects						
Intercept		18280351.96	1	18280351.96	417.5782475	2.43882E-15
Genotype		479372.5079	2	239686.254	5.475155296	0.012198718
Error		919318.4597	21	43777.06951		

Student t test

Sample1	Sample2	Statistic	dof	cohens_d	p_value	p_adj(FDR BH)	Rejects(FDR 5%)
PdgfraCre;Tbx1+/+	WT;Tbx1+/flox	1.782324381	15	0.866053977	0.094944335	0.18988867	FALSE
PdgfraCre;Tbx1+/+	WT;Tbx1+/+	2.254227774	13	1.166673712	0.042077619	0.182512156	FALSE
WT;Tbx1+/flox	WT;Tbx1+/+	1.0781018	14	0.543312238	0.299214264	0.414296673	FALSE
PdgfraCre;Tbx1+/+	WT;Tbx1+/flox	2.69065136	15	1.307421554	0.016770132	0.182512156	FALSE
PdgfraCre;Tbx1+/+	WT;Tbx1+/+	2.532927569	13	1.31091456	0.024986314	0.182512156	FALSE
WT;Tbx1+/flox	WT;Tbx1+/+	-0.231693882	14	-0.116762741	0.820128066	0.820128066	FALSE
PdgfraCre;Tbx1+/+	WT;Tbx1+/flox	1.870796877	15	0.909043883	0.081011856	0.182512156	FALSE
PdgfraCre;Tbx1+/+	WT;Tbx1+/+	1.571756012	13	0.813461019	0.140019642	0.22912305	FALSE
WT;Tbx1+/flox	WT;Tbx1+/+	-0.554475257	14	-0.279429264	0.588002519	0.661502834	FALSE
PdgfraCre;Tbx1+/+	WT;Tbx1+/flox	1.92146405	15	0.933663704	0.073882743	0.182512156	FALSE
PdgfraCre;Tbx1+/+	WT;Tbx1+/+	2.057488232	13	1.064851326	0.060276832	0.182512156	FALSE
WT;Tbx1+/flox	WT;Tbx1+/+	0.70823831	14	0.35691856	0.490422016	0.630542591	FALSE
PdgfraCre;Tbx1+/+	WT;Tbx1+/flox	1.967124166	15	0.955850532	0.06794745	0.182512156	FALSE
PdgfraCre;Tbx1+/+	WT;Tbx1+/+	0.620765095	13	0.321276459	0.545484347	0.654581216	FALSE
WT;Tbx1+/flox	WT;Tbx1+/+	-1.390976099	14	-0.700986064	0.185945611	0.278918417	FALSE
PdgfraCre;Tbx1+/+	WT;Tbx1+/flox	1.663575002	15	0.808352151	0.116943757	0.210498763	FALSE
PdgfraCre;Tbx1+/+	WT;Tbx1+/+	-0.308231337	13	-0.159524872	0.762789645	0.807659625	FALSE
WT;Tbx1+/flox	WT;Tbx1+/+	-1.879743998	14	-0.947301933	0.081116514	0.182512156	FALSE

Figure	Measurement	Month	Time (min)	Genotype	# of samples	Average	s.e.m	Shapiro-Wilk test Statistic	Shapiro-Wilk test p_value	Shapiro-Wilk test p_adj(FDR BH)	Shapiro-Wilk test Rejects(FDR 5%)	Levene test Statistic	Levene test df1	Levene test df2	Levene test p_value	Levene test p_adj(FDR BH)	Levene test Rejects(FDR 5%)	Student t test Sample1	Student t test Sample2	Student t test Statistic	Student t test dof	Student t test cohens_d	Student t test p_value	Student t test p_adj(FDR BH)	Student t test Rejects(FDR 5%)
Figure 8D	Total Distance (cm)	2	5	oTbx1+/+	20	582.5324674	39.81366145	0.961805113	0.580510261	0.964595553	FALSE	2.027577552	1	28	0.165516111	0.496548332	FALSE	oTbx1+/-	oTbx1+/+	-0.200159227	28	-0.077521335	0.842802741	0.9640554	FALSE
				oTbx1+/-	10	565.9321735	87.02480436	0.952194518	0.694501499	0.964595553	FALSE														
			10	oTbx1+/+	20	465.0152343	28.92161572	0.976249885	0.877119898	0.964595553	FALSE	3.110488944	1	28	0.088700281	0.496548332	FALSE	oTbx1+/-	oTbx1+/+	0.243505064	28	0.094309106	0.809389409	0.9640554	FALSE
				oTbx1+/-	10	478.4165818	52.4441209	0.848827274	0.056251555	0.675018657	FALSE														
			15	oTbx1+/+	20	361.7175911	28.74548525	0.979861932	0.932306056	0.964595553	FALSE	0.864912718	1	28	0.360316817	0.530231581	FALSE	oTbx1+/-	oTbx1+/+	0.892772198	28	0.345769186	0.379588252	0.9640554	FALSE
				oTbx1+/-	10	409.8879946	50.49069356	0.979893494	0.964595553	0.964595553	FALSE														
			20	oTbx1+/+	20	348.215865	27.97211407	0.978671917	0.915818525	0.964595553	FALSE	0.608602693	1	28	0.441859651	0.530231581	FALSE	oTbx1+/-	oTbx1+/+	-0.897736865	28	-0.347691993	0.376980718	0.9640554	FALSE
				oTbx1+/-	10	300.6010342	50.30866599	0.93172014	0.465023493	0.964595553	FALSE														
			25	oTbx1+/+	20	299.1055367	24.94704284	0.974019572	0.836412834	0.964595553	FALSE	0.876820379	1	28	0.357080786	0.530231581	FALSE	oTbx1+/-	oTbx1+/+	-0.703264717	28	-0.272373254	0.487697769	0.9640554	FALSE
				oTbx1+/-	10	264.0208722	50.34200893	0.938023496	0.531237334	0.964595553	FALSE														
			30	oTbx1+/+	20	255.362162	39.42744784	0.949277247	0.356252313	0.964595553	FALSE	0.036907756	1	28	0.849039501	0.849039501	FALSE	oTbx1+/-	oTbx1+/+	-0.045470044	28	-0.017610472	0.9640554	0.9640554	FALSE

Repeated Measures ANOVA

		Type III Sum of Squares	df	Mean Square	F	Sig.
Within Subjects						
Time	Greenhouse-Geisser	1995853.076	3.660164031	545290.6098	26.86051187	1.71481E-14
Time * Genotype	Greenhouse-Geisser	40039.66219	3.660164031	10939.30814	0.538860217	0.691877512
Error(Time)	Greenhouse-Geisser	2080522.01	102.4845929	20300.82719		
Between Subjects						
Intercept		23339048.01	1	23339048.01	306.4591211	1.2929E-16
Genotype		1846.055051	1	1846.055051	0.024240081	0.87739263
Error		2132399.721	28	76157.13288		

Measurement	Month	Time (min)	Genotype	# of samples	Average	s.e.m	Shapiro-Wilk test Statistic	Shapiro-Wilk test p_value	Shapiro-Wilk test p_adj(FDR BH)	Shapiro-Wilk test Rejects(FDR 5%)	Levene test Statistic	Levene test df1	Levene test df2	Levene test p_value	Levene test p_adj(FDR BH)	Levene test Rejects(FDR 5%)	Student t test Sample1	Student t test Sample2	Student t test Statistic	Student t test dof	Student t test cohens_d	Student t test p_value	Student t test p_adj(FDR BH)	Student t test Rejects(FDR 5%)
Total Distance (cm)	2	5	PdgfraCre;Tbx1+/+	8	675.3377481	67.21069573	0.960970017	0.819288618	0.90097253	FALSE	0.513944781	2	17	0.60713361	0.845882843	FALSE	PdgfraCre;Tbx1+/+	WT;Tbx1+/flox	2.318778914	12	1.25228374	0.038853127	0.145180864	FALSE
			WT;Tbx1+/+	6	576.9360505	60.27675931	0.947046048	0.716310322	0.90097253	FALSE							PdgfraCre;Tbx1+/+	WT;Tbx1+/+	1.049097419	12	0.566577362	0.314803416	0.404747249	FALSE
			WT;Tbx1+/flox	6	464.38851	54.01971119	0.932193779	0.597146871	0.90097253	FALSE							WT;Tbx1+/flox	WT;Tbx1+/+	-1.390491666	10	-0.802800737	0.194547247	0.291820871	FALSE
		10	PdgfraCre;Tbx1+/+	8	563.3077705	39.36525666	0.91827703	0.416039464	0.90097253	FALSE	0.142545825	2	17	0.86817344	0.86817344	FALSE	PdgfraCre;Tbx1+/+	WT;Tbx1+/flox	3.212491801	12	1.734943863	0.007457649	0.134237677	FALSE
			WT;Tbx1+/+	6	423.8291928	36.86712279	0.939986406	0.659089302	0.90097253	FALSE							PdgfraCre;Tbx1+/+	WT;Tbx1+/+	2.504995321	12	1.352852094	0.027660714	0.145180864	FALSE
			WT;Tbx1+/flox	6	375.1445608	42.57179879	0.896122527	0.351518024	0.90097253	FALSE							WT;Tbx1+/flox	WT;Tbx1+/+	-0.864483291	10	-0.499109661	0.407581081	0.489097297	FALSE
		15	PdgfraCre;Tbx1+/+	8	412.9964819	53.1536322	0.970729632	0.903671601	0.903671601	FALSE	1.538099909	2	17	0.243233282	0.518147214	FALSE	PdgfraCre;Tbx1+/+	WT;Tbx1+/flox	1.951155687	12	1.053744506	0.074776993	0.154898089	FALSE
			WT;Tbx1+/+	6	384.9906002	24.8709437	0.960076551	0.820330406	0.90097253	FALSE							PdgfraCre;Tbx1+/+	WT;Tbx1+/+	0.427254885	12	0.23074401	0.676759782	0.716569181	FALSE
			WT;Tbx1+/flox	6	270.0727277	45.65896481	0.885730035	0.296415795	0.90097253	FALSE							WT;Tbx1+/flox	WT;Tbx1+/+	-2.210243188	10	-1.2760845	0.051539445	0.154618335	FALSE
		20	PdgfraCre;Tbx1+/+	8	383.3626534	47.27633929	0.962488762	0.833447547	0.90097253	FALSE	0.356989008	2	17	0.704902369	0.845882843	FALSE	PdgfraCre;Tbx1+/+	WT;Tbx1+/flox	1.870093843	12	1.009966107	0.086054494	0.154898089	FALSE
			WT;Tbx1+/+	6	392.8098267	35.00674422	0.93743225	0.638585233	0.90097253	FALSE							PdgfraCre;Tbx1+/+	WT;Tbx1+/+	-0.150587648	12	-0.081326625	0.882802665	0.882802665	FALSE
			WT;Tbx1+/flox	6	256.7595188	45.97104537	0.889647485	0.316344886	0.90097253	FALSE							WT;Tbx1+/flox	WT;Tbx1+/+	-2.354527304	10	-1.359386973	0.040328018	0.145180864	FALSE
		25	PdgfraCre;Tbx1+/+	8	364.6078814	41.60013821	0.951382549	0.72516182	0.90097253	FALSE	1.850493244	2	17	0.187452819	0.518147214	FALSE	PdgfraCre;Tbx1+/+	WT;Tbx1+/flox	2.664033886	12	1.438742736	0.02063703	0.145180864	FALSE
			WT;Tbx1+/+	6	296.9929018	29.92382991	0.964127822	0.8509185	0.90097253	FALSE							PdgfraCre;Tbx1+/+	WT;Tbx1+/+	1.232745856	12	0.665758853	0.241276061	0.334074546	FALSE
			WT;Tbx1+/flox	6	213.881712	34.05386391	0.910326291	0.438546447	0.90097253	FALSE							WT;Tbx1+/flox	WT;Tbx1+/+	-1.833339471	10	-1.058479037	0.096646438	0.158148716	FALSE
		30	PdgfraCre;Tbx1+/+	8	325.6745739	75.49961398	0.953377125	0.745179396	0.90097253	FALSE	1.463867976	2	17	0.259073607	0.518147214	FALSE	PdgfraCre;Tbx1+/+	WT;Tbx1+/flox	1.942251174	12	1.048935519	0.075945879	0.154898089	FALSE
			WT;Tbx1+/+	6	277.1861365	55.16889694	0.929847805	0.578927051	0.90097253	FALSE							PdgfraCre;Tbx1+/+	WT;Tbx1+/+	0.485421275	12	0.262157451	0.636119338	0.715634256	FALSE
			WT;Tbx1+/flox	6	139.7883048	43.83595818	0.905323563	0.40635214	0.90097253	FALSE							WT;Tbx1+/flox	WT;Tbx1+/+	-1.949896567	10	-1.125773308	0.079761998	0.154898089	FALSE

Repeated Measures ANOVA

		Type III Sum of Squares	df	Mean Square	F	Sig.
Within subjects						
Time	Sphericity Assumed	1366149.157	5	273229.8314	19.2608065	9.05321E-13
Time * Genotype	Sphericity Assumed	56104.56039	10	5610.456039	0.395498206	0.94529822
Error(Time)	Sphericity Assumed	1205792.482	85	14185.7939		
Between subjects						
Intercept		16804988	1	16804988	552.5624347	2.10342E-14
Genotype		579823.9342	2	289911.9671	9.532554405	0.001673302
Error		517018.1288	17	30412.83111		

						Shapiro-Wilk test		Levene test				Linear Mixed Model						Fisher's r-to-Z transformation					
Figure	Measurement	Genotype	# of Samples	Average	s.e.m	Statistic	p_value	Statistic	df1	df2	p_value	factor	F	df1	df2	p_value	Measurement	N	Pearson's r	p_value (correlation)	Z transformed correlation	Z statistic	p_value (Z statistic)
Figure 9B	g-ratio	oTbx1+/+	4423	0.742132168	0.001178885	0.983206272	1.62E-22	1.670711318	1	6738	0.196207608	Genotype	0.055858571	1	6736	0.813172794	g-ratio vs Axon Diameter (oTbx1+/+)	4423	0.626809	0.00E+00	0.736142587	-1.466330096	0.14255838
		oTbx1+/-	2317	0.736721572	0.001594201	0.98563242	1.56E-14					Axon Diameter	4117.938128	1	6736	0	g-ratio vs Axon Diameter (oTbx1+/-)	2317	0.649115	2.53E-277	0.773767499		
												Genotype:Axon Diameter	1.497334759	1	6736	0.22112471							

Figure	Measurement	Axon Diameter	Genotype	# of samples	Average	s.e.m	Shapiro-Wilk test statistic	Shapiro-Wilk test p_value	Shapiro-Wilk test p_adj(FDR BH)	Shapiro-Wilk test Rejects (FDR 5%)	Levene test Statistic	Levene test df1	Levene test df2	Levene test p_value	Levene test p_adj(FDR BH)	Levene test Rejects (FDR 5%)
Figure 9C	Axon Number	200	oTbx1+/+	145	0.131034483	0.035632184	0.341078043	8.80283E-23	5.47732E-22	TRUE	0.036618062	1	210	0.848429647	0.961107197	FALSE
			oTbx1+/-	67	0.119402985	0.045226142	0.358457863	1.42881E-15	3.63697E-15	TRUE						
		300	oTbx1+/+	145	0.662068966	0.111254037	0.56666255	6.46568E-19	2.78522E-18	TRUE	8.05053552	1	210	0.004994777	0.139853743	FALSE
			oTbx1+/-	67	1.313432836	0.207512627	0.771918416	7.85361E-09	1.25658E-08	TRUE						
		400	oTbx1+/+	145	1.8	0.180622593	0.794955611	5.68057E-13	1.13611E-12	TRUE	0.146243949	1	210	0.70253768	0.961107197	FALSE
			oTbx1+/-	67	3.268656716	0.268656716	0.922051668	0.000442592	0.000495703	TRUE						
		500	oTbx1+/+	145	3.04137931	0.201497236	0.927050591	9.02246E-07	1.29553E-06	TRUE	0.171565279	1	210	0.679147179	0.961107197	FALSE
			oTbx1+/-	67	4.253731343	0.309171785	0.915763259	0.000238829	0.000278634	TRUE						
		600	oTbx1+/+	145	4.020689655	0.224134984	0.938970745	6.20047E-06	8.26729E-06	TRUE	1.592773869	1	210	0.20833013	0.729155453	FALSE
			oTbx1+/-	67	5.059701493	0.405123562	0.891388595	2.6243E-05	3.26579E-05	TRUE						
		700	oTbx1+/+	145	3.806896552	0.19605705	0.943566203	1.3749E-05	1.79057E-05	TRUE	0.742076712	1	210	0.389978983	0.880618111	FALSE
			oTbx1+/-	67	4.865671642	0.359591407	0.867092669	3.69424E-06	5.04579E-06	TRUE						
		800	oTbx1+/+	145	3.593103448	0.177654081	0.944682121	1.67654E-05	2.13378E-05	TRUE	0.310912228	1	210	0.577714827	0.951530303	FALSE
			oTbx1+/-	67	3.671641791	0.28484093	0.922504842	0.000463096	0.000508498	TRUE						
		900	oTbx1+/+	145	3.220689655	0.160658656	0.954623818	0.000107914	0.000128578	TRUE	0.7278997	1	210	0.394536889	0.880618111	FALSE
			oTbx1+/-	67	3.014925373	0.261758774	0.920220673	0.000369011	0.000421727	TRUE						
		1000	oTbx1+/+	145	2.668965517	0.155380873	0.935009897	3.20007E-06	4.4801E-06	TRUE	0.684857725	1	210	0.408858409	0.880618111	FALSE
			oTbx1+/-	67	2.432835821	0.207528892	0.930607498	0.001061447	0.001143097	TRUE						
		1100	oTbx1+/+	145	1.972413793	0.103086853	0.925580502	7.20232E-07	1.09008E-06	TRUE	6.478227093	1	210	0.011638138	0.162933933	FALSE
			oTbx1+/-	67	1.880597015	0.19667336	0.894105256	3.31308E-05	4.03331E-05	TRUE						
		1200	oTbx1+/+	145	1.448275862	0.097345533	0.886540353	3.87729E-09	6.38613E-09	TRUE	3.69443342	1	210	0.055947631	0.391633419	FALSE
			oTbx1+/-	67	0.970149254	0.114467183	0.829086244	2.4814E-07	3.85995E-07	TRUE						
		1300	oTbx1+/+	145	1.144827586	0.093351451	0.832913399	1.46897E-11	2.65362E-11	TRUE	0.321086438	1	210	0.571560581	0.951530303	FALSE
			oTbx1+/-	67	1.029850746	0.112474228	0.847671866	8.85128E-07	1.29553E-06	TRUE						
		1400	oTbx1+/+	145	0.910344828	0.080656574	0.778914571	1.6278E-13	3.37617E-13	TRUE	0.011174349	1	210	0.915914309	0.961107197	FALSE
			oTbx1+/-	67	0.656716418	0.113638558	0.720096111	5.37756E-10	9.12555E-10	TRUE						
		1500	oTbx1+/+	145	0.537931034	0.067820962	0.664089799	9.36116E-17	2.66433E-16	TRUE	0.241876622	1	210	0.623367675	0.961107197	FALSE
			oTbx1+/-	67	0.47761194	0.104961083	0.599906087	3.1492E-12	6.08121E-12	TRUE						
		1600	oTbx1+/+	145	0.372413793	0.050802777	0.625598192	1.17036E-17	3.8677E-17	TRUE	6.61207E-05	1	210	0.993519823	0.993519823	FALSE
			oTbx1+/-	67	0.373134328	0.070006205	0.64398396	1.80164E-11	3.15287E-11	TRUE						
		1700	oTbx1+/+	145	0.317241379	0.042326328	0.607726872	4.70168E-18	1.7553E-17	TRUE	0.107856086	1	210	0.742925516	0.961107197	FALSE
			oTbx1+/-	67	0.343283582	0.072283423	0.60768044	4.24081E-12	7.91618E-12	TRUE						
		1800	oTbx1+/+	145	0.262068966	0.045926697	0.525665522	1.0219E-19	4.76887E-19	TRUE	1.66949102	1	210	0.197746792	0.729155453	FALSE
			oTbx1+/-	67	0.164179104	0.050313423	0.439795375	1.44797E-14	3.24346E-14	TRUE						
		1900	oTbx1+/+	145	0.124137931	0.029169144	0.382323027	3.6823E-22	2.06209E-21	TRUE	0.981731842	1	210	0.322911885	0.880618111	FALSE
			oTbx1+/-	67	0.179104478	0.05176825	0.462751687	2.90876E-14	6.26502E-14	TRUE						
		2000	oTbx1+/+	145	0.151724138	0.032944622	0.41921103	1.4113E-21	7.1848E-21	TRUE	0.095627397	1	210	0.757448003	0.961107197	FALSE
			oTbx1+/-	67	0.134328358	0.041974785	0.403025091	4.94005E-15	1.15268E-14	TRUE						
		2100	oTbx1+/+	145	0.096551724	0.026486709	0.326505065	5.39777E-23	3.77844E-22	TRUE	0.561931824	1	210	0.454321862	0.908643725	FALSE
			oTbx1+/-	67	0.134328358	0.047054932	0.38790673	3.21939E-15	7.83851E-15	TRUE						
		2200	oTbx1+/+	145	0.082758621	0.024958679	0.294410527	1.89092E-23	1.51274E-22	TRUE	0.036086921	1	210	0.8495196	0.961107197	FALSE
			oTbx1+/-	67	0.074626866	0.032347005	0.289320052	2.35055E-16	6.26812E-16	TRUE						
		2300	oTbx1+/+	145	0.027586207	0.013648669	0.151343524	2.64901E-25	2.96689E-24	TRUE	1.882778001	1	210	0.171482662	0.729155453	FALSE
			oTbx1+/-	67	0	0	1	1	1	FALSE						
		2400	oTbx1+/+	145	0.055172414	0.021395989	0.218779445	1.83508E-24	1.71274E-23	TRUE	0.012885239	1	210	0.90973217	0.961107197	FALSE
			oTbx1+/-	67	0.059701493	0.036094986	0.207609415	3.26996E-17	1.01732E-16	TRUE						
		2500	oTbx1+/+	145	0.027586207	0.013648669	0.151343524	2.64901E-25	2.96689E-24	TRUE	0.008464882	1	210	0.92678194	0.961107197	FALSE
			oTbx1+/-	67	0.029850746	0.020947148	0.162513554	1.17412E-17	3.8677E-17	TRUE						
		2600	oTbx1+/+	145	0.006896552	0.006896552	0.056594372	2.12105E-26	5.93893E-25	TRUE	5.644026015	1	210	0.018414322	0.171867004	FALSE
			oTbx1+/-	67	0.059701493	0.02916443	0.252678573	9.51548E-17	2.66433E-16	TRUE						
		2700	oTbx1+/+	145	0	0	1	1	1	FALSE	2.176243568	1	210	0.14165388	0.729155453	FALSE
			oTbx1+/-	67	0.014925373	0.014925373	0.10137707	3.12269E-18	1.24907E-17	TRUE						
		2800	oTbx1+/+	145	0.013793103	0.009719273	0.093628466	5.5507E-26	1.03613E-24	TRUE	0.928222721	1	210	0.336433275	0.880618111	FALSE
			oTbx1+/-	67	0	0	1	1	1	FALSE						
		2900	oTbx1+/+	145	0.006896552	0.006896552	0.056594372	2.12105E-26	5.93893E-25	TRUE	0.460888365	1	210	0.497956586	0.929518961	FALSE
			oTbx1+/-	67	0	0	1	1	1	FALSE						

LMM (setting session id as random effect) Source	F	df1	df2	Sig.
Corrected Model	133.9074722	55	5880	0
genotype	7.655858881	1	5880	0.005676512
binned_Axon_Diameter	246.5223833	27	5880	0
genotype * binned_Axon_Diameter	6.336275377	27	5880	0

LMM (setting both mouse id and session id as random effects) Source	F	df1	df2	Sig.
Corrected Model	133.7784885	55	5880	0
genotype	0.561757486	1	5880	0.453582974
binned_Axon_Diameter	246.5223833	27	5880	0
genotype * binned_Axon_Diameter	6.336275377	27	5880	0

Mann-Whitney U test Statistic	R (Z score)	p_value	p_adj(FDR BH)	Rejects (FDR 5%)	Mann-Whitney U test (300-1400nm) Statistic	R (Z score)	p_value	p_adj(FDR BH)	Rejects (FDR 5%)
4856	-0.000248086	0.996365794	0.996365794	FALSE					
3574.5	-0.212196465	0.00037454	0.00524356	TRUE	3574.5	-0.212196465	0.00037454	0.00224724	TRUE
2713	-0.354680685	1.48147E-07	4.14811E-06	TRUE	2713	-0.354680685	1.48147E-07	1.77776E-06	TRUE
3448.5	-0.233035713	0.00062617	0.00584425	TRUE	3448.5	-0.233035713	0.00062617	0.002504679	TRUE
4021	-0.138349449	0.042188689	0.147660412	FALSE	4021	-0.138349449	0.042188689	0.072323467	FALSE
3861.5	-0.16472929	0.015562111	0.087147822	FALSE	3861.5	-0.16472929	0.015562111	0.037349066	TRUE
4841	0.002728949	0.968922578	0.996365794	FALSE	4841	0.002728949	0.968922578	0.968922578	FALSE
4439	0.069216072	0.308357041	0.626862409	FALSE	4439	0.069216072	0.308357041	0.411142721	FALSE
4552.5	0.05044421	0.456622851	0.741419141	FALSE	4552.5	0.05044421	0.456622851	0.547947421	FALSE
4436	0.069712245	0.298569389	0.626862409	FALSE	4436	0.069712245	0.298569389	0.411142721	FALSE
3707	0.190282177	0.003824339	0.026770374	TRUE	3707	0.190282177	0.003824339	0.011473017	TRUE
4732.5	0.020673857	0.752577581	0.996365794	FALSE	4732.5	0.020673857	0.752577581	0.820993725	FALSE
3984	0.144468911	0.023473363	0.093893452	FALSE	3984	0.144468911	0.023473363	0.046946726	TRUE
4530.5	0.054082809	0.358207091	0.626862409	FALSE					
4780.5	-0.012735096	0.820278888	0.996365794	FALSE					
4852	0.00090965	0.987880394	0.996365794	FALSE					
4529	0.054330895	0.249807126	0.626862409	FALSE					
4626.5	-0.038205287	0.34420146	0.626862409	FALSE					
4831	0.004382858	0.916278431	0.996365794	FALSE					
4710.5	-0.024312455	0.495563538	0.741419141	FALSE					
4849	0.001405822	0.966419652	0.996365794	FALSE					
4723.5	0.022162374	0.17251315	0.483036819	FALSE					
4842.5	0.002480863	0.924256179	0.996365794	FALSE					
4846.5	-0.001819299	0.929852964	0.996365794	FALSE					
4601	-0.042422754	0.019005936	0.088694366	FALSE					
4785	-0.011990837	0.144023867	0.448074253	FALSE					
4790.5	0.011081187	0.338862118	0.626862409	FALSE					
4824	0.005540594	0.503105846	0.741419141	FALSE					

Figure	# of samples	Chi squared test Statistic	dof	p_value	Kolmogorov-Smirnov test Distance	p_value
Figure 9D	6740	109.7085231	27	6.22E-12	0.108947998	3.59E-16

							Shapiro-Wilk test				Levene test						Mann-Witney U test						
Figure	Measurement	PND	Genotype	# of Samples	Average	s.e.m	Statistic	p_value	p_adj(FDR BH)	Rejects(FDR 5%)	Statistic	df1	df2	p_value	p_adj(FDR BH)	Rejects(FDR 5%)	Sample1	Sample2	Statistic	R (Z score)	p_value	p_adj(FDR BH)	Rejects(FDR 5%)
Figure S1	Weight	P8	oTbx1+/+	27	4.6	0.125064086	0.922948078	0.046515575	0.186062298	FALSE	0.639894198	1	36	0.428996273	0.428996273	FALSE	oTbx1+/+	oTbx1+/-	140	0.044382036	0.799797921	0.91732983	FALSE
			oTbx1+/-	11	4.454545455	0.237931861	0.980904629	0.970981671	0.970981671	FALSE													
		P12	oTbx1+/+	30	6.54	0.155482194	0.986169448	0.955380174	0.970981671	FALSE	1.973777187	1	40	0.167766267	0.428996273	FALSE	oTbx1+/+	oTbx1+/-	153	0.115996334	0.465855659	0.91732983	FALSE
			oTbx1+/-	12	6.225	0.351861931	0.915390828	0.249993706	0.499987413	FALSE													
		1M	oTbx1+/+	27	16.15925926	0.252241194	0.863150358	0.002121269	0.016970151	TRUE	0.856989714	1	36	0.360747027	0.428996273	FALSE	oTbx1+/+	oTbx1+/-	135.5	-0.067878408	0.703523286	0.91732983	FALSE
			oTbx1+/-	11	16.37272727	0.447232075	0.942333972	0.548313562	0.80806296	FALSE													
		2M	oTbx1+/+	21	23.78571429	0.385837723	0.943028092	0.24996769	0.499987413	FALSE	1.523319488	1	29	0.227026429	0.428996273	FALSE	oTbx1+/+	oTbx1+/-	102	0.022769128	0.91732983	0.91732983	FALSE
			oTbx1+/-	10	23.53	0.736515822	0.94467026	0.60604722	0.80806296	FALSE													

						Shapiro-Wilk test				Levene test						Mann-Witney U test						
	Measurement	PND	Genotype	# of Samples	Average	s.e.m	Statistic	p_value	p_adj(FDR BH)	Rejects(FDR 5%)	Statistic	df1	df2	p_value	p_adj(FDR BH)	Rejects(FDR 5%)	Sample1	Sample2	Statistic	R (Z score)	p_value	p_adj(FDR BH)	Rejects(FDR 5%)
	Weight	P8	PdgfraCre;WT	8	4.35	0.205287255	0.866045239	0.137839188	0.413517564	FALSE	0.127476314	2	24	0.880906332	0.880906332	FALSE	PdgfraCre;WT	WT;Tbx1+/flox	18	-0.367573522	0.160528361	0.872562731	FALSE
			WT;Tbx1+/flox	8	4.7375	0.203485257	0.753919531	0.009024632	0.054147793	FALSE							PdgfraCre;WT	WT;WT	29.5	-0.274679021	0.272287052	0.872562731	FALSE
			WT;WT	11	4.681818182	0.225153758	0.91199385	0.257472583	0.617934199	FALSE							WT;Tbx1+/flox	WT;WT	40.5	-0.066301833	0.840385277	1	FALSE
		P12	PdgfraCre;WT	9	6.477777778	0.227777778	0.921953577	0.408659184	0.700558602	FALSE	1.743649374	2	27	0.194001478	0.776005912	FALSE	PdgfraCre;WT	WT;Tbx1+/flox	30.5	-0.20813018	0.436281366	0.872562731	FALSE
			WT;Tbx1+/flox	9	6.788888889	0.217590623	0.947010301	0.657291765	0.876389021	FALSE							PdgfraCre;WT	WT;WT	52.5	0.023262105	0.97227231	1	FALSE
			WT;WT	12	6.4	0.31454633	0.994973684	0.999999306	0.999999306	FALSE							WT;Tbx1+/flox	WT;WT	42	0.186096842	0.422107304	0.872562731	FALSE
		1M	PdgfraCre;WT	8	16.3625	0.287189273	0.934767327	0.560437988	0.840656982	FALSE	0.176982173	2	24	0.838878203	0.880906332	FALSE	PdgfraCre;WT	WT;Tbx1+/flox	31	0.116690007	0.672974085	1	FALSE
			WT;Tbx1+/flox	9	15.78888889	0.590537525	0.763341553	0.007737799	0.054147793	FALSE							PdgfraCre;WT	WT;WT	40	0	1	1	FALSE
			WT;WT	10	16.33	0.381240665	0.925384317	0.404055022	0.700558602	FALSE							WT;Tbx1+/flox	WT;WT	42	-0.056195149	0.842105263	1	FALSE
		2M	PdgfraCre;WT	8	24.3875	0.578309575	0.794950867	0.025269633	0.101078534	FALSE	0.889390233	2	18	0.428210148	0.856420296	FALSE	PdgfraCre;WT	WT;Tbx1+/flox	26	0.05976143	0.866511267	1	FALSE
			WT;Tbx1+/flox	7	23.91428571	0.525279323	0.958737507	0.807832827	0.969399392	FALSE							PdgfraCre;WT	WT;WT	14.5	0.327781141	0.282384282	0.872562731	FALSE
			WT;WT	6	22.83333333	0.889818958	0.974279891	0.919850787	0.999999306	FALSE							WT;Tbx1+/flox	WT;WT	14	0.277350098	0.365967366	0.872562731	FALSE

*including P11 and P13

**At the beginning of the behavioral battery (RSI) at each age

						Shapiro-Wilk test		Levene test				Linear Mixed Model						Fisher's r-to-Z transformation					
Figure	Measurement	Genotype	# of Samples	Average	s.e.m	Statistic	p_value	Statistic	df1	df2	p_value	factor	F	df1	df2	p_value	Measurement	N	Pearson's r	p_value (correlation)	Z transformed correlation	Z statistic	p_value (Z statistic)
Figure S2	myelin thickness (nm)	oTbx1+/+	4423	298.4267488	1.598178651	0.883548319	0.00E+00	18.9486008	1	6738	1.36273E-05	Genotype	0.007407354	1	6736	0.931416522	myelin thickness vs Axon Diameter (oTbx1+/+)	4423	0.309679	6.35E-99	0.320189803	-2.190862775	0.028461724
		oTbx1+/-	2317	281.3171899	1.943145919	0.89264971	1.85E-37					Axon Diameter	755.8280666	1	6736	0	myelin thickness vs Axon Diameter (oTbx1+/-)	2317	0.359582	1.15E-71	0.376405671		
												Genotype:Axon Diameter	0.05543768	1	6736	0.813865028							